Title
DIELECTRIC LOSS AND FARADAY ROTATION AND PHOTOSYNTHETIC SYSTEMS

Author
Bogomolni, Roberto A.

Publication Date
1972-08-01

DIELECTRIC LOSS AND FARADAY ROTATION IN PHOTOSYNTHETIC SYSTEMS

Roberto A. Bogomolni
(Ph.D. thesis)

August 1972

AEC Contract No. W-7405-eng-48

DISCLAIMER

Dedication

to my parents

to my wife Beatriz

to my son Martin

DIELECTRIC LOSS AND FARADAY ROTATION IN PHOTOSYNTHETIC SYSTEMS

Contents

Contents (continued)

Contents (continued)

DIELECTRIC LOSS AND FARADAY ROTATION IN PHOTOSYNTHETIC SYSTEMS

Roberto Alejandro Bogomolni

Lawrence Berkeley Laboratory
University of California
Berkeley, California

August 1972

ABSTRACT

A central problem in photosynthesis is the manner in which electromagnetic radiation in the visible region of the spectrum is converted into chemical potential. Early theories proposed that properties analogous to those exhibited by inorganic photoconductors might account for the required separation of unit positive and negative charged species. Previous attempts to detect such liberated charge carriers in photosynthetic materials have produced inconclusive results.

An electrodeless method employing microwave techniques has been used successfully to detect light induced mobile charge carriers. The Faraday rotation at microwave frequencies has been detected and used to determine the signs and Hall mobilities of these carriers.

Charge carriers of both negative and positive signs have been detected with Hall mobilities of about 1 cm^2/volt-sec with quantum yields between 0.1% and 1%. The photoconductivity action spectrum is similar to the action spectrum for photosynthesis, indicating that the process is sensitized by the same pigments. The rise times of the photoconductivity are shorter than the response time of the instrument, 10^{-5} sec.

The signals have been observed in samples of intact green leaves, in intact chloroplasts and sub-chloroplast fractions from Spinacea oleracea, and from the photosynthetic bacterium R. spheroides and its chromatophores. The signals were absent in a mutant of R. spheroides which lacks the reaction center pigments and is incapable of living photosynthetically. This observation provides evidence that the generation of the photocarriers takes place either in the reaction centers or in structures closely associated with them.

The activation energies for the photogeneration of the mobile charges are of the order of 0.2 to 0.4 eV. Superposition of pulses and continuous actinic light confirmed the existence of traps.

The charge transport properties in photosynthetic materials are consistent with a process involving multiple trapping, possibly in association with charge transfer processes involving the primary donors and acceptors. The data are inconsistent with earlier proposals which invoked charge migration through conduction bands.

Measurements on well characterized inorganic semiconductors, pigments extracted from photosynthetic materials, and pigment-protein complexes were performed and used as controls.

Photoinduced microwave absorption and luminescence measurements on a ZnO semiconductor-electrolyte solution interface indicated that surface states exist and can be detected.

ACKNOWLEDGMENTS

I wish to express my gratitude to Dr. Melvin Calvin for making possible my residence at the Laboratory of Chemical Biodynamics, and for his constant interest, constructive criticism, and encouragement.

This work would not have been possible without the daily guidance, advice, encouragement and contributions, both in inspiration and transpiration, of Dr. Melvin P. Klein. As the best teacher I have ever had, and as a friend, I thank him for making my graduate student years a delightful experience.

I am indebted to Dr. Kenneth Sauer and Dr. Alan Portis for the many valuable discussions that greatly contributed to my understanding of the experimental data.

I express my thanks to Dr. David Gill, who, in the first two years of my residence, contributed with infinite patience and inspiration to clarify my understanding of the basic principles of modern physics and spectroscopy, and for the priviledge of having him share with me his enormous wealth of human values that have so much enriched my spirit.

It was a wonderful experience to be associated with Dr. Helmut Tributsch and Dr. Günter Petermann, with whom I collaborated in part of the work presented in Chapter IV, and with my classmate and friend Ramesh Agarwal, who dedicated to me many hours of fruitful discussion.

I extend my thanks to the staff and students of the Laboratory of Chemical Biodynamics, and in particular to Mrs. Marilyn Taylor and to Evie Litton, who typed the original of this work.

Finally, I thank my parents and sister for the years of understanding encouragement and support, and to my friend and companion, my beloved wife Beatriz who provided me with the support so much needed in the hours of frustration, and who did not hesitate in renouncing her personal interests to make the fulfillment of this work possible.

This was supported, in part, by the U. S. Atomic Energy Commission.

PREFACE

Life in any of its facets is exciting to an inquiring mind. Man, as part of such phenomenon, is probably the most intriguing of all. The essence of the complex machinery that is able to study itself through the use of a process we call "thought" - whose very nature is beyond our present understanding - that creates new elements unknown to nature before, as forms of art or mathematical abstractions, and sometimes produces its own destruction for no other purpose than that of destruction itself, is paralleled in grandeur by very few "natural phenomena".

In a drive of absolute insolence, man created science to "discover" the rules that govern such natural phenomena. As a result, we have today some laws that probably Nature itself does not abide with, and through natural sciences such as physics and chemistry man is trying to teach nature how things happen.

Among the abstract concepts created is that of "energy"; a great deal of scientific effort has been spent in understanding what we regard as different forms of such an entity. Under the present laws, forms of energy are interconvertible, and the total energy of the universe remains unchanged. The conversion process is sometimes called energy transduction and the systems responsible for that are called "transducers".

Life systems as a whole are energy transducers; energy is absorbed in several forms to be converted into chemical bonds or to produce work. The state of ordering that characterizes a living system requires a continuous supply of energy, since it is a feature of this strange machine to continuously perform work, build and destroy itself to replace worn out parts. Energy is continuously degraded to keep the entropy constant.

There seems to be a unique internal currency of energy in living systems; it is the chemical energy stored in an apparently trivial phosphate ester bond in the molecule of ATP. Since life on earth has only one supply of external energy, it has learned to transduce it into forms that ultimately could be converted into such phosphate bonds. Thus electromagnetic radiation from the sun is converted into usable chemical potential by a transducer system which we are still rather far from understanding completely.

The study of life systems has provided other examples of energy transduction processes. Although none has been completely unveiled at present, in the deepest sense, a great deal of knowledge about them has been obtained in the past half century. Figure 1 shows some of the known transducers. The arrows indicate the direction in which they operate. Sometimes I ask myself whether production of "thought" through brain activity is not a form of energy transduction, but in such case the question of which form of energy is "thought" shows me that our present state of knowledge is much weaker than our insolence towards nature, and helps me to commit myself to continue searching for answers for as long as I live.

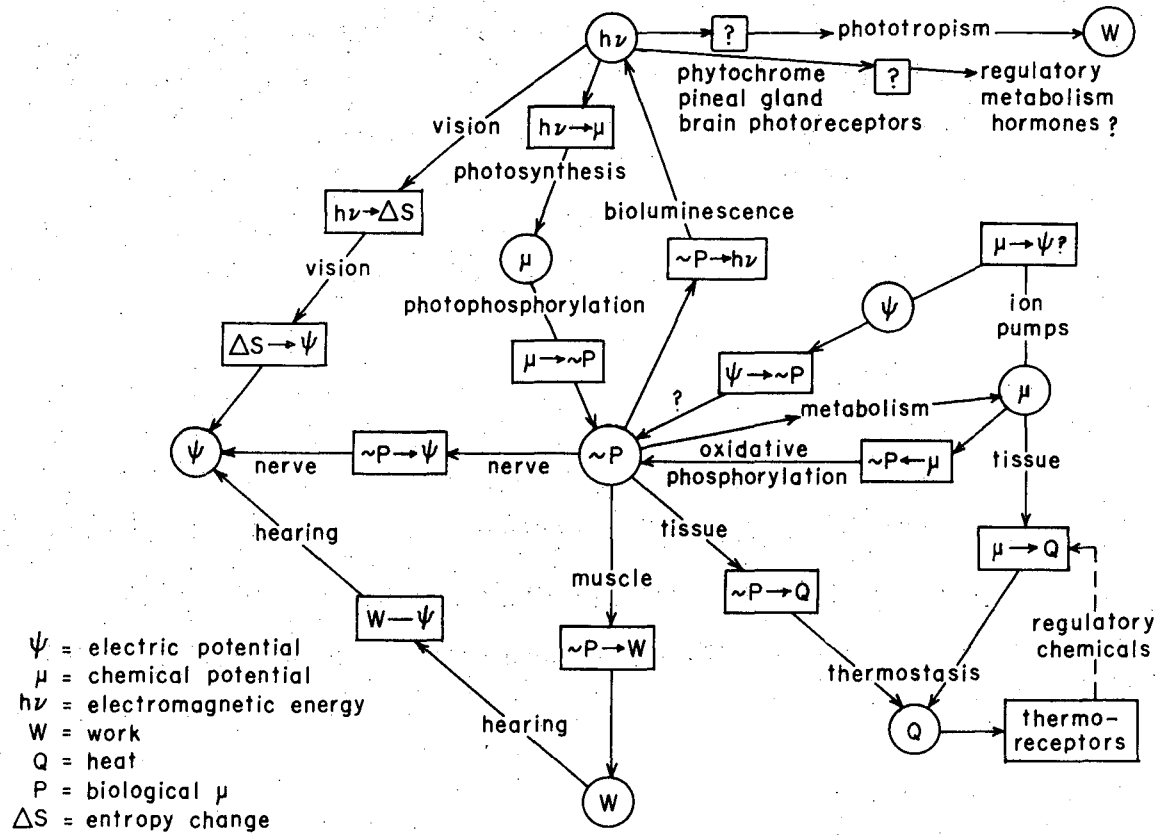

SOME ENERGY TRANSDUCERS IN BIOLOGY

XBL726-4665

Figure 1. The biological transducers are shown in rectangular boxes. Each consists of a complex molecular structure. Energy forms are enclosed in circles. The definition of symbols is given at the left of the figure.

I. THE PROBLEM OF ENERGY CONVERSION IN PHOTOSYNTHESIS

GENERAL INTRODUCTION

The problem of energy conversion in photosynthesis has been repeatedly and variously formulated as more knowledge of the overall process was acquired. Thorough historical surveys of photosynthesis are available in the literature, notably Rabinowitch (1945-1956), and it is my intention in part A only to introduce arguments leading to the present picture of the photosynthetic process, with special emphasis on the energy conversion steps.

The experimental observations are presented in a more or less chronological sequence. As much as possible, I have tried to separate experimental facts from speculation. In part B, I summarize the observations on "in vivo" systems at the time when this experiment was proposed. Part C contains the current speculation to account for the particular transducer that focuses my attention:

$$h\nu \longrightarrow \text{Chemical Potential}$$

In part D, I present the experiment and discuss some of the limitations one could foresee before performing the measurements.

A. Historical Review

By the end of the last century, the process of photosynthesis was regarded as,

$$CO_2 + H_2O \xrightarrow[\text{plant cell}]{\text{light}} (COH_2) + O_2$$

basic unit of carbohydrate

The early work of Engleman (1881) and later Willstätter et al. (1918) clearly established the role of chlorophyll as a contributing factor for carbon dioxide fixation. Willstätter was also the first to approach the problem from the kinetic point of view. He found that the time needed for the assimilation of a molecule of CO_2 was 20 seconds per molecule of chlorophyll at maximum rate. It was also realized from their early experiments that, although the absence of chlorophyll resulted in inhibition of the process, there was another limiting factor independent of chlorophyll present in photosynthetic systems.

Willstätter and Stoll (1918), and later Emerson (1929), working on etiolated leaves and Chlorella cells, respectively, found that the rate of photosynthesis could be very large in organisms with very low chlorophyll contents, even larger than for others with ten times as much pigment. Thus the concept of some kind of limiting enzymatic factor other than chlorophyll leads to the question of how many molecules of pigment were needed per such factor to produce a molecule of oxygen or to take up a molecule of CO_2. Emerson and Arnold (1932) utilizing light in the form of short flashes found the surprising result that for every molecule of oxygen evolved the Chlorella cell suspension had about 2,500 molecules of pigment. At this time a long controversy was initiated between the schools of Otto Warburg and Emerson in trying to give an answer to the question:

How many light quanta are needed to produce an oxygen or to fix a carbon dioxide molecule? Values of four quanta per oxygen obtained by Warburg (1922, 1954) could not be reproduced by most investigators. From the experimental values of 6 to 10 obtained by Emerson (1941) and many others and from thermodynamic considerations, a value close to 8 was accepted by most. From these experiments Emerson and Arnold suggested that some kind of system containing about 2,500 chlorophyll molecules per enzymatic limiting factor was the operational unit responsible for the assimilation of a molecule of CO_2. The energy of eight quanta was collected by the pigments with the formation of some kind of unstable photoproduct efficiently stored at the enzymatic center; when the necessary amount was collected, a molecule of CO_2 was absorbed or an O_2 was released. Gaffron and Wohl (1936) performed experiments with extremely low values for the light intensity, such that a photon was absorbed every several minutes, on the average, per chlorophyll molecule. Contrary to any previous supposition, the rates of oxygen evolution or CO_2 fixation were established with no lag in time. The conclusion was that a large number of pigment molecules cooperated in funneling the energy to a reaction center with high efficiency. The concept of the present photosynthetic unit was born, and from then to the present time the efforts of many investigators contributed to the elucidation of the chemical structure of such a unit and its dynamics. Studies using organisms that do not evolve oxygen led Van Niel (1931) to the conclusion that donors of reducing power replaced water in such system. Water was regarded as one among several possible hydrogen donors. This argument facilitated separating the oxygen evolving step from

the CO_2 reduction. Gaffron's experiments with hydrogen-adapted algae, which were induced to replace water for hydrogen gas, supported this view. It took some time until Hill (1939) was able to replace CO_2 by electron acceptors such as ferricyanide or oxidant dyes. The dark reactions leading to CO_2 fixation were clearly separated from the light-dependent oxidation of water.

A feature of the history of photosynthesis has been the strong dependence upon technological and theoretical developments in various areas of physics and physical chemistry. Thus, great momentum was given in the forties to the biochemistry of photosynthesis by the introduction of radioisotope tracers by Ruben, and Kamen et al. (1941). Oxygen was proven to come from water with ^{18}O. The first attempts to study carbon paths with ^{11}C were also performed in the early forties. The discovery of carbon-14 was the crucial step for development in the area of biochemistry of CO_2 fixation. Calvin, Bassham et al. (1957) during that decade and the first half of the 1950's clarified the dark reactions leading to the synthesis of glucose.

The interest of excellent physicists in the problem provided new ideas which led to fruitful research. Franck and Teller (1938) discussed the concept of energy migration in the photosynthetic unit, following early suggestions of Gaffron (1936). By that time people were inclined to think more in terms of diffusion of chemical species than migration of electromagnetic energy among pigment molecules. The experimental evidence for energy transfer in other areas of research was non-existent by that time. The Russian group of Terenin (1940) and later Lewis and Kasha (1945) worked on the idea of a long-lived metastable electronic state, such as a triplet state of the

chlorophyll or chlorophyll-protein-lipid complexes *in vivo*, to account for the extremely low yield of fluorescence *in vivo* (not known precisely at that time) and the efficient transfer of excitation energy between molecules without its loss as heat or chemistry. This is the time in the evolution of the ideas in photosynthesis when speculation began to rise in importance. Very often theories for the functioning of the photosynthetic apparatus, although physically correct, were proven to be wrong by the newly acquired experimental evidence. Structural as well as functional evidence kept destroying theories almost as fast as they were voiced. Unfortunately, Nature did not choose the nice and easy ways that we might envision.

A careful look at the literature shows an almost incredible wealth of experimental data that escapes the capabilities of a lifetime to read. Theories tried to fit as much of such experimental data as possible. The main difficulty in using experimental results is the variety of conditions under which the same systems were studied. The ideal of the biological experimenter is to study the living system in its unperturbed condition. It is an unavoidable fact that the process of measurement constitutes a perturbation on the system. In reality, in most cases it is not only a perturbation. We destroy life to disentangle its mysteries. Quite frequently the measurement has very little to do with the life process. It is a formidable task for a newcomer to the field to read the literature critically in order to separate the observer from the observable. Nevertheless, fundamental steps are relatively easy to locate. Such is the observation made by Emerson and Lewis (1943) of the sudden drop in quantum yield for photosynthetic activity at wavelengths longer than 700 nm. Why

does not light absorbed by the pigments in green plants promote photosynthesis? It was again Emerson (1957) who found, reviewing early observations by Warburg, another surprising result: a cooperative effect of light at relatively shorter wavelengths with far red radiation. The total yield of photosynthesis was larger than that expected by adding the energies of the two light sources. This enhancement effect and the red drop effect are not found in bacteria.

Arnon (1951) found that ATP was produced in chloroplasts by light. Vishniac and Ochoa (1951) found that NADPH was also produced by a light reaction, thus providing the necessary reducing power and the energy needed to perform the CO_2 fixation, respectively.

At this point, three effectively separate processes may be sorted out from the energy conversion step: (a) oxygen evolution (in green algae and higher plants), (b) phosphorylation and production of reducing power in the photoact (common to all photosynthetic organisms), and (c) carbon dioxide fixation.

Measurements of important quantities such as the fluorescence yield had to wait until rather recent times. Latimer (1956) reported a fluorescent yield close to 2% extrapolated to zero light intensity. The lifetime of the fluorescence, which should reflect the efficiency of the quenching process, is a parameter of considerable importance. Recent measurements for "in vivo" systems in chloroplasts and algae give values ranging from 0.6 to 1.5 x 10^{-9} sec (Brody and Rabinowitch, 1957) which, when compared with a natural lifetime for the singlet excited state of chlorophyll a of 1.5 x 10^{-8} sec, does not predict the low value of fluorescence yield observed. The argument is that the fluorescence yield is related to the lifetime in a linear fashion,

provided a first order quenching process is assumed, namely: Yield = $\tau_{\text{in vivo}}/\tau_{\text{natural}}$. Values obtained for chlorophyll a *in vitro* are perfectly consistent with the fluorescence yield of 33%; the measured lifetime is 5×10^{-9}. Therefore $5 \times 10^{-9}/1.5 \times 10^{-8} = 0.33$. If two different forms of chlorophyll a fluorescent and a non-fluorescent are assumed to exist, it is possible to fit the observed discrepancy. Fluorescence yield is strongly dependent upon light intensity, indicating light saturation effects on the quencher.

The role of pigments other than chlorophyll in photosynthetic organisms was studied by Haxo and Blinks (1950), and Franck *et al.* (1937-1960). Energy transfer from pigments such as phycobilins to chlorophyll was clearly established. Fluorescence emitted by chlorophyll, as well as photosynthetic activity, *e.g.* carbon fixation, is promoted more efficiently by light absorbed by that accessory pigment than by chlorophyll a itself. These pigments as well as the entire carotenoid group are now regarded as complementary for energy gathering at wavelengths at which chlorophyll does not absorb. Mutants of bacteria having no other pigment than bacteriochlorophyll performed photosynthesis with reasonable efficiency, thus showing that such pigments are not essential.

New evidence on the functioning of the photosynthetic unit was obtained by Duysens (1952) and later Chance *et al.* (1952), Goedheer (1955), and Witt *et al.* (1955) during the 1950's. Light induced absorbance changes at different wavelengths were observed when light at the chlorophyll absorption band acted upon photosynthetic systems. The study of the photochemistry by this approach yielded valuable information concerning the intermediate components of the electron

transferring system. A light induced absorbance change at 870 nm was observed by Duysens (1952). It was later attributed to some form of photochemistry of bacteriochlorophyll, and the system responsible for that activity was named P870. Cytochromes were identified as intermediates in the photochemical steps, and a considerable effort was spent in obtaining kinetic information. Fast flashes were sent to the samples and the transient absorbance changes were followed. Many evanescent components, as Kamen (1963) calls the seemingly disconnected observations, were available by the end of the decade.

The huge number of experimental observations was condensed in a remarkable way by Hill and Bendall (1960) by proposing a two-light-reaction-in-series mechanism for the photo act in green plants and green algae. The red drop and the enhancement effects are explained in a very natural way in such a picture. The location of the intermediate components responsible for the transfer of reducing power between the two photosystems was left for further work. Thus some of the evanescence was constrained. Figure 2 is based on that series formulation.

The work of the last decade has enriched that initial picture with descriptions of new intermediates and their reaction kinetics. Kok et al. (1956) found in green plants and algae absorbance changes at 700 nm which were similar to the one at 870 nm, in bacteria. The component was designated P700. Work of Clayton et al. (1963-1972) in bacteria leads to the isolation of pigment-protein complexes containing most of the long wavelength pigment P870 (Reed and Clayton, 1968). The 870 nm band is completely bleached by light in this structure.

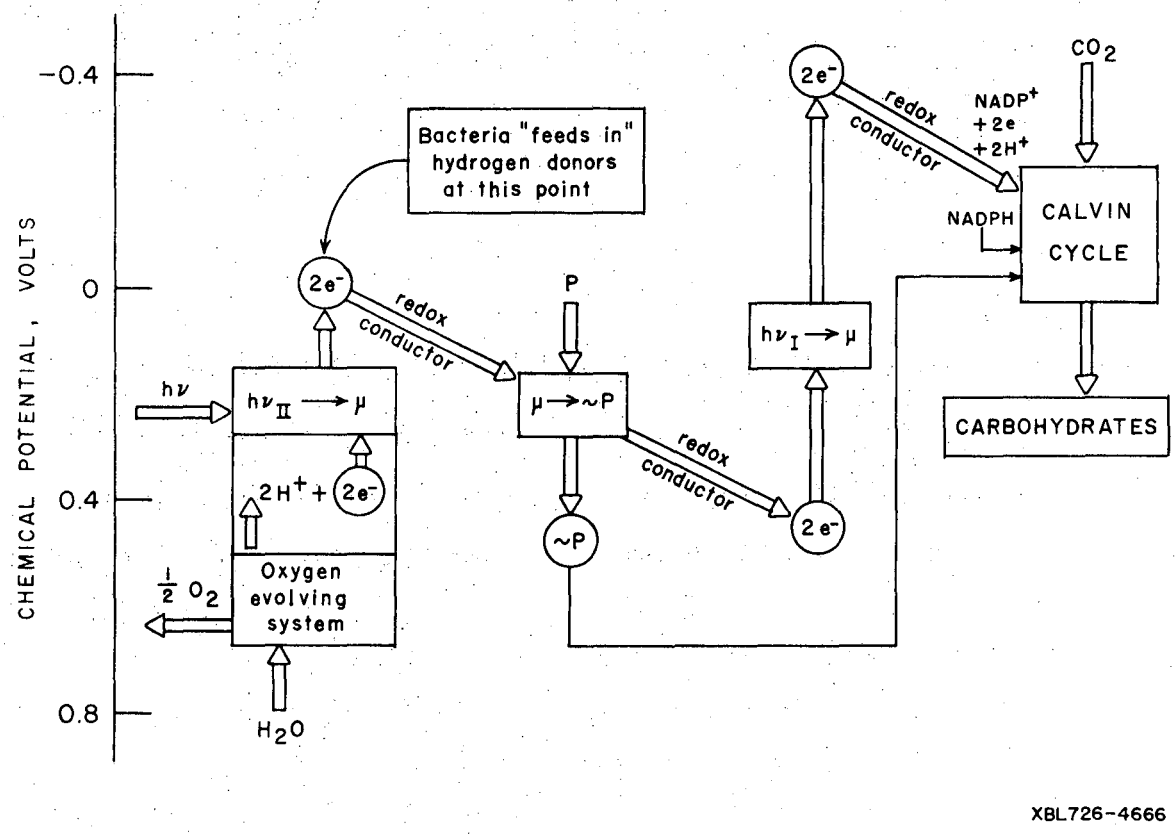

Figure 2. Series formulation of photosynthetic electron transport with special emphasis on the transducers. The fact that a two electron transfer is depicted does not indicate that such is the correct mechanism; it is shown in that manner for stoichiometric reasons.

The previously proposed reaction center of the photosynthetic unit was finally found. The fraction of the pigments contained in such structures is called reaction center pigment. The remainder, which also has been isolated in some cases as a protein complex (Thornberg and Olson, 1970), is called antenna or light-gathering pigment.

The study of photosynthesis in purple and green bacteria was a decisive step in the understanding of the process of early photochemistry. The fact that bacterial mutations are rather easy to produce encouraged efforts to obtain species with damaged or incomplete photosynthetic structures. Stanier and Sistrom (1961) produced mutants of R. spheroides which were unable to grow photosynthetically but apparently contained the normal amount of pigments. The lack of the light-induced absorbance change at 870 nm in this organism was regarded as further evidence for the existence of a primary photochemical center, possibly a form of bacteriochlorophyll absorbing at that wavelength. Mutants of algae lacking the 700 nm absorbance change were also reported. Evidence for a reaction center at the O_2 evolving photosystem has been found (Witt, 1968), but no characterization of the chemical species is available yet. Current work at Levine's laboratory with algal mutants with damage at the oxygen site might help to clarify this point.

Use of the herbicide DCMU proved that inhibition of oxygen evolution does not inhibit cytochrome oxidation by far red light, provided that an electron donor replaces the oxygen evolving system. Oxidation of cytochrome f by 670 nm light is completely inhibited in the presence of DCMU. Studies of fluorescence in Chlorella have shown

that inhibitors have an effect on the emission intensity, suggesting that the fluorescent species is the pigment fraction associated with oxygen evolution. The action of far red light on the 700 nm ΔOD can be substituted by oxidizing agents such as ferricyanide. DCMU inhibits the 700 nm change (chlorophyll oxidation) by short wavelength light when far red is substituted by ferricyanide. These observations give further strong support to the series scheme of Figure 2.

Structural evidence is of major importance in the understanding of the photosynthetic machinery. The lamellar structure in chloroplasts contains particles of different sizes. Some were identified as enzyme components. Park et al. (1963) found small particles, about 100 Å by 160 Å x 180 Å with molecular weight 2×10^6, intimately associated with the membrane structures - thylakoids - containing most of the pigments and able to perform the Hill reaction. They were initially identified as the photosynthetic units, and called quantasomes. Separation of single membrane forms (stroma lamellae) from the compact membrane stacks (grana lamellae) in chloroplasts has shown that the two light reactions are performed in the latter, while only Photosystem I is present in the former (Park, 1971). Lamallae seen in the chromatophores of photosynthetic bacteria might have evolved, with the incorporation of photosystem II, into what is found in higher organisms. Considerable effort is underway in order to clarify the function associated with the observed structures.

Very valuable information on the molecular organization of the pigments in several isolated structures was obtained by Sauer et al. using circular dichroism techniques. Bacteriochlorophyll molecules in

the reaction centers of bacteria appeared to be trimers (Sauer et al., 1968). The antenna pigments of a blue-green algae (Chloropseudomonas ethylica) might be composed of units of four or five molecules embedded in a protein matrix. Strong exciton interaction among the pigments was found in such structures (Philipson and Sauer, 1972). Evidence for such strong interaction in the pigment aggregates has been found in intact quantasome preparations (Sauer, 1965).

Crystalline chlorophyll absorbs at much longer wavelengths (745 nm for chlorophyll a) than does the "in vivo" pigment. Highly dispersed (low concentration) solutions, in which chlorophyll is in the monomeric form, absorb at much shorter wavelengths. Thus, current thinking envisions the antenna pigments to be in the form of aggregates of a small number of molecules in a protein or lipoprotein environment. Evidence from fluorescence depolarization in oriented structures (Euglena cells and chloroplast quantasome fractions) showed that the main pigment fraction absorbing at 680 nm is very likely to be in an array with a complex organization. Work on the molecular organization will contribute to rule out current (or introduce new) speculation about the dynamics of these systems. All present efforts to determine molecular structure rely on spectroscopic techniques, which in a sense is the microscope we use to "look" at the structures. A significant step in understanding the structure-function relation in biology would come when such a molecular microscope could be coupled with spectroscopy. It is an unfortunate fact that our technical development is unable to construct an X-ray microscope with resolution of atomic dimensions.

B. Experimental Observations

1. Structural

-The photosynthetic apparatus is located in membranous structures which, with progressive evolution, are contained in differentiated organelles. The membranous structures are common to all photosynthetic systems, with several variants of organization.

-The relevant molecular species, pigments, and electron transfer proteins, are contained in such membrane structures in a densely packed environment. Molecular translational motion is highly constrained.

-The pigment molecules show very strong electronic interactions. Exciton splitting due to the interaction of a few chlorophyll molecules is observed. The aggregation of the antenna pigments in some species might be an ensemble of small units containing a few pigment molecules.

-The pigments can be split into two fractions in the form of protein complexes. Energy gathering complexes containing a few tens of bacteriochlorophyll molecules in bacterial chromatophores, and photochemical reaction center complexes with just a few molecules of chlorophyll.

-One of the two photosystems in chloroplasts has been isolated, and corresponds to the apparently single photosystem of bacteria.

2. Operational

-About 2,500 chlorophyll molecules are needed to fix a CO_2 molecule or to evolve an O_2 in higher systems.

-Eight quanta are needed for such a process.

-Four units of reducing power (4 e^-) are produced, at a potential around -0.4 volts. This fact is common to all photosynthetic systems. The potential of the donor is +0.8 for oxygen evolging organisms, and about zero for non-O_2-evolving.

-Some of the light energy is lost radiatively as fluorescence, the in vivo fluorescence yield being about 2.5%.

-Fluorescence induced by polarized incident radiation shows a large degree of depolarization.

-The lifetime of fluorescence is 0.5×10^{-9} sec. The natural radiation lifetime for chlorophyll a is 1.5×10^{-8} sec. There is strong evidence that the light induced absorbance changes at 870 nm in bacteria (purple bacteria) and at 700 nm in chloroplasts are the result of photooxidation of the reaction center pigment. Mutants of bacteria unable to grow photosynthetically but containing apparently healthy antenna pigments lack such absorbance changes. The absorbance changes are reversible in bacteria down to temperatures of 1°K. They are not reversible in chloroplasts at low temperatures.

Experimental facts which have been omitted in part A because they were not needed for the gross view of Figure 2 are not introduced.

-In 1951 Arnold and Strehler found light emission in photosynthetic tissues at times when the fluorescence should have been completely excinct. It can be observed many seconds after an exciting flash. The wavelength of the emission is identical with that of the fluorescence of the light harvesting (680 nm) chlorophyll. The

same phenomenon has been observed in bacterial chromatophores. This delayed fluorescence is regarded as a reverse process. It is still evident with comparable intensity at low temperatures, indicating that at least part of it is not dependent on enzymatic factors. The decay of this radiation follows a second order decay over many orders of magnitude in time. Delayed light emission at the same wavelength can also be induced by action of redox agents (Fleishman, 1968-1971).

-Commoner, Heise and Townsend (1954-1956) found an EPR signal induced by light in photosynthetic material. Later this effect was studied extensively by Calvin et al. (1958-1963). The EPR signal is produced by light, even if the samples are dried or frozen, suggesting that the species responsible for such an effect is connected with primary "physical" events in the photosynthetic process.

-In recent work in bacteria, Feher et al. (1970), and separately, Bolton et al. (1971) showed that the paramagnetic species is very likely to be the cation radical of the reaction center bacteriochlorophyll. The kinetics in the isolated reaction center particles is not the same as in intact chromatophores, but in every case the kinetics of the EPR signal are very closely correlated with that of the 870 nm absorption changes. The EPR spectrum shows no hyperfine structure. The formation of a radical at one site implies that another unpaired electron will be either free or form part of another radical species.

-Another radical signal has been detected in reaction center preparations (Feher, 1970), but it has not been identified with any

chemical species. That signal is very broad and has a rather low g value. Both the EPR signal and the absorbance change are reversible in bacterial chromatophores even at liuqid helium temperatures. That is not the case in chloroplasts where freezing or drying, "freezes in" the EPR signal and the absorbance changes (Bolton, 1971; Androes, 1963).

-Measurements by Chance et al. (1966) and by Parson et al. (1968, 1969) with laser excitation, showed that the first electron donor to the chlorophyll cation is very probably a cytochrome molecule. This oxidation of the cytochrome is temperature-dependent from room temperature to 120°K, the half-reaction times being 2 μsec and 2 msec respectively; below such temperature the reaction rate is temperature insensitive. The activation energy is 0.14 eV.

-The first electron receptor has not yet been identified.

-A shift in the absorption wavelength at 515 nm detected by Witt et al. (1968) and also studied by Fleishman and Clayton (1968) has been attributed to the effect of a light-induced electric field (10^6 volts/cm) on the carotenoid molecules (Stark effect). Part of such a shift can be seen even at 1°K. The voltage across the thylakoid membranes has been estimated to be 250 mv. The onset time for the fields was estimated to be less than 10^{-8} sec (Witt, 1969).

-Substances which are known to affect the permeability of membranes to ions are also effective inhibitors of the carotenoid shift. The delayed light emission, and the process of photoproduction of ATP seem to be related to such trans-membrane fields.

-An interesting effect of an electric field on the delayed light emission has been reported. Arnold (1970), and later Ellenson (1971), have shown that an electric field applied to a suspension of chloroplasts increases the intensity of delayed fluorescence. The physical integrity of the thylakoid membrane is essential for the effect.

From the EPR vs ΔOD experiments, it seems that the primary photochemistry is the production of an oxidized chlorophyll radical. It is not clear how the charge transfer takes place, or how to explain the series of chemical redox reactions that follow among membrane components that are fixed in position. Molecular collision chemistry does not apply in this situation. Distinction between membrane-bound and unbound components is essential for its interpretation. The system it is clearly in a "solid state" matrix where charge migrates in some form. Although light absorbed by reaction center pigments promotes charge splitting very efficiently, it is not known how the system operates under normal conditions, e.g. when the antenna system is the energy donor. It could well be that charge and not excitation energy is transferred to the reaction center complex. These considerations are already part of the speculation that follows.

C. Current Theories

Speculation to account for the energy conversion steps has promoted very useful research and helped to formulate the problem in more precise terms.

The hν to $_{\mu}$ converter is envisioned as shown in Figure 3. Capture of a photon by any of the antenna pigments results in the excitation of the whole ensemble through a process of energy migration. The times involved would depend upon the mechanism of transfer. Two possible ways are currently considered. A dipole-induced dipole mechanism postulated by Forster in the 1940's would result in a dependence of the rate of transfer as the inverse 6th power of the separation between molecules. The typical rate of transfer is about 10^{12} sec^{-1} and the optimal separation about 70 Å. The other mechanism is based on the strong interaction between molecules in an ensemble that leads to exciton levels (Bay and Pearlstein (1963, 1966, 1970; Robinson, 1966). Thus, the overlapping of the electron wavefunctions causes the excitation of any molecule to be immediately delocalized and shared by all the neighbors. Depending on the strength of the interaction, the rates of transfer may vary from 10^{12} sec^{-1} to 10^{14} sec^{-1}. The distance between molecules ranges from 5 to 15 Å. The dependence on separation distance in this model goes as the inverse 3rd power. Fluorescence depolarization and fluorescence yield data strongly support rapid migration of excitation energy. It can be seen that either of the two mechanisms would assure a large number of transfers within the lifetime of the excited state, as measured "in vivo", facilitating the trapping at some photochemical center by a collision process.

The trapping of excitation at a photochemical form of the pigment at the reaction center follows. Such trapping centers would be responsible for the fast and efficient separation of an electron (reducing

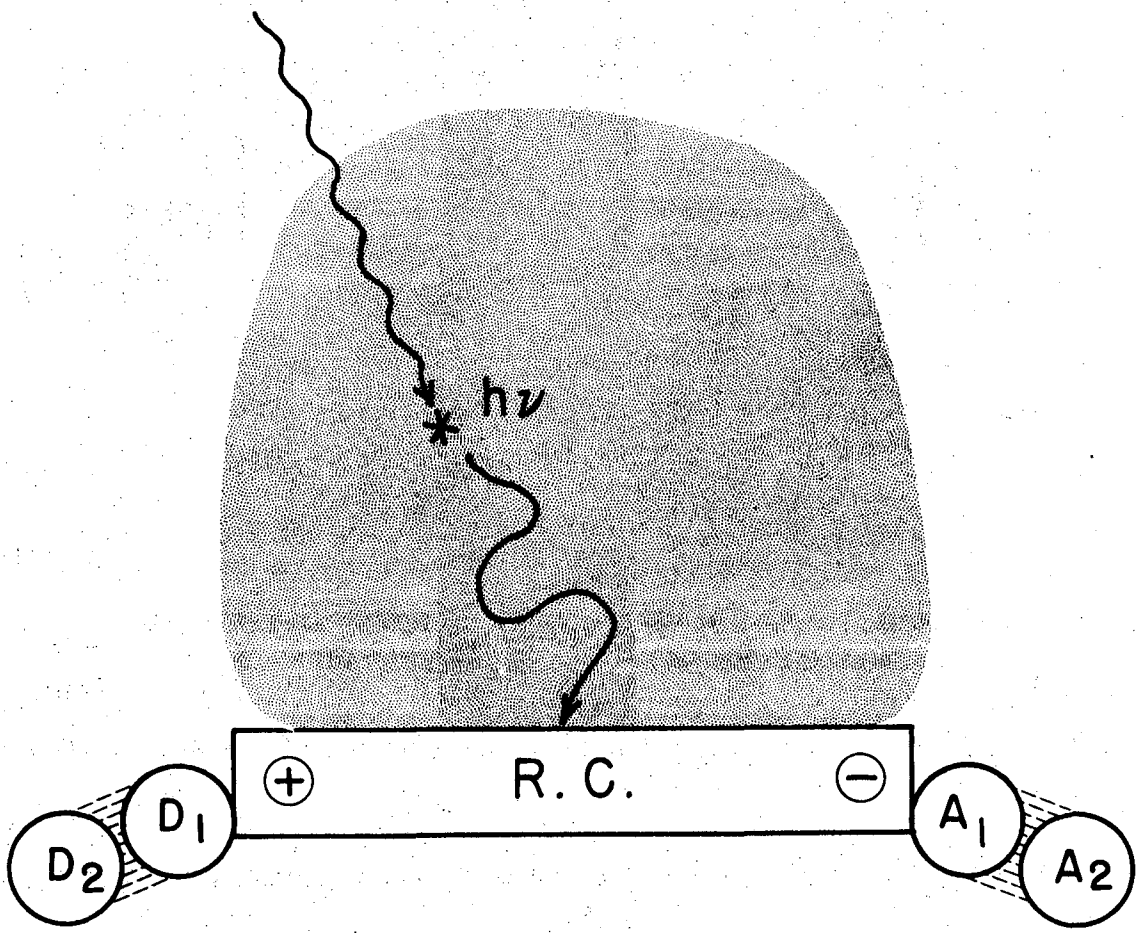

XBL723-4587

Figure 3. Current scheme for the functioning of the hν→μ converter. a) A photon is absorbed by an antenna pigment molecule. b) Energy migrates. c) Energy is trapped at a photochemical reaction center complex, R.C., where charge separation occurs. d) An electron and a hole are produced, and a sequence of electron transfer reactions begins among several membrane bound donors and acceptors.

chemical potential) from a hole (oxidizing potential) in the protein-pigment complexes. Close association with a donor and an acceptor induces charge transfer by tunneling or semiconduction. The tunneling mechanism is favored by the temperature insensitivity of the process below 120°K. However, the large activation energy at higher temperatures cannot be accounted for by the tunneling mechanism unless large vibrations or conformation changes of the donor or acceptor molecules are postulated.

This mechanism for the development of chemical reducing power from light can account for most of the observables. For instance, the fast rising electric field reflected as a shift in the absorption peak of carotene molecules at 1°K might be the result of the primary charge separation; the associated fields in the molecular environment could be very large. The absorption changes and the EPR signals are other indications of that primary photochemistry.

The emission of delayed fluorescence in green material has to be accounted for in this mechanism as resulting from the existence of some kind of metastable state in the light harvesting pigments.

Following early suggestions of Szent-Gyorgyi (1941) and Katz (1949), several investigators, notable Calvin and Arnold, speculated on the possibility of using arguments then currently employed in the field of solid state physics of semiconductors. Knowledge of semiconduction properties of organic pigments was almost nil at that time. Nevertheless, some interesting features of a solid state type argument for the interpretation of the process were foreseen.

The solid state models envisioned that the photon energy which is harvested and funneled to the special sites leads to the creation of

an electron - hole pair. By virtue of the molecular organization of the proteins, lipids and pigments in the relevant units, they are considered to possess some sort of collective electronic structure which provides the pathway for the migration of the photoliberated charges. Since the mobilities of the electron and the hole may be quite different, these models have the attraction of providing a mechanism for physically separating the units of charge and thereby separating the primary units of reducing and oxidizing power. Should these rather "free" charges exist, effects such as changes in the dielectric properties of the material can be expected. Stemming from these suggestions, a number of experiments in various laboratories were designed to test such effects. Arnold and Sherwood (1956) studied the resistivity and thermoluminescence of chloroplasts, and Arnold and Clayton (1960) studied the delayed light emission, spectral changes and photoconductivity in chromatophores of R. spheroides. It was concluded from these experiments that separation of positive from negative charges was responsible for the observed effects.

Extensive investigations on the conductivity of pigments related to the photosynthetic apparatus have been carried out in several laboratories since then, by Rosenberg et al. (1961), Terenin et al. (1959-1965), and Blummenfeld (1970). More recently, a study of the semiconductor properties of films of chloroplasts and chromatophores of bacteria by Litvin et al. (1967) showed that the light induced changes in conductivity of these materials are indeed sensitized by chlorophyll, and they estimated a relatively high quantum yield.

Since no value for the mobilities of the carriers are available from direct measruements, it was impossible to establish the correct order of magnitude for quantum yields.

While all the experiments mentioned above are indeed suggestive of the existence of charge migration connected to the primary events, they are by no means conclusive. Most measurements were performed by conventional methods which require the presence of electrodes. If any free charges were liberated in the photosynthetic structures they would be required to traverse many membranes and lamellar components to reach the electrodes. This is a demand far from that which might be expected to occur in their normal functioning. Thus any charge produced at the central sites would be remotely related to the observed effects. By means of the condenser method developed by Terenin and Putzeiko (1959), attempts were made by McCree to detect free charges, in a variety of material ranging from chloroplasts to a whole leaf, with negative results, thus tending to rule out the process of charge transfer in photosynthesis. The condenser method has the advantage that it avoids the use of electrodes and, therefore, eliminates the possible charge injection at the electrode junction, a fact that has been repeatedly pointed to as a possible pitfall in the previous measurements.

Theories for the functioning of the photosynthetic energy conversion, based on the relative position of the π-π^* and n-π^* levels in different forms of chlorophyll were developed by Franck et al., and resumed in the paper by Franck, Rosemberg and Weiss, Jr. (1962). Since there is considerable evidence that such a model is not supported

by new experimental observations, I will only refer to it as one of the remarkable examples of very intelligent speculation on the available data.

D. The Proposed Experiment: Advantages and Limitations

The strongest evidence against the use of the solid state models was based on the apparently low quantum yields. I felt that these experiments were still inconclusive. If the charge migration takes place in small regions, as should be expected, the measurement of photoconductivity at very high frequencies would give a more realistic picture of the situation, because the diffusion length of the charge carriers during one period of the accelerating electric field becomes of the order of the intermolecular distances in the photosynthetic apparatus. Therefore, I decided to look for free charge carriers, if any, by means of an electrode-less method: the measurement of photo-induced dielectric loss at microwave frequencies. This method has been used in the past to perform studies on inorganic photoconductors and spectral sensitization of photoconductivity by Terenin (1965). Microwave techniques also provide means for a complete characterization of the charge carriers through measurements of the Hall effect. The sign and mobility may be obtained directly, thus providing conclusive data for the evaluation of quantum yield. Portis et al. (1958) developed a microwave method for the measurement of the Hall effect, and it was then used for the study of photoconductivity in PbS and CdS and for measurement of Faraday rotation (Teaney (1960). Later, Teaney, Klein and Portis (1961), using the same technique, developed

an electron paramagnetic resonance spectrometer, which is basically the electronic arrangement used in the measurements reported in this dissertation.

Measurements of Hall mobilities in proteins and DNA by means of this technique have been reported by Trukhan (1966), and a very recent report of measurements of the action spectrum of microwave photoconductivity in green photosynthetic materials by Blyumenfeld (1970) coincides very closely with measurements already obtained in this work.

The main limitation that may be foreseen is of a biological sort. The rather unphysiological state of the samples (in the dry state) might raise skepticism about the biological meaning of such measurements. The fact that primary processes such as cytochrome oxidation or light induced absorbance changes occur in such conditions encourages the performance of the experiment.

II. EXPERIMENTAL TECHNIQUES AND PROCEDURES

A. Theory of Measurements

1. Conductivity

The measurements of conductivity at microwave frequencies consists of measuring the imaginary part of the complex dielectric constant that characterizes the propagation of electromagnetic radiation through a conducting medium.

$$\varepsilon = \varepsilon' + i\varepsilon'' \qquad (1)$$

The imaginary part, ε'', represents the losses due to all mechanisms that contribute to the conductivity at the applied frequency. The real part, ε', determines the velocity of the radiation in the medium. Both parts are frequency-dependent. It can be shown that $\varepsilon'' = K\frac{\sigma}{\omega}$, where σ is the conductivity, ω is the applied radian frequency, and K is a constant that depends upon the system of units used. In our case, K = 1. In optical measurements ε'' is proportional to the quantity usually known as absorption coefficient, and ε' is related to the index of refraction.

For performing such measurements it is assumed that a sample, located at a site in a cavity resonator where the electric field is a maximum acts only as a small perturbation. Thus the field configuration differs only slightly from that of the empty cavity. The difference in the real part of the dielectric constant between sample

and vacuum will induce a shift in frequency of the resonator given by:

$$\frac{f_1 - f_0}{f_1} = \frac{\Delta\varepsilon'}{2} \frac{\int_v E^2 dv}{\int_V E^2 dV} \qquad (2)$$

where v and V are the volumes of the sample and the cavity, respectively, and $\Delta\varepsilon'$ is the change in the real part of the dielectric constant. E is the electric field.

The quality factor of a resonator, defined as

$$Q = \frac{\text{energy stored} \times 2\pi f_0}{\text{average power dissipated}} , \qquad (3)$$

is associated with the losses due to the finite conductivity of the metal that constitutes the walls of the empty cavity. When a sample is introduced into the cavity, the change in Q due to the sample losses is given by

$$\frac{1}{Q_1} - \frac{1}{Q_0} = \Delta\varepsilon'' \frac{\int_v E^2 dv}{\int_V E^2 dV} \qquad (4)$$

where Q_1 is the new quality factor, and $\Delta\varepsilon''$ is the change in the imaginary part of the dielectric constant. The measurement of Q provides the data to evaluate $\Delta\varepsilon''$ and, consequently, σ, the conductivity.

The ratio of integrals:

$$\eta = \frac{\int_v E^2 dv}{\int_V E^2 dV} \qquad (5)$$

is usually called the filling factor. It can be evaluated for the mode of excitation of interest, giving typically

$$\eta = C \frac{v}{V} \qquad (6)$$

Two cylindrical cavities were used in this work: a TE_{011} operated in the reflection configuration, as depicted in Figure 4, and a TE_{111} which was used as a transmission cavity, and will be described in in part 2.

A theoretical calculation for the filling factor for a sample in the form of a thin piece of cylinder located at the antinode of the electric field in a TE_{011} cavity is given in Appendix I. The result shows that the radius of the cavity, a, the cavity height, d, and the sample height, h, should satisfy certain conditions to permit an exact evaluation of C. If $h/d \leq 1/10$ and the sample is located at $r = 0.58\ a$, the theoretical value for C is 4.2.

The samples were not in the form of a piece of cylinder but in the form of a thin disc. Therefore the previous calculation provides only an approximate value for the filling factor. Taking advantage of the fact that the thin disc geometry is ideal for the TE_{111} bimodal cavity, for which there is a theoretical calculation of the filling factor by von Aulock and Rowen (1957), I performed measurements of the conductivity on the same sample in both cavities in order to test experimentally the filling factor value.

The average of ten measurements resulted in a value of $C = 3.0 \pm 0.4$; therefore, the value of the filling factor that was used in the calculations was

$$\eta = 3.0 \frac{v}{V} \ , \qquad (7)$$

and the samples were standardized to a radius of about 3 mm, which is close to d/10. The filling factor for the TE_{111} cavity was calculated

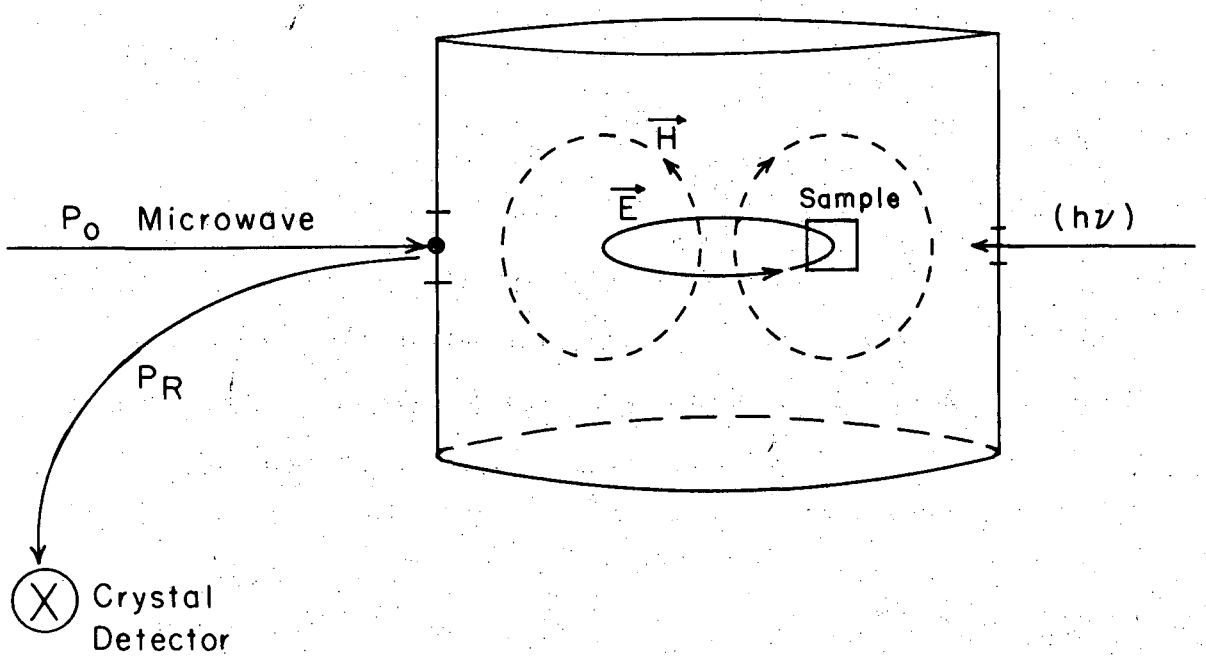

XBL 706-5264

Figure 4. The scheme shows the lines of maximum $\vec{E}$ and $\vec{H}$ fields for the TE_{011} cavity. P_o, the incident power, is a constant; therefore any photoinduced power absorption by the sample is measured as a decrease in reflected power, P_R, by the crystal detector, X.

from von Aulock and Rowen's work resulting in

$$n = 1.9 \frac{v}{V} \quad , \tag{8}$$

provided the sample is in the form of a thin disk having a radius smaller than one half of the cavity radius.

The Q of a cavity may be calculated from the bandwidth at half power of the absorption curve of the resonator, Δf.

$$Q_o = K \frac{f_o}{\Delta f} \quad , \tag{9}$$

where f_o is the resonance frequency, and K a constant that depends on the losses in the system that couples the resonator to the microwave circuit.

The value of K for the TE_{011} cavity is $K = (1 + \beta)$, giving

$$Q_o = (1 + \beta) \frac{f}{\Delta f} \quad , \tag{10}$$

where β is the coupling coefficient. The empty cavity unloaded Q, was about 10,500.

It can be shown that β is related to the Voltage Standing Wave Ratio, VSWR = r. For the undercoupled case, $\beta = \frac{1}{r}$, overcoupled case, $\beta = r$, where

$$r = \frac{1 + \Gamma}{1 - \Gamma} \quad , \tag{11}$$

Γ is the reflection coefficient. It is the measured quantity in my experimental arrangement. The readings from the reflectometer are obtained as values of r. A conversion table gives the values of β. It is important to know whether one is in the undercoupled or the

overcoupled situation. The distinction is very simple in the case where there is a variable coupling mechanism such as a dielectric stub that effectively enlarges the coupling iris for microwaves, or a piece of metal that acts as an antenna to couple power from the waveguide into the cavity. Such a deposition was provided in the TE_{011} cavity. The bimodal TE_{111} cavity which had a fixed coupling at the input, was constructed to be always in an undercoupled situation. Detailed treatment of the subject of microwave measurements is given by Slater (1946), Birnbaum (1949), Feher (1957), and Ginzton (1957).

The value of K for the bimodal cavity is:

$$K = 0.64 \left[(1 + \beta_1)(1 + \beta_2)\right]^{1/2} \tag{12}$$

giving

$$Q_o = 0.64 \left[(1 + \beta_1)(1 + \beta_2)\right]^{1/2} \frac{f_o}{\Delta f} \tag{13}$$

provided $\beta_1 \cong \beta_2$, which was always the case. Typical values for β were $\beta_1 = 0.16$ and $\beta_2 = 0.06 - 0.18$. The empty cavity unloaded Q was 5,500.

The conductivity of a sample σ, is given by:

$$\sigma = \frac{1}{9 \times 10''} \frac{f_o}{2\eta} \left[\frac{1}{Q_s} - \frac{1}{Q_o} \right] \Omega^{-1}\ cm^{-1} \tag{14}$$

where Q_o is the empty cavity unloaded Q, and Q_s the quality factor with the sample in place, f_o is the resonant frequency and η the filling factor.

The photoconductivity is measured as a change in reflected (or transmitted) microwave power, P_2, when light is impinging on the

sample. Provided the changes are small, e.g., $\frac{\Delta\sigma}{\sigma} = 10^{-3}$, the fractional change in conductivity, or sensitivity, is related to the fractional change in reflected power as follows:

TE_{011}: (reflection)

$$\left(\frac{\Delta P_2}{P_2}\right)_{\text{reflected}} = (1 + \beta_1)\left[\frac{1}{Q_s} - \frac{1}{Q_o}\right]Q_o \frac{\Delta\sigma}{\sigma} \qquad (15)$$

TE_{111}: (transmission)

$$\left(\frac{\Delta P_2}{P_2}\right)_{\text{transmitted}} = \left(\frac{1}{1+\beta_1} + \frac{1}{1+\beta_2}\right)\left[\frac{1}{Q_s} - \frac{1}{Q_o}\right]Q_o \frac{\Delta\sigma}{\sigma} \qquad (16)$$

When backing material, such as styofoam, is used to support the sample, the values of Q_o in the formulas should be replaced by Q_b; the quality factor with the supporting material in place. It is assumed that the backing material perturbs very little the cavity field distribution. Figure 4 depicts very schematically the field distribution for the TE_{011} cavity and the measurement configuration.

2. Bimodal cavity operation: the microwave Hall effect

The theory of operation of the bimodal cavity has been given in great detail by Portis and Teaney (1958). The general formulas given below have been taken from their work. The formulas that apply to our particular case have been taken from the work of Snowden (1960). Minor changes are introduced to agree with my experimental arrangement; e.g. linear detector instead of "square law", and the units.

The bimodal cavity is a TE_{111} cylindrical cavity excited simultaneously in two orthogonal modes which, in the absence of asymmetry,

are degenerate in frequency, coupling and quality factors; i.e., the electric fields are equal. In such a case the microwaves in the cavity are linearly polarized. Figure 5a shows the waveguide and cavity's field distribution.

Due to asymmetry and imperfections, neither of the above conditions is fulfilled in the actual case. The microwaves are elliptically polarized due to differences in the frequencies and phase angle between the two modes. Four metallic plugs, labeled 1, 2, 3, and 4 in Figure 5b, provide a source of external capacitance, which affects the mode frequencies and phase angles. After proper tuning with the capacitive plugs a linearly polarized field may be obtained.

The linearly polarized field may be regarded as the resultant of two components oriented at 90° with respect to each other. They are labeled x and y in Figure 6b. The introduction of a piece of resistive material at position 5, which introduced loss in the mode x, would result in an effective rotation of the plane of polarization of the resultant cavity field. Two resistive plugs at positions 5 and 6 are provided for the purpose of rotating the cavity fields.

The electric field of the input and output waveguides are made to be orthogonal to each other. In Figure 6a, where the cavity fields are polarized in the horizontal direction, if the output waveguide field is in the vertical direction, no microwave radiation should couple through. It is said that the cavity is in its "balanced" condition.

A simple explanation of how the bimodal cavity provides a measurement of the Hall mobility is as follows: A resistive plug #5 is introduced which induces a rotation in the plane of polarization,

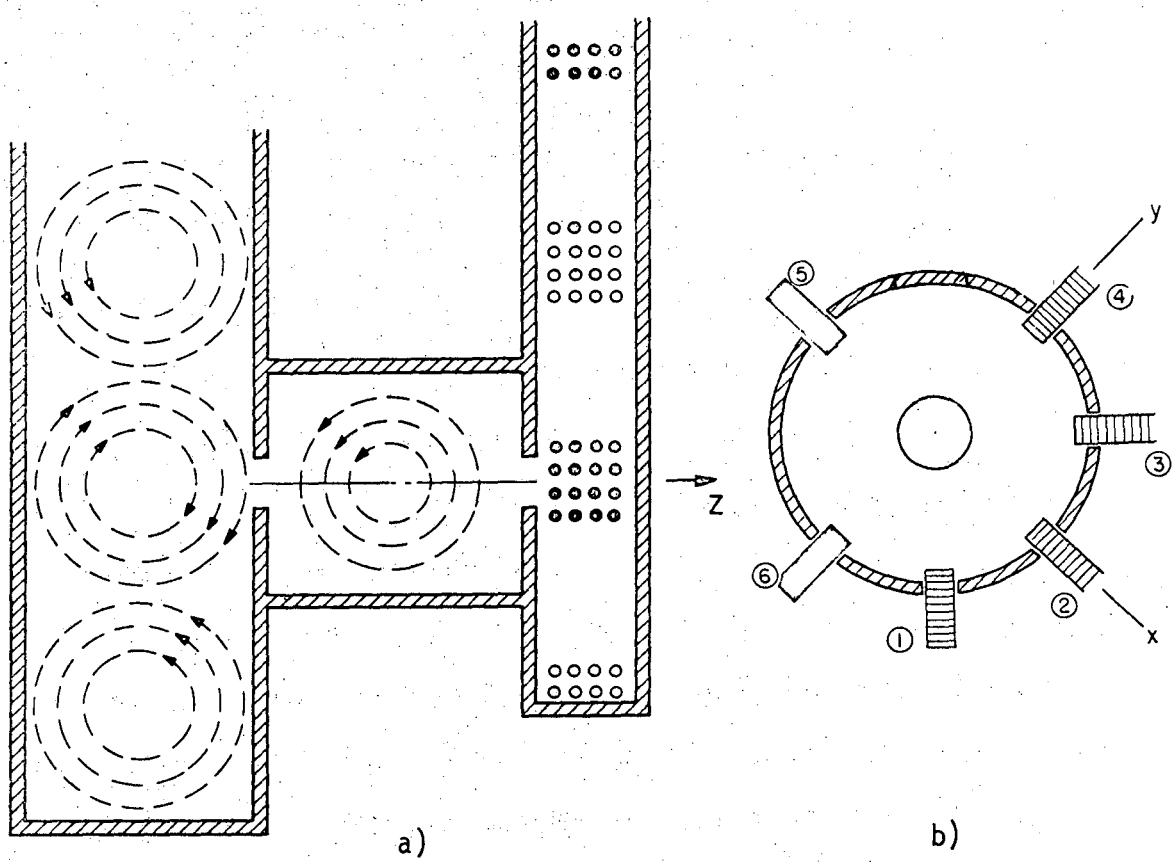

Figure 5. Bimodal cavity TE_{111}.

XBL 723-4582

a) The bimodal cavity is shown in a longitudinal section along the z axis. Power is coupled into the cavity from the narrow face of the waveguide at the left, which is short-circuited 3/4 wavelength from the coupling iris. For simplicity, only the magnetic field lines are shown. Microwave power is coupled out at the broad face of the output waveguide at the right. The dots depict the magnetic field lines, which are perpendicular to the plane of the page and consequently orthogonal with respect to the input waveguide. b) Transverse section showing the four capacitive and two resistive plugs.

Legend to Figure 6. Microwave Hall Effect measurement

a) Transverse section at the center of the TE_{111} cavity showing the balance situation. The radiation is linearly polarized. Only the maximum intensity electric field line is shown for simplicity. The output waveguide only couples through microwave radiation with electric field components in the vertical direction. Therefore, no power is detected at the output waveguide.

b) The horizontal field is decomposed into two orthogonal components, x and y. The arrow shows the effect of the resistive plug #5, which introduces losses in the mode x.

c) The resultant field is effectively rotated. The vertical component produces power coupling into the output waveguide. The cavity is said to be in a resistive unbalance. The fields remain linearly polarized under this type of unbalance.

d) Shows the current, j, induced in a sample by the microwave electric field.

e) A steady magnetic field, H, is applied in the direction perpendicular to the plane of the page. The Lorentz force acts on the moving charges; the currents are forced to oscillate at an angle $\theta = \mu \cdot H$ with respect to the applied electric field, μ is the carrier mobility. The situation is depicted for holes.

f) The result is an additional rotation, which is observed as an increase in coupled power. The effect for electrons would be a rotation towards balance, with a consequent decrease in power coupled through.

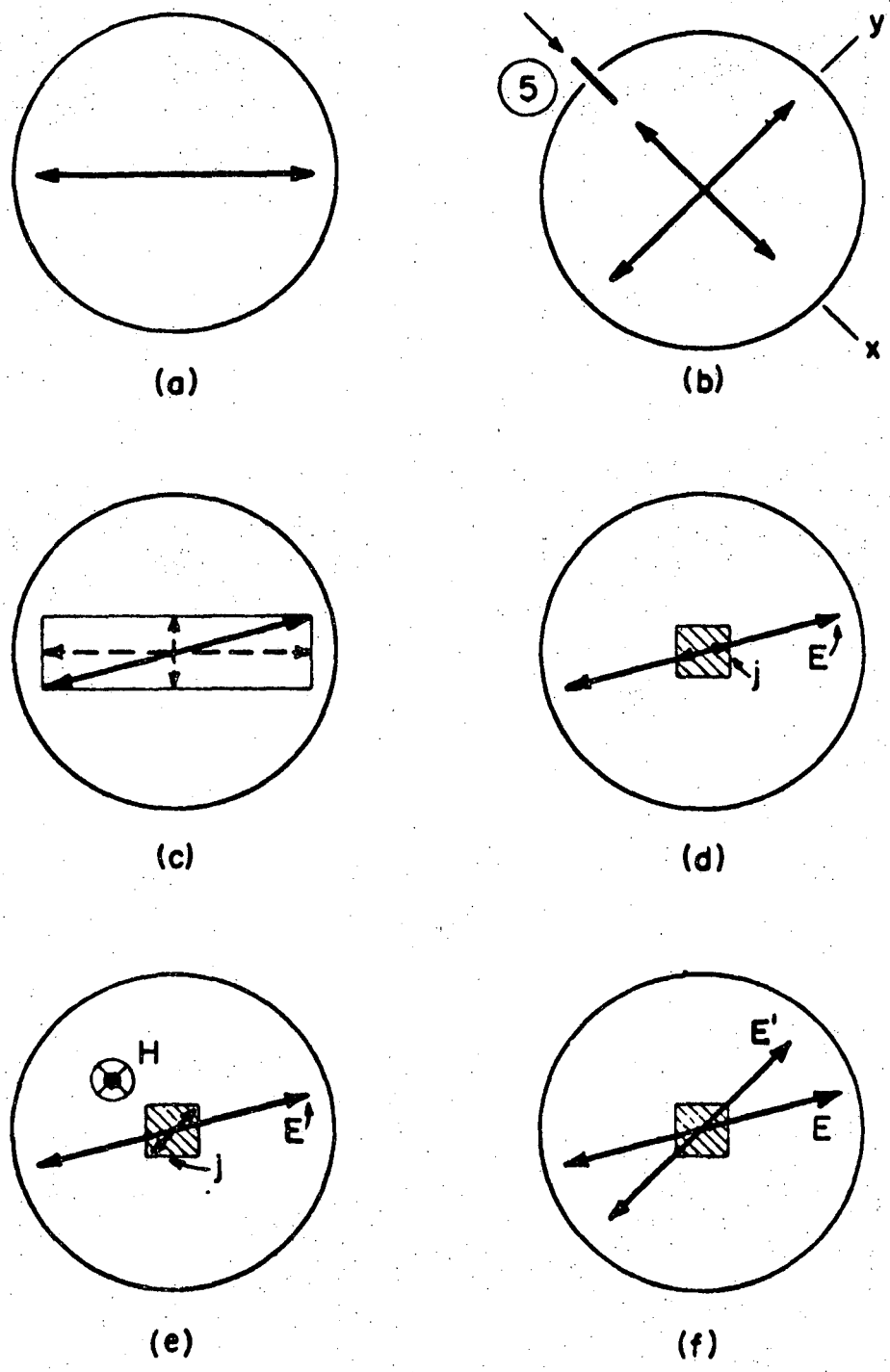

XBL 723-4581

Figure 6

as shown in Figure 6c. This rotation is seen at the output waveguide as an amount of coupled power proportional to the component of the fields in the vertical direction. This coupled power will be labeled P_2 in the formulas. This initial unbalance which results from a rotation of the cavity electric fields is called a resistive unbalance.

A magnetic field is applied in a direction perpendicular to the plane of the page and pointing towards it. If the sample has charge carriers, the magnetic field will act upon the currents produced in the sample by the microwave electric field. The Lorentz force makes the currents oscillate at an angle with respect to the microwave fields. This is a Hall angle $\theta_H = \mu B$ where μ is the mobility and B the magnetic induction. The rotated currents will produce a radiation field in the direction of the current, resulting in a further rotation of the fields in the cavity, when it is added to the applied field. Figure 6d and 6e show this action for holes. A magnetic field in the opposite direction would induce a rotation in the reverse sense. The rotation for holes is seen at the output waveguide as an increase in coupled power, Figure 6f. The reverse field would result in a decrease in coupled power. Knowledge of the initial position of the cavity fields and the direction of the applied magnetic field gives unambiguously the sign of the charge carriers. The fractional change in coupled power is related to the Hall angle and hence to the mobility. It is emphasized that an initial rotation must be introduced in order to determine the sign of the carriers, and that for a pure rotation measurement it is only the "in phase" component of the vertical component of the microwave fields with respect to the applied field that

is measured. The initial rotation introduced by a resistive plug, accomplishes this latter requirement.

The unbalance power is related to the mobility by

$$\frac{\Delta P_2}{P_2} = \frac{2 \operatorname{cosec} 2\theta}{[(1+\beta_1)(1+\beta_2)]^{1/2}} \frac{\Delta Q}{Q} \mu H \qquad (17)$$

where ΔP_2 is the change in coupled power, P_2 is the initial unbalance, H is the applied magnetic field in Tesla (Weber/m^2), μ is the mobility in m^2/volt sec. θ is defined by

$$\frac{P_2}{P_2^{max}} = \sin^2 2\theta \qquad (18)$$

where P_2^{max} is the maximum possible coupled power; it is measured by completely unbalancing the cavity with a metallic plug. In that case the fields in the cavity are circularly polarized; the vertical component being equal to the horizontal, giving the maximum possible coupling. For small coupling, it can be shown that

$$\operatorname{cosec} 2\theta = \left[\frac{P_2^{max}}{P_2}\right]^{1/2} . \qquad (19)$$

The effect of a sample on the cavity has been studied by Teaney and Portis from the point of view of the equivalent circuit of lumped elements. Thus the sample is characterized by a complex impedance that in the general case is a tensor quantity. The resistive unbalance for such a situation gives for the fractional change in coupled power (very small coupling):

$$\frac{\Delta P_2}{P_2} = \frac{2 \operatorname{cosec} 2\theta}{[(1+\beta_1)(1+\beta_2)]^{1/2}} \left[\frac{r_{xx}-r_{yy}}{R} + \frac{r_{xy}-r_{yx}}{R}\right] - \left(\frac{1}{1+\beta_1} + \frac{1}{1+\beta_2}\right) \frac{r_{xx}+r_{yy}}{R} -$$

$$- \left(\frac{1}{1+\beta_1} - \frac{1}{1+\beta_2} \right) \frac{r_{xy} + r_{yx}}{R} \qquad (20)$$

The first term is a rotation term that has two components, the first due to sample anisotropy and the second due to the off-diagonal elements of the impedance tensor. The second term is a measurement of the decrease in cavity excitation due to the finite resistivity of the sample. The third has the same meaning but for the off-diagonal elements of the resistivity. In the absence of a magnetic field and for an isotropic sample the first term is zero. Where light is introduced a power unbalance proportional to the photoconductivity of the sample is detected. If the sample is not isotropic or the illumination is not perfectly homogeneous, a spurious rotation due to the first term would also contribute to the signal.

When a magnetic field is applied, it is only the difference between the off-diagonal components of the impedance tensor that is responsible for any excess unbalance. The second term would not be affected by the magnetic field unless an effect such as magnetoconductivity is considered.

Since $\frac{r_{xx}}{R} = \frac{\Delta Q}{Q}$, and $\frac{r_{xy}}{R}$ is given directly by the unbalance due to the magnetic field in Eq. (20), the Hall angle $\theta = \mu B$ is given by the ratio:

$$\mu B = \frac{r_{xy}/R}{r_{xx}/R} = \frac{\Delta P_2/P_2}{\Delta Q/Q} \left[\frac{2 \operatorname{cosec} 2\theta}{[(1+\beta_1)(1+\beta_2)]^{1/2}} \right]^{-1} \qquad (21)$$

after rearrangement of the expression above. It is clear from these considerations that the excess unbalance introduced by the magnetic field with no illumination gives the mobility and sign of the dark

charge carriers. The sign and mobility of the photocarriers is obtained from the excess unbalance introduced by the magnetic field which will be added to or subtracted from the normal photoconductivity signal which is present simultaneously. This is accomplished without complications when a lock-in technique is used. A signal produced by light modulation is synchronously detected; then a magnetic field is applied in both directions. The excess signal determines only the contribution to the rotation due to the photocarriers, since only the modulated component of the rotation signal is measured by the lock-in amplifier. Some of my measurements were done in this fashion. Only an average value for the mobility is provided by this method. If there are equal numbers of charge carriers with different mobilities, this measurement provides a value equal to the difference in mobility. The situation becomes more complicated when there are charge carriers in different concentrations, having different lifetimes. Pulse techniques provide in this case a deeper insight into the problem. The time evolution of the photoconductivity and rotation signals might resolve the several components.

B. Instrumental

1. Microwave Instrument

Basically the measurement of the photoconductivity and the Hall effect consist of measurements of changes in microwave power intensity. A simple microwave detector diode at the output of the bimodal cavity, or at the reflected-power arm of a directional coupler, as shown in Figure 4 for the TE_{011} cavity, would provide such a measurement.

Such was actually the arrangement that I used in most of the preliminary measurements.

The simple system has many limitations and as it is customary in the field of microwave measurements in cavities, I built a microwave bridge.

The full description and analysis of the bridge is given by Teaney, Klein and Portis (1961). Very few modifications were introduced to the original system. They included the replacement of a magic tee by a microwave ferrite circulator, the use of Gunn diode oscillators for some measurements instead of klystrons as local oscillators, and the automatic frequency lock between the main and local oscillators.

A brief description follows: Microwave power was generated by an ultrastable X-band oscillator (Laboratory for Electronics, 814.A, Boston, Mass.). The power reflected by the TE_{011} cylindrical cavity was sent, via a ferrite circulator, to a superheterodyne receiver. The frequency of the oscillator was automatically adjusted to the cavity frequency by a conventional servo-mechanism. A fraction of the power provided by the main oxcillator was directed to a bucking arm, which was also used as a reference for relative power measurements. The local oscillator was a Gunn diode (Intradyne OD 45 WV, Palo Alto, Ca.), which was automatically tuned 60 MHz above the main oscillator by a servo-mechanism. The receiver used a LEL (Varian, N. Y.) balanced 60 MHz mixer-preamplifier. The resultant 60 MHz signal was sent to a dual phase-sensitive detector. A fraction of the microwave power provided by the oscillator was directed to a second LEL balanced

mixer in order to obtain a coherent reference voltage for the 60 MHz phase sensitive detector. The phase of the reference voltage was adjusted by a microwave phase shifter at the main oscillator input to the second mixer.

The superheterodyne receiver was designed and built in collaboration with M. P. Klein and Branko Leskovar, and is given in the Lawrence Berkeley Laboratory schematics 10X- 1540 P-I, 1550 P-I and 1721 P-I. The Gunn oscillator automatic frequency lock is described in the Lawrence Berkeley Laboratory schematics 10X- 1651 P-I.

The coupling coefficients were obtained by measurements of the reflection coefficient. A reflectometer arrangement is provided in the cavity arm of the circulator. The 100% reflection is calibrated by replacing the cavity by a short. A Hewlett-Packard 16A Ratiometer instrument provided readings of percent reflection which were converted to coupling coefficient values by computation. Provision was also made for frequency markers for the measurements of the cavity Q. The local oscillator was frequency modulated and some of its power, taken via a 20 dB doupler, was introduced through another 20 dB coupler located immediately after the output of the main oscillator. When the frequency of the local oscillator coincided with that of the main oscillator, the beat frequency signal appeared in the scope as a small pip; signals above and below that are spaced at the modulation frequency and provide the necessary calibration (details are given by Snowden, 1959). The main oscillator was frequency swept by the sawtooth of the scope. The cavity absorption signal was observed in the reflected power detector of the reflectometer. Measurement of

the width at half power provided the values for the loaded Q's. The measurements of Q performed in that way were reproducible to about 20%. Figure 7a shows a typical cavity absorption trace. To increase the accuracy of these measurements it is rather simple to obtain the derivative of the absorption signal from this arrangement, and the peaks on the derivative give the frequency positions with more precision. For a perfectly Lorenzian line shape the width at half power is related to the separation of the peaks in the derivative by

$$\Delta\nu_{1/2} = \sqrt{3}\,\Delta\nu(\text{inflection})$$

The Gunn oscillator was frequency modulated to a depth of about 1/4 of the cavity's width at half power, the voltage for the modulation being provided by the reference of a PAR JB-6 (Princeton Applied Research, Princeton, New Jersey) lock-in amplifier. A slow sawtooth, 10^{-2} Hz, was superimposed on the small modulation. The reflected power from the cavity was sampled as before and sent to the lock-in signal channel. As the Gunn oscillator was swept slowly through the cavity, the lock-in output was sent to a recorder and provided the derivative of the cavity absorption. The calibrating pips, this time obtained by modulation of the main kystron, appeared also at the output of the lock-in amplifier giving the needed calibration. With this technique an accuracy of a few percent was obtained. A typical trace is shown in Figure 7b.

The bucking and measuring arm was provided with a microwave PIN diode switch that has a response time of 10^{-8} sec. This device was used as a source of microwave modulation when the lock-in technique was used for light-induced effects, such as photo-losses or photo hall

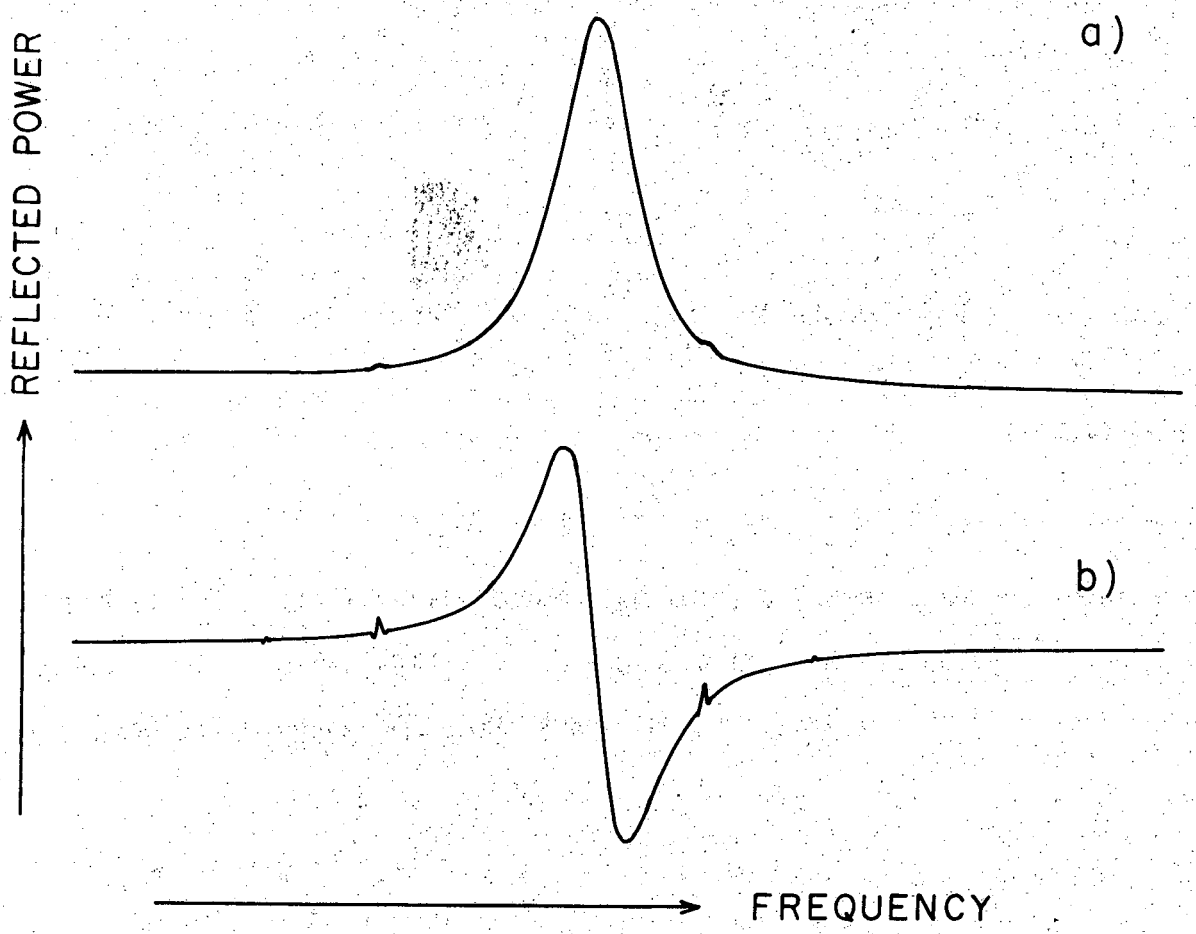

Figure 7. a) Typical cavity absorption trace as seen at the ratiometer output. b) The derivative as obtained at the lock-in output. The calibration beeps are 4 MHz apart in this example.

mobilities. In such cases the microwaves in the branch circuit were 100% modulated by the PIN diode by the same pulse generator that drives the light chopper. The phase of this signal was turned 180 degrees with respect to the signal coming from the cavity, so that it was possible to balance the lock-in amplifier reading to zero. This method provides a direct reading on the calibrated attenuator of P reflected. A second PIN diode was located in the reflected power arm from the cavity. In some cases a "Replacement method" was used to measure the modulation depth introduced by the sample absorption. That was the case in measurements of Hall mobilities where small changes in coupled power are to be measured. Since the parameter in that measurement is the modulation depth, $\Delta P_2/P_2$, this was a very convenient procedure. Figure 8 shows the typical arrangement for the reflection cavity. The transmission bimodal cavity was coupled to the system by removing the circulator, as shown in Figure 8b.

A signal averaging computer replaced the lock-in amplifier in many measurements. The instrument was a Northern Scientific, Madison, Wisconsin.

2. Magnetic Field

A 12-inch magnet with a gap of about 2 inches was powered by a modified Varian V 2100 power supply provided with a polarity reversing switch. Magnetic field intensities were determined with a Bell-240 Incremental Gaussmeter. The calibration values on the Hall probe were taken as correct. The magnetic field was swept by a Hewlett-Packard low frequency function generator. The field could be swept in intervals of about 2.5 kgauss. The maximum field available was 11 kgauss.

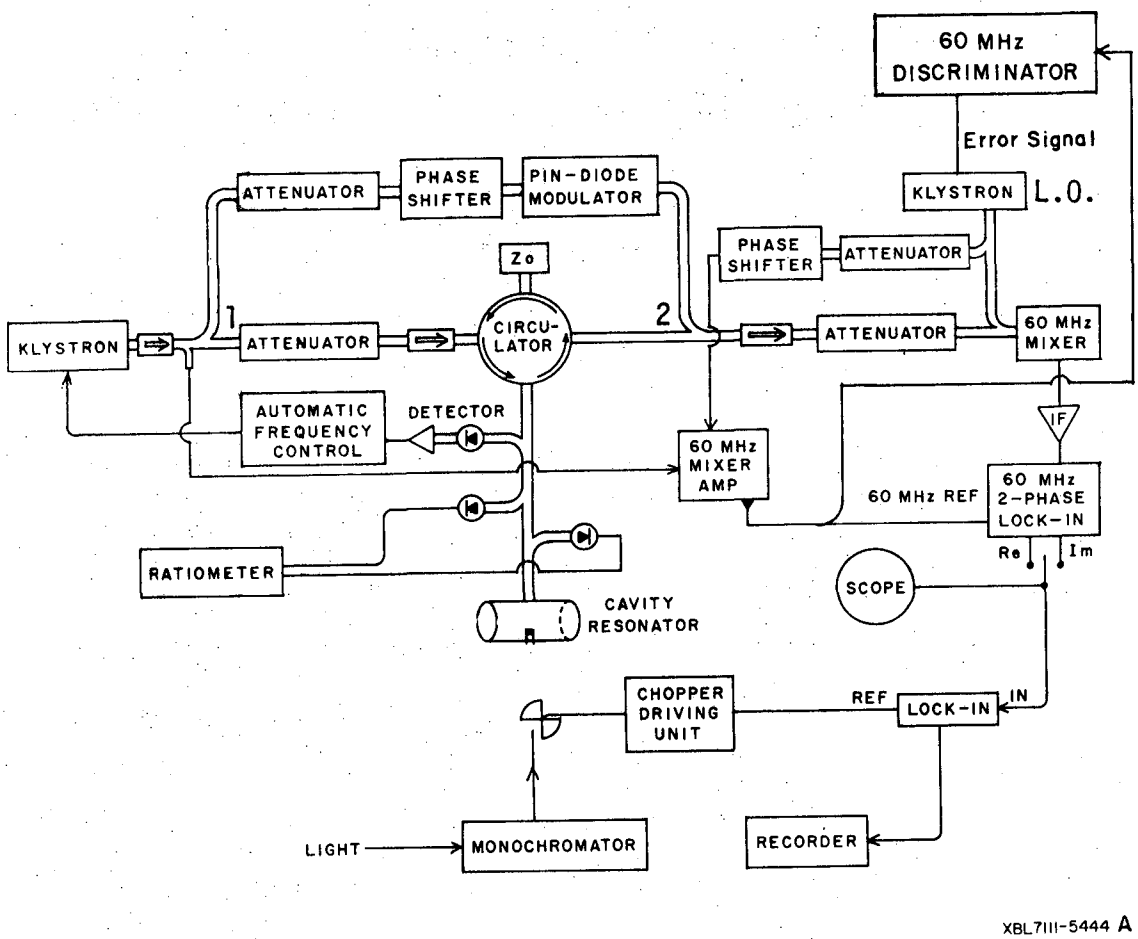

Figure 8a. Microwave instrument. The description is given in the text. The klystron-labeled L.O. (local oscillator) was replaced by a Gunn oscillator for the microwave Hall effect measurements. Modification of the system at points marked 1 and 2, was required for the attachment of the bimodal (transmission) cavity, shown in Figure 8b.

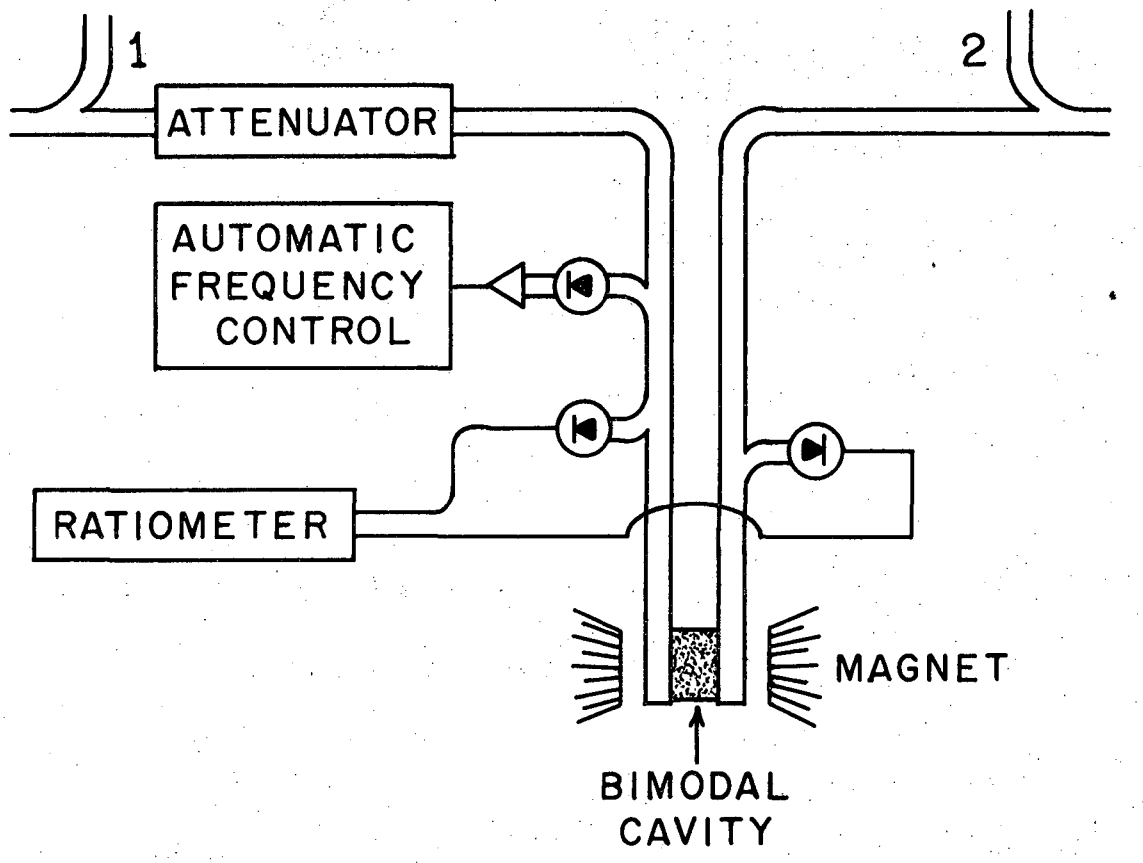

XBL7111-5444B

Figure 8b. Modified arrangement to insert the bimodal cavity. Points marked 1 and 2 correspond to those in Figure 8a.

3. Light Sources

Pulsed light is introduced into the cavity by a quartz light-pipe. The light source was a 650 watt Tungsten-iodine lamp with a filament temperature of 3.400°K (General Electric, Cleveland, Ohio) chopped by a stepping motor (Model 55-100, Cedar Engineering, Minneapolis, Minn.). The motor was driven by a Tektronix 160 pulse generator unit. Light pulses varying from 6 to 100 msec in width were obtained in this way. The rise time for the 6 msec flashes was about one msec. The delay between pulses had a minimum value of 10 msec and could be extended to several seconds. Shorter pulses (0.7 - 2 msec) were obtained by using a rotating disc chopper. The fastest flashes were provided by a 50 joule Xe flash unit (I.L.C., Sunnyvale, California) that delivers 5 joules of white light (between 400 and 700 nm) per flash. The duration of each flash is about 20 μsec at 1/3 of the peak power, and the interval between flashes can vary from 200 μsec to several seconds. Since not more than 10% of the total available light was collected, an upper limit of 0.5 joule per flash was available. Measurements of light energy at the sample site gave 0.1 joule/flash as an upper limit due to losses in the light pipe, reflections, etc.

Monochromatic light was obtained by means of interference filters that gave a rather poor resolution ($\pm$ 20 nm) but enough light to make the measurements possible. The infrared radiation was filtered by 5 cm of H_2O plus a Corning 1-59 glass filter.

A Baush and Lomb grating monochromator with automatic scanning with a 900 watt Xenon lamp (Osram, West Germany) provided about 10^{15}

photons/cm^2 sec with a bandwidth of 5 nm. Some measurements of the action spectra in pigment samples, as well as measurements described in Chapter III, were performed with automatic scanning of the light wavelength. The intensity provided by this source was not sufficient for measurements in most biological samples.

A passively Q switched ruby laser was used for the rise time and saturation experiments. A solution of a dye was used for Q switching, giving at best a pair of 30 msec pulses spaced over several microseconds. The estimated intensity of the unattenuated beam was about 2/3 Joule/flash at 694 nm.

One msec flashes were provided by a camera strobe (Cornet 100, R. Bosch Inc., West Germany). About 2×10^{-2} Joules/flash of white light were available at the strobe output. Collection of the light was not very efficient due to the small area of the light-pipe used to introduce illumination into the cavity. I estimate that only 10% was collected at the light-pipe input. Infrared was filtered with a Corning 1-59 glass filter and monochromatic light obtained with interference filters. Measurements with a silicon photocell (S1020 International Rectifier, El Segundo, Ca.) in place of the sample indicated a total energy over the 1 msec flash of about 10^{-3} Joules of white light. The measurement of the light intensity for the flash sources is rather difficult to perform since the voltage output of the photocell gives values proportional to the light power input. Therefore, time integration of the scope traces were necessary to obtain the total energy in the light flash. Nevertheless, the values are correct to a factor of about 2 or 3. Since no conclusions will be introduced needing more precision, the values given are sufficiently accurate.

4. Sample Holders

The samples were located in place by means of a styrofoam support which at the same time was part of the temperature regulation system. The styrofoam contained channels for the flow of nitrogen. The temperature of the gas was regulated by servomechanism. To measure the temperature I located a Cu-constantan thermocouple at the flow output as it cannot be located inside of the cavity for technical reasons. The maximum temperature difference between the sample site and the monitoring position was measured and never exceeded 2°C (Figure 9).

A sample of polycrystalline CdS was at all times contained in the cavity and could be illuminated alternatively to the experimental sample, thus providing a reference signal originating in the same cavity. If I express the results relative to this signal, namely

$$\frac{(\Delta\,\sigma/\sigma)_{\text{sample}}}{(\Delta\,\sigma/\sigma)_{\text{CdS}}} = \left(\frac{\Delta\sigma}{\sigma}\right)_{\text{relative}}$$

a complete independence with respect to variations in the instrumental constants is obtained. This procedure was very useful in the temperature measurements to avoid errors due to changes in the cavity Q resulting from changes in the temperature of the walls or accidental accumulation of condensed H_2O.

A variety of biological specimens were tested. They included whole leaves, chloroplasts and subchloroplast fractions, photosynthetic bacteria and the chromatophore fraction isolated from them.

The samples were mounted between microscope cover glasses and sealed with parafin, as shown in the following side view:

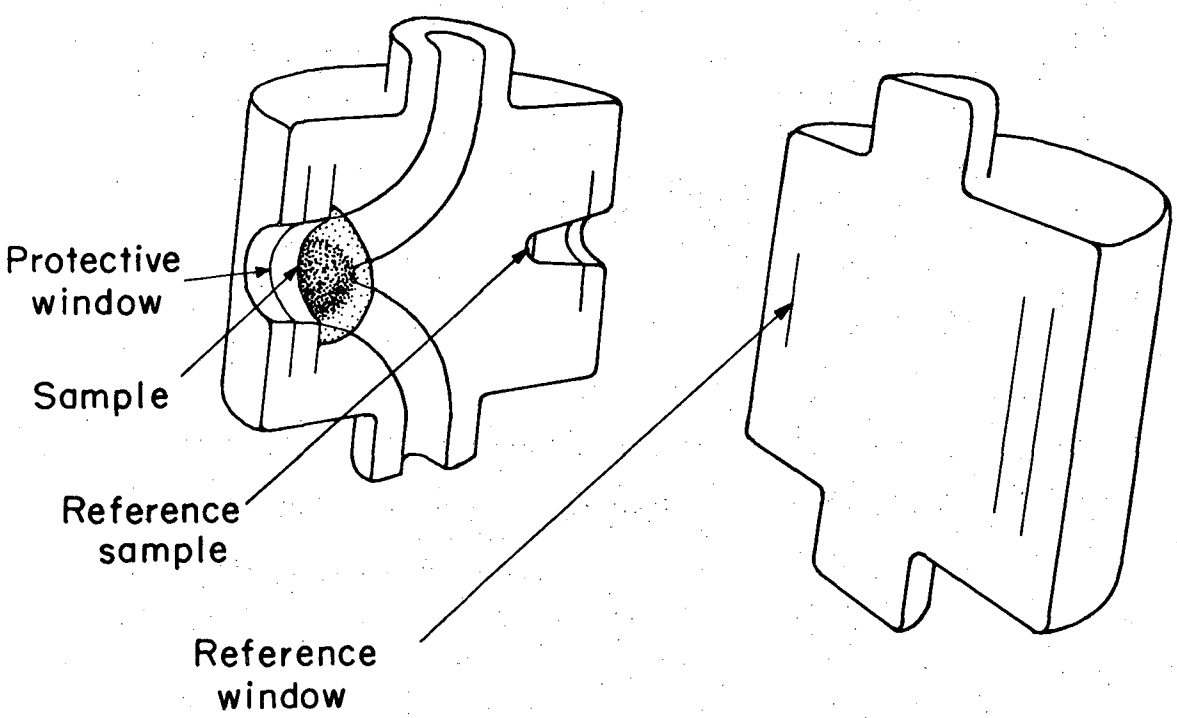

Figure 9. The two halves of the styrofoam support are shown separately. The protective window was a piece of quartz coverglass and it is not in place in the diagram for simplicity.

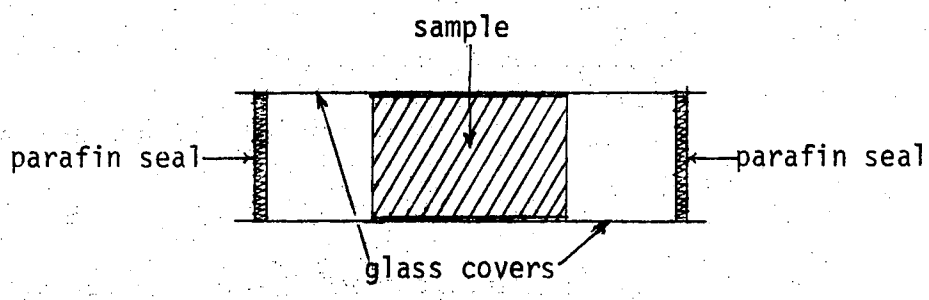

In this way the shape of the specimen was that of a very thin disc. Polycrystalline material was simply mounted between the cover glasses to obtain a layer as thin as possible. In every case the samples were opaque to visible light. Leaf samples were cut to a 2 mm by 2 mm size and mounted between the cover glasses in a similar way.

C. Estimation of Experimental Error

1. Dark conductivity Measurements

The main instrumental source of error in these measurements are the values of the width at half power in the cavity resonance plot. The beat oscillator calibration, although very precise, is not the limiting factor. The width of the pips and the relative instabilities of the swept klystron introduced a large dispersion in the values obtained after successive measurements. A reproducibility of about 30% is a reasonable estimate. Positioning the sample several times to test the extent of this source of random error showed that it was possible to reproduce values better than the error in the Q measurements when the styrofoam holder was used. The presentation of the derivative of the cavity absorption curve permitted a reduction of the uncertainty in Q to 3-4%.

The uncertainty in the values for the filling factor could make all my measurements in error by at most a factor of 1.5 when the TE_{011} cavity was used. This systematic error would apply to almost all my samples. Calibration of the filling factor was made by measuring the same sample in the TE_{111} cavity for which the filling factor for a flat disc-shaped sample is well known. The limiting factor in the measurements is the volume of the sample, which enters the calculation of the filling factor. The uncertainty in the sample volume is almost 100%.

2. Light-induced Measurements

Measurements were mostly performed using computer averaging techniques or lock-in detection. In both the averager and lock-in systems the main contribution to the noise was the low frequency microphonics. Unfortunately, in these measurements the time constants involved were of the order of 1 Hz. Detection at such low frequencies is very unfavorable for noise elimination. If a large number of scans were possible in the averager or a large time constant in the lock-in, this source of noise could be overcome. The other sources of noise, such as frequency instability of the oscillator or the typical 1/f noise, were much smaller than the microphonics. It is interesting to note that the part of the microphonic noise introduced by changes in the resonance frequency of the cavity due to strain or other mechanical factors is largely suppressed by the automatic frequency control system. Therefore, the error is estimated in all measurements for the particular cases and indicated in the form of vertical lines in the plots, or as the last significant figure expressed in the values quoted.

3. Light Intensities

The light intensities were measured with a silicon photocell (S1020, by International Rectifier Co., El Segundo, Ca.) located at the sample position. It was previously calibrated against a thermopile over the whole spectrum. It was also calibrated for the three typical sources of white light used: a 3,400 K source (quartz iodine tungsten source), a 2,800 K (tungsten filament lamp) and a Xenon arc. In these cases the energy of white incident light will be expressed in watts/cm^2. When monochromatic light was obtained with interference filters, the light intensities were expressed in photons/$cm^2 \cdot$sec. The energy of the photon at the center of the bandwidth was used for the calculations. In all these situations in which a continuous source was used, the error in the light intensities is never larger than 10-20%. Since light pulses were obtained by chopping these sources, the calculated energy per pulse has the same limits of error. Light intensities were varied by means of Kodak neutral density filters previously calibrated in a Cary 14 Spectrophotometer.

When fast flashes from Xenon flash lamps or laser source was used, the situation was worse. Saturation of the light detectors was encountered very often. The extremely large peak powers developed by these sources were attenuated to reasonable values for the detectors by means of neutral density filters previously calibrated. I estimate that the actual values for the light intensities of the Xenon flash are within about $\pm$ 50% of the values reported. For the laser the values could be off by a factor of 3 or 4. Due to this uncertainty, values from the laser experiments are used only for order of magnitude calculations.

4. Biological Limitations

Biological systems are characterized by very large random variations. In these experiments I found no exception to the rule. Conductivities varied by factors as large as 4 or 5 in samples of the same batch. The same comment applies to photoconductivities. By contrast, the values of kinetic parameters and thermal activation energies were quite reproducible in different samples. Dispersion in the values of activation energies was about 20%.

5. Instrumental Limitations

The noise power, P_n, is contributed mainly by crystal detector noise and frequency microphonics from the microwave generator. The latter is more relevant when the circulator bridge is used, as the frequency dependence of bridge unbalance is the limiting factor. When the bimodal cavity replaces the bridge, the large isolation that may be achieved and the fact that balance is essentially frequency-independent, the noise power is reduced to the detector quality.

The sensitivity of the instrument used in my measurements has been studied in detail by Teaney, Klein and Portis (1961), and estimation of the sensitivity limit for the bridge, assuming a bandwidth equal to the high frequency limit of 1 KHz (equal value), gives for $P_s/P_n = 1$, where P_s is the power in the signal, a limit of 10^{-5} for $\Delta P_2/P_2$. By means of averaging techniques it is possible to improve that value as $\sqrt{n}$, where n is the number of passes added in the computer averager. The lock-in arrangement greatly increases the sensitivity by reducing the bandwidth. That was the reason to use

it for measurements of action spectra, where there was no need for time resolution.

The bimodal cavity with the superheterodyne detector at values of isolation (P_2^{max}/P_2) of 80 dB gives a lower measurable limit of 10^{-2} cm^2/volt sec for the mobility at a field of 10^4 gauss.

It is of interest to know the ultimate limit of sensitivity that could be achieved if the noise power were reduced to zero (e.g. by infinite time averaging). The sensitivity of the superheterodyne detector is about 10^{-16} watts and, since it is a linear detector, $\frac{\Delta Q}{Q} = [\frac{\Delta P}{R}]^{1/2}$ (Feher, 1957). At an incident power of 0.1 watt, this gives $\Delta Q/Q = 10^{-8}$ as a lower limit.

The time resolution is limited by the intermediate frequency amplifier bandwidth to 5×10^{-7} sec. In measurements when the automatic frequency control is required, the time resolution is given by the stabilizer modulation frequency. In my case it was 60 KHz, giving 10^{-4} sec as a lower limit.

D. Materials

1. Chemicals

Chlorophyll a: Chromatographically purified chlorophyll was kindly provided to me by Dr. A. Schultz*(Sauer et al., 1966).

Bacteriochlorophyll: Obtained from Dr. A. Schultz.*

Chromatographically purified methyl chlorophyllide was obtained from Dr. H. Tributsch (Tributsch, 1969).

*The pigments were purified in 1966, and kept in a desiccator in the dark. I used them without further treatment during 1969.

Eosine (Y) and β-carotene (all trans) from J. T. Baker, New Jersey. Rhodamine b was obtained from Matheson, Coleman & Bell, New Jersey. Bovine serum albumin was obtained from Armour Pharmaceutical Co., Chicago, Ill. All the above compounds were used without further purification for the microwave measurements.

Polycrystalline CdS, reagent grade, was from Baker & Adamson, New York; PbS Reagent, Baker & Adamson, New York; Cu_2O, reagent grade, from Allied Chem., New York. Single crystals of undoped ZnO were obtained as a gift from Dr. G. Heiland, Technische Universitaet Aachen, Germany.

2. Biological Material

Bacteria: Rhodopseudomonas spheroides

Four different strains of this bacteria were used in these measurements. The normal wild type purple strain, a green mutant lacking some carotenoid pigments (Cohen-Bazire, Sistrom and Stanier, 1957; Griffiths and Stanier, 1956), its carotenoidless blue green mutant R-26 (Crouse, Feldman, and Clayton, 1963), and its non-photosynthetic mutant PM-8 (Sistrom and Clayton, 1964).

Wild type R. spheroides was grown in a modified Hutner's medium (Cohen, Sistrom, and Stanier, 1957) and harvested at the end of the exponential growth phase. Strain R-26 was grown according to the method of Sistrom and Clayton (1964) in a yeast extract medium (Cohen et al., 1957). Strain G.A. and its non-photosynthetic mutant were grown following Sistrom (1960).

The preparation procedure to obtain chromatophores was standard for all mutants as follows: The bacteria were harvested by centrifugation and washed twice with 0.1 M Tris-HCl buffer, pH 7.8. For

large volume cultures the harvesting was performed in a continuous flow Sharples centrifuge. For small volumes a Sorval RB-2 centrifuge was used. After harvesting, the cells were either stored at 0°C and used for measurements or further processed to obtain chromatophores.

All operations from this point were performed at temperatures close to 0°C. The tris-washed cells were resuspended in about five times their wet volume of 0.05 M Tris-HCl buffer, pH 7.8, which was the buffer used for the rest of the procedure. The suspension was either passed twice through an Aminco-Franch pressure cell at 20,000 psi or sonicated at 20 KHz for 5 minutes at a nominal power of 70 Watts in a sonicator (Ultrasonics, Inc., Model W185, Plainview, New Jersey). The resulting suspension was centrifuged at 20,000 x g for 30 minutes to remove cell debris. The supernatant was resuspended in buffer and centrifuged in a Spinco L2 centrifuge in a type 50.1 rotor at 144,000 x g for 90 minutes. This last centrifugation was repeated twice. The resulting pellet was either removed with a spatula and mounted in the usual way between cover glasses for measurements in the wet state, or resuspended in buffer. If the suspension was not optically clear, the material was sonicated under the same conditions as above and centrifuged at 20,000 x g. The clean supernatant was used for testing absorption spectra, photoinduced EPR measurements and photoinduced absorption changes needed for a complete characterization of the material. Drops of the solution were deposited on the cover glasses and allowed to evaporate under a flow of dry nitrogen gas. This procedure yielded optically clean films. In order to increase the amount of sample,

the operation was repeated up to ten times, such that a stack of layers was deposited.

Two alternative methods were used in order to obtain lyophilized samples. The solution was directly lyophilized and the resultant material mounted between cover glasses under a dry nitrogen gas atmosphere and sealed with parafin; or the chromatophore pellet was taken with a spatula, mounted in the cover glass and then lyophilized and sealed with parafin.

Bacteriochlorophyll content was determined from the clear solution absorbance. An extinction coefficient ε = 127 mM^{-1} cm^{-1} was used (Clayton, 1966).

3. Preparation of Chloroplasts

Spinach (Spinacia oleracea, var. early hybrid No. 7) was grown in vermiculite in a growth chamber under controlled conditions similar to those of Sauer and Park (1965); light intensity was approximately 3200 f-c in 10 hr light/14 hr dark cycles, temperature 18°C, leaves harvested six to eight weeks after germination. The leaves, rinsed with cold distilled water and ribs removed, were then stored at -20°C for 10 min. Ten g of leaves was homogenized 10 to 15 sec in 50 ml of 0.5 M sucrose, 0.1 M tricine pH 7.6 buffer in a Waring blendor at 0°C. The resultant homogenate was strained through 8 layers of cheese-cloth, centrifuged at 100 g for 10 min and the precipitate was resuspended in 1 ml of 0.5 M sucrose, 0.05 M tricine, pH 7.6, and stored at 0°C.

4. Subchloroplast Fractions

Subchloroplast fractions were isolated by the method of Park and Pon (1961). The 600 x g fraction was used as chloroplasts in the early experiments. The Jensen and Bassham (1966) method was used later for intact chloroplasts. No difference was observed between intact and broken chloroplasts in the microwave measurements. Therefore broken preparations were used most of the time. The typical total amount of chlorophyll in the chloroplast sample was 0.02 mg/sample. The typical amount of chlorophyll contained in the leaf samples was about 0.08 mg, measured as described by Vernon (1960). The subchloroplast specimen was the 145,000 x g fraction from Park and Pon, and will be referred to as lamellar fragments or quantasome aggregates in the experiments.

III. MEASUREMENTS IN STANDARD SAMPLES, SOME PIGMENTS AND PROTEIN PIGMENT MIXTURES

A. Inorganic Semiconductors

I performed some measurements on samples for which microwave parameters are available in the literature. The results on such standards are summarized in Table I-A.

For some of the samples, the observation of pulsed photoconductivity was performed here for the first time, as in the cases of CdS and ZnO single crystals. Data on PbS was available from Snowden (1959). Dark mobilities for polycrystalline ZnO and Cu_2O are reported by Eley (1970) as 90 $\pm$ 15% cm^2/volt sec and 54 $\pm$ 15% cm^2/volt sec respectively. Trukhan (1965), reported 110 $\pm$ 40 cm^2/volt sec for a polycrystalline sample of ZnO, and that was probably the first time a microwave Hall effect was observed in such a sample.

Portis (1958) reported values of +10 cm^2 volt sec for the mobilities for Cu_2O in polycrystalline form at room temperature. The same author obtained values around 200 cm^2 volt sec for the photomobility of polycrystalline CdS.

The agreement of my data with such measurements is satisfactory considering the variability in composition of polycrystalline samples.

Table I-A. Standards

Sample	σ_{dark}	Excitation λ	$\frac{\Delta\sigma}{\sigma}$ (4)	μ_{dark} (1)	μ_{light} (2)
	Ω^{-1} cm^{-1}	nm		cm^2/volt sec	cm^2/volt sec
CdS polycrystalline	10^{-3}	500	10^{-1} - 10^{-2}	-250 ± 20%	-200 ± 50%
ZnO single crystal undoped	10^{-3}	380	5×10^{-3}	-90 ± 20%	-80 ± 15%
Cu_2O polycrystalline	10^{-4}	550	8×10^{-5}	+20 ± 40%	---
PbS polycrystalline	10^{-5}	700 - 900	10^{-2}	+17 ± 40%	+50 ± 50%
ZnO polycrystalline	10^{-2} - 10^{-3}	380	10^{-3}	-85 ± 50%	+50 ± 50% -80 ± 50% (3)

(1) and (2): The dispersion in the values is due to variability among several samples. The reported value is an average over several samples. (3) Some ZnO polycrystalline samples yielded positive photomobilities and some negative ones within the reported range. (4) Standardized to an incident light intensity of 10^{-3} watts/cm^2.

B. Measurements on Pigments and Some Pigment Protein Mixtures

In order to establish whether there is any similarity in the photoconducting behavior of living systems with their constituent pigments in the crystalline state, I tested samples of chlorophyll a (kindly provided to me by Dr. A. Schultz), methyl chlorophyllide a, and β-carotene. I also tested some known sensitizer pigments such as rhodamine B and eosine.

An easily available protein, bovine serum albumin, which is used as a protein standard in 1% solution (by weight), was mixed with equal amounts of 1% solution in acetone pigment and allowed to evaporate in the standard sample holders. At the same time, samples of pure pigment and pure protein were prepared in the same way. The results are summarized in Table I-B.

C. Benzene Solution

When chlorophyll crystals were introduced in benzene, the absorption spectrum showed main absorption peaks at 678-685 nm and 740 nm, the latter being the largest in intensity. With a 1 msec flash, a signal was obtained that followed the flash in its rise, decayed in 30 msec to about one half the initial value, and took one to two seconds to decay completely. Upon heating the solution to 60°C, the 740 nm peak practically disappeared, and almost no effect was detected but for a slowly rising and decaying signal much smaller than before. The remaining absorption was at around 670 nm.

Table I-B. Photoconductivity of Pigments and Pigment-Protein Mixtures

Sample	σ_{dark}	Light source*	$\Delta\sigma/\sigma$	Rise Time	Decay Time				Observations
					Fast		Slow		
	$ohm^{-1}cm^{-1}$	1) 20 μs xenon flash 2) 1 msec xenon flash	Fraction of dark conductivity	sec	$\tau_{1/2}$ sec	% of signal	$\tau_{1/2}$ sec	% of signal	
Chlorophyll a	$2x10^{-5}$	(1)	10^{-4}	Follows flash rise time	$300x10^{-6}$	70	Total decay in 10^{-2} sec	30	Maximum effect at wavelengths longer than 700 nm
β-Carotene	10^{-5}	(1)	$5x10^{-5}$	Follows flash shape	follows flash	100	---		
Eosine	10^{-5}	(1)	10^{-6}	10^{-2}	---	---	5	100	
Bovin Serum albumin (BSA)	$1.5x10^{-4}$	---	---	---	---	---	---	---	Showed no photosignal to visible light, but a small visible light was observed when 1-58 Corning glass IR absorbing filter was removed.
Eosine-BSA (mix)	10^{-4}	(2)	10^{-3}	Follows flash	10^{-2}	70	$5x10^{-1}$	30	
Me Chlorophyllide BSA (mix)	$5x10^{-5}$	(2)	10^{-4}	Follows flash	$4x10^{-3}$	25	$3x10^{-1}$	75	
Rhodamine B-BSA (mix)	10^{-4}	(2)	10^{-3}	Follows flash	$4x10^{-3}$	75	1	25	
Chlorophyll a-BSA (mix)	10^{-4}	(2)	$5x10^{-3}$	Follows flash	$20x10^{-3}$	30	0.5-2	70	

*5 millijoules per flash of white light; an infrared absorbing 1-58 Corning glass filter was always located in front of the light pipe.

An ethanol solution gave the same slow effect, but upon addition of water to about 50% the 740 nm absorption peak reappeared, and with it the signal that followed the rise of the flash; in this case about one fourth decayed in 30 msec and the rest was almost stabilized, and took almost a minute to decay.

It seems that the presence of microcrystalline or highly aggregated forms are responsible for these observations. The presence of water seems to stabilize the signal. It is interesting to note that similar experiments performed by Douglas and Albrecht (1972), in which currents were measured across electrodes located in the solution, gave similar results - with the difference that a very fast decay in the microsec range followed by a msec component was observed. In our case the fast component could not be seen due to the flash duration and its decay tail, which is of the order of a msec. Douglas and Albrecht concluded that charge separation occurs in the crystallites giving rise to a fast polarization of the surface of the crystals followed by the discharge contributed to dissolution of pigment ions. The slow decay was inhibited by freezing the solution. Such a mechanism would be consistent with the microwave loss measurements if they arise from bulk charge carriers separated in the crystals after light excitation.

From the pigment protein mixtures it can be concluded that in none of the samples did the dark loss show a significant change as compared with the separated components. In almost all of them, a rather large photosignal was obtained - notably for BSA mixtures of eosine and chlorophyll a. Eosine is known to form complexes with

human serum albumin (Grossweiner, 1967). The pigments in polycrystalline form were very insensitive to light excitation as compared with biological materials.

No measurements of the Hall mobilities were performed for the pigments and the protein pigment samples. The microwave technique is not sensitive enough for the very low photosignals produced by the pigments alone. However, it may be possible to obtain the values for the more sensitive BSA-pigment samples by increasing the amount of sample. These measurements are worth future efforts, because they could contribute to our understanding of the mechanism of sensitization observed here, and to determine the possibility of biological implications for such a mechanism.

IV. STUDIES IN A MODEL SYSTEM
THE ZnO-WATER INTERFACE

A. Introduction

While performing the measurements in photosynthetic systems, I had the opportunity to study with Dr. H. Tributsch some of the interesting features of the electrochemistry of semiconducting electrodes (Memming and Tributsch, 1971). Pigment molecules promoted to the excited state by light act as charge donors to the conduction band of the semiconductor. Photocurrents are produced in such systems with quantum yields as high as 50%. Thus an illuminated solution of chlorophyllide in water, in contact with the electrode, yields photocurrents that very closely follow the absorption spectrum of the pigment.

The similarity between this effect and the functioning of the photosynthetic apparatus is evident, because the photocurrent is equivalent to a charge that has been lifted to a higher chemical potential.

When an electric field is applied to such a system, almost all the voltage drop occurs across a very thin section on the surface of the semiconductor. The solution and the semiconductor itself are good conductors, and the limiting process for the generation of current is the electrolytic junction. Space charge layers in the semiconductor and Helmholtz layers in the interface experience the

entire magnitude of the applied field.

The availability of a phenomenon that was more or less understood in terms of charge injection, and the fact that an applied electric field could modulate such effects, made very attractive the idea of using such a system as a sort of calibration for the microwave absorption measurements that I had underway on photosynthetic materials. Moreover, the fact that some previous attempts to introduce samples with relatively large water content were successful encouraged us to perform the experiment.

Two separate experiments were designed. In the first one, illumination of the semiconductor surface while it was located in the microwave cavity and simultaneously contacted both to a voltage source and to a system to detect the photocurrents. Charges (mainly holes) generated by light would contribute to the microwave losses and at the same time be accelerated by the static field. In a second stage we intended to incorporate a pigment in the solution to produce the charge injection from the excited state of the pigment. In the first experiment ultraviolet light simply raises electrons from the valence to the conduction band of the semiconductor. In the second case, far red light that is not absorbed by the ZnO crystal could only have an effect on the pigment. In both cases we hoped to measure the microwave loss contributed by the charge carriers.

The result of the first experiment and some unexpected effects of the applied electric field upon the luminescence of the ZnO electrode are reported in this chapter (Petermann, Tributsch, and

Bogomolni, 1972). No extrapolations to photosynthesis are intended from these measurements, but they clearly show that measurements of such surface charge carriers are possible with the microwave technique.

B. The Electrochemical Cell

One of the difficult experimental problems results from the introduction of large amounts of water into the microwave cavity. For optimal detection of microwave absorption due to charge carriers, the surface of the electrode must be placed in a resonator at a site of maximal electric field. Since we wished to investigate an electrode in contact with an aqueous electrolyte, and since water strongly absorbs microwaves, we had to abandon this arrangement and look for a compromise solution. We found it in the cylindrical TE_{011} cavity resonator which is depicted in Figure 10. This resonator, which had a typical resonance frequency of 9.5×10^9 Hz, had a cylindrical opening in which the electric field decays exponentially (a waveguide beyond cutoff).

We constructed a small cylindrical electrochemical cell, consisting of the sample electrode, the aqueous electrolyte and a counter electrode, which fitted into this opening. The position of the electrode surface was adjustable within the electrical field of the cavity resonator. The geometry for the arrangement of the metal wires of the electrochemical cell was chosen so that they did not act as antennae for the leakage of microwaves from the cavity.

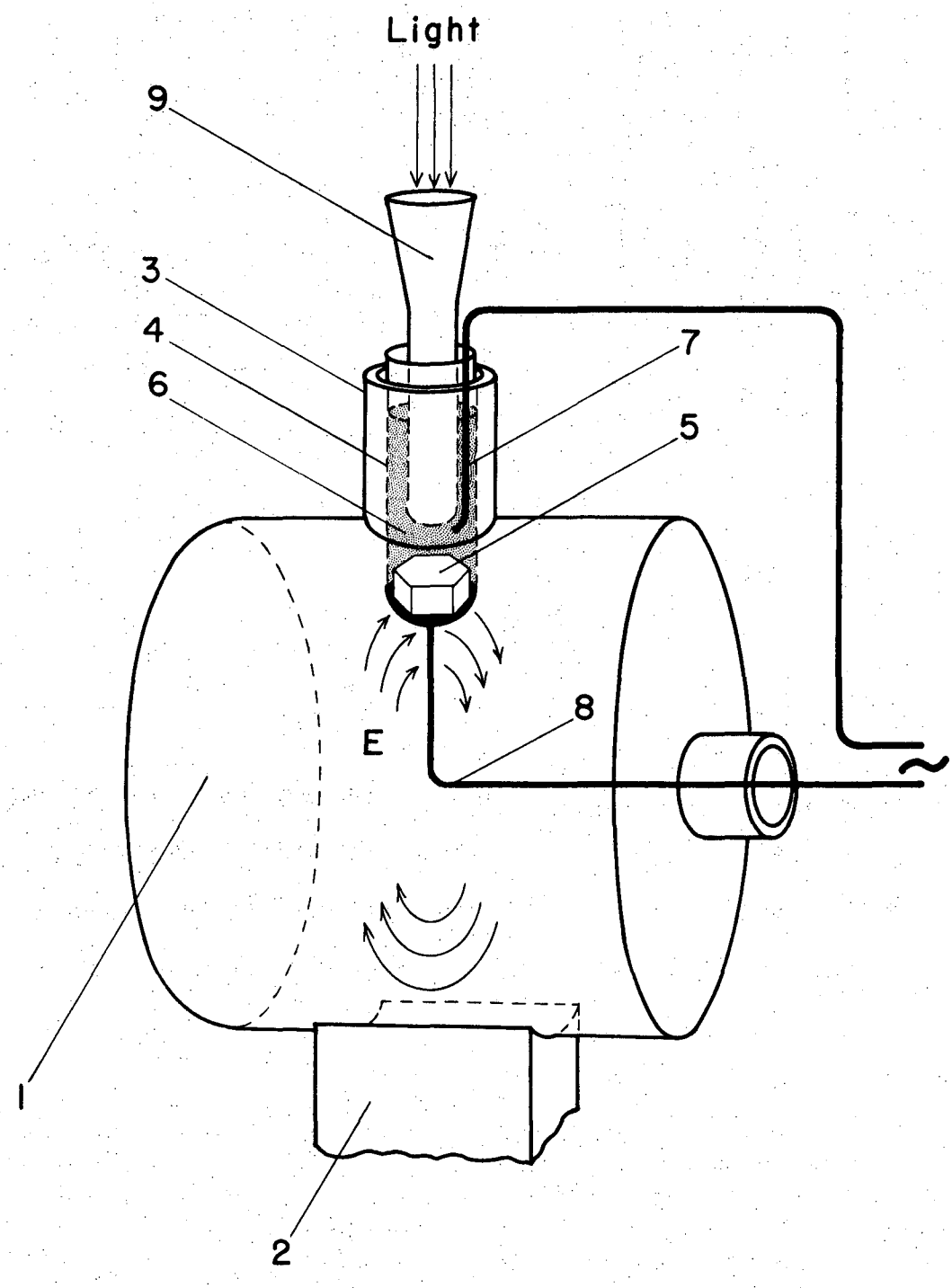

Figure 10. The electrochemical cell. XBL7110-5400

1: TE_{011} cylindrical cavity. 2: Waveguide. 3: Waveguide beyond cutoff and support. 4: Quartz cylindrical cell. 5: ZnO crystal. 6: Electrolyte. 7: Counter electrode; platinum. 8: Connecting wire. 9: Light pipe.

For the microwave experiments single crystals of zinc oxide (10^{-2} to 10^{-3} Ω^{-1} cm^{-1}) were selected. (Note: We are indebted to Prof. G. Heiland, Technische Universitaet, Aachen, Germany, for his generous gift of single crystals.) From the several cm long and approximately 4 mm thick hexagonal needle crystals we split 2 to 4 mm high discs and prepared them as electrodes. The contacts were made by diffusion of indium into one surface (1 hr, 700°C). The surfaces, which were exposed to the electrolyte, were produced by cleaving the contacted crystal with a blade. The counter electrode was a platinum wire. Although not ideal, it has been used as a reference electrode too, because of the small size of the electrochemical cell (two-electrode arrangement). Aqueous 1 M KCl solution has been used as electrolyte. A pH of 2 was adjusted by addition of HCl. Electrode potentials were controlled with a potentiostat (Wenking fast rise: 1 μsec). The electrochemical setup is shown in Figure 11.

C. Photoinduced Microwave Loss, Photocurrents, and Luminescence Applied Voltage Dependence

When a periodic electric potential was applied to the zinc oxide electrode, a synchronous modulation of microwave absorption was observed. The microwave absorption changes due to variations of the electrode potential were so pronounced that they could conveniently be measured in a quasi-stationary way. Figure 12 depicts the dependence of microwave absorption on the electrode potential for two different velocities of potential changes. A clear hysteresis

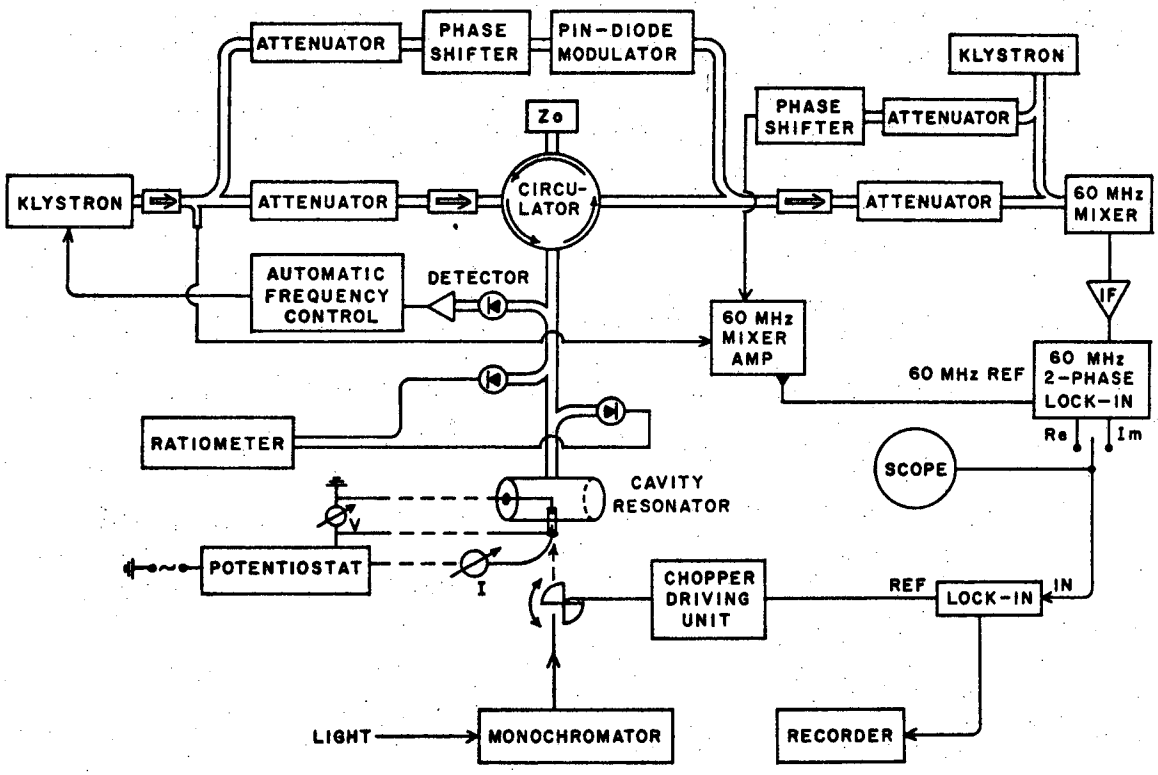

Figure 11. Essentially the microwave arrangement is the same described in Chapter II. Included in the diagram are the electrochemical cell in the cavity and the typical measuring system. V - indicates a lock-in voltmeter, Model 131, Brower Lab., Inc., Westboro, Mass. I - is an electrometer, Keithley Model 610 A.

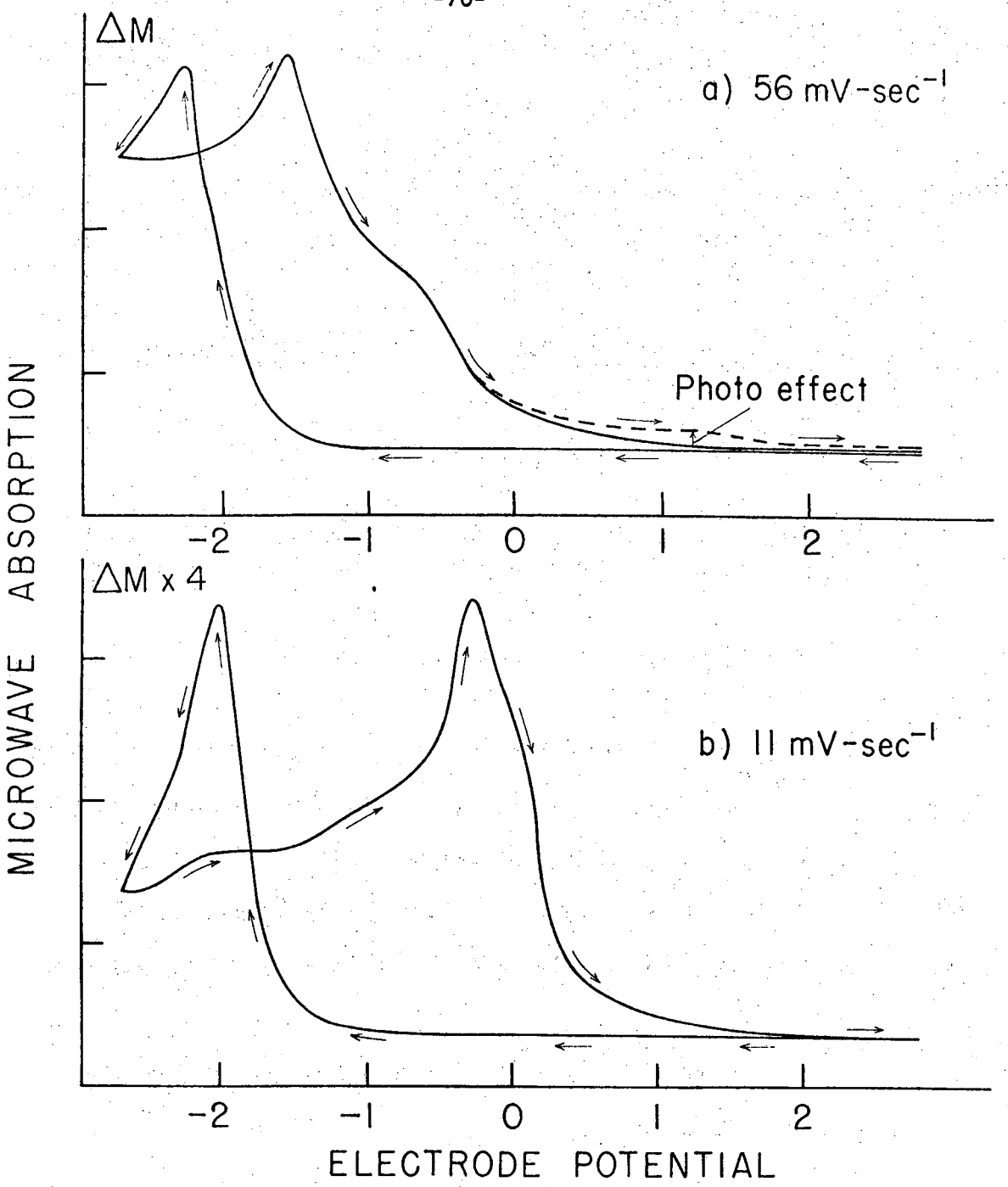

XBL7111-5442

Figure 12. Microwave absorption vs. electrode potential. ZnO electrode, pH 2, KCl 1 M electrolyte. The absorption of microwave power is shown in arbitrary units; the electrode potential is given in volts. The arrows indicate the direction of sweep. a) shows the effect of voltage on the dark microwave absorption, and the region where the photoeffect was found. b) slower sweep rate. The vertical axis scale was reduced 4 times. Only dark absorption is shown.

can be observed which is more pronounced in the slower dynamic measurement.

This behavior may best be described by comparison with a current-voltage diagram for the same electrode (Figure 13). When the electrode potential is changed towards negative values, microwave absorption increases considerably and passes over a maximum. The electrode behavior in this potential range is characterized by hydrogen evolution and by a partial reduction of the zinc oxide to zinc (cathodic current in Figure 4). When the potential changes are reversed, the electrode surface is reoxidized. This is reflected in an anodic current peak which is higher and apparently shifted towards more positive potentials after prolonged cathodic reduction. The reoxidation process of the electrode surface seems to be reflected in the second microwave absorption peak, which is surpassed during transition from negative to positive electrode potentials. At sufficiently high anodic potentials, finally, current flow is limited by a boundary layer in the n-conducting semiconductor surface. Microwave absorption in this region reaches a constant value. Under modulated light and synchronous detection, DC photocurrents showing the behavior depicted in Figure 16b are observed.

The ZnO crystal showed bulk microwave photoconductivity when illuminated before addition of the electrolyte in contact with air. The transient changes in microwave absorption due to the photocarriers were as fast as the light pulses. When electrolyte was added but with no electric field applied, a 20- to 40-fold increase in the microwave photoeffect was observed. The kinetics of the

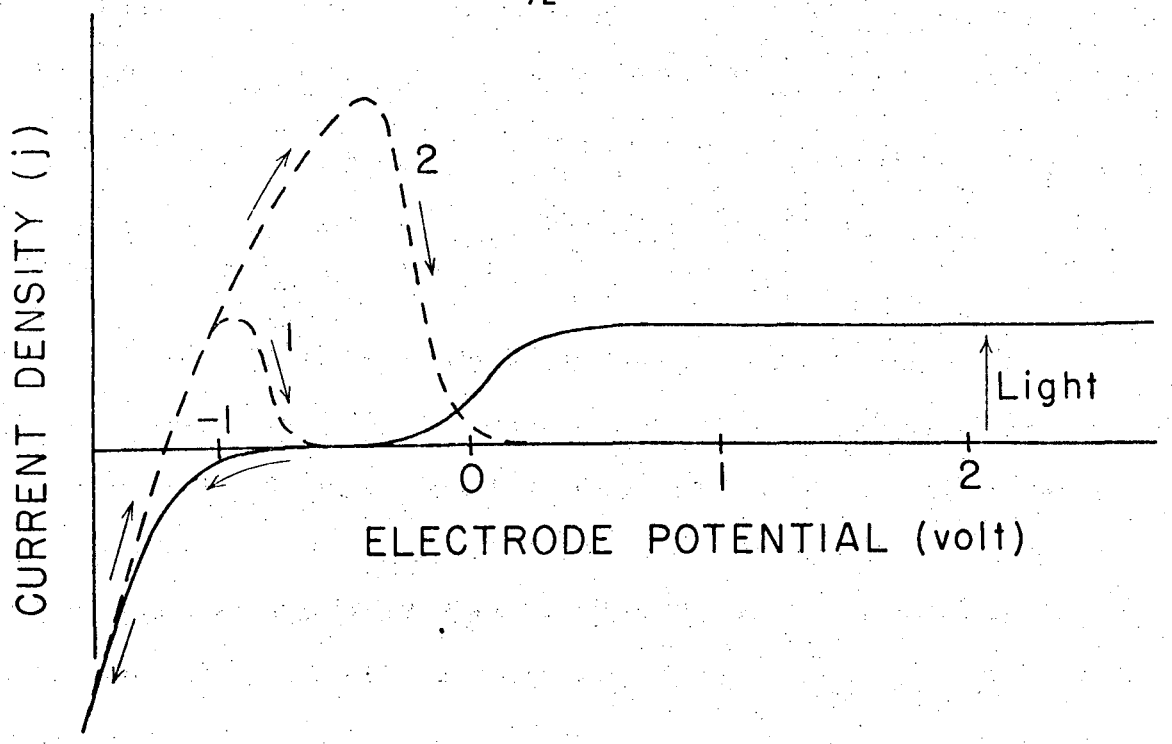

XBL7111-5443

Figure 13. Solid line: Illumination of the zinc oxide electrode gives rise to an anodic photocurrent, which shows a limiting behavior at positive potentials. It arises from the generation of holes in the valence band of the semiconductor. Holes are minority carriers in this n-type material and initiate electrochemical reactions at the semiconductor surface which lead to its photocorrosion - e.g., Zn^{++} ions dissolve into the solution. Broken line: At negative potentials Zn^{++} is reduced to metallic Zn°. The broken line shows the effect of reoxidation of Zn° on the currents when the electrode returns to positive potentials. 1: Shows the effect of a 56 mvolt/sec sweep rate. 2: Sweep rate 11 mvolt/sec. The typical dark current is included in Figure 18; essentially no current flows at positive potentials in the dark.

transients showed also a marked change; the rise as well as the decay times were in this case of several milliseconds as compared with the microsecond responses of the dry crystal.

The voltage dependence of the microwave photoeffect is shown in Figure 14. The photoeffect appeared to be very dependent on the pretreatment of the surfaces; in some samples a maximum effect was obtained at about one volt and complete disappearance of the photoinduced losses occurred at 4-5 volts. The variations over many samples are shown as a shaded area.

The kinetics of the effects are shown for zero volts and at maximum effect for 2 volts, in Figure 15.

Simultaneous measurement of the DC photocurrents and the microwave photoeffect is shown in Figure 16. In this particular sample the maximum effect occurred very close to zero volts. The competitive nature of the effect is observed in these experiments. The rise of DC photocurrents accompanied the drop in microwave absorption.

At this stage a very interesting effect was observed. The ZnO crystals are known to possess a green luminescence, which we usually observed. However, when an electric field was applied to the crystal a marked decrease in luminescence was found which paralleled the change in microwave photoeffect. Figure 17 shows the effect of the field on the green fluorescence as measured by introducing the electrochemical cell in a Hitachi spectrofluorometer.

Fluorescence and DC photocurrent were measured in separate experiments in collaboration with Dr. Günter Petermann. Figure 18 shows the result. A clear correlation between the drop in light

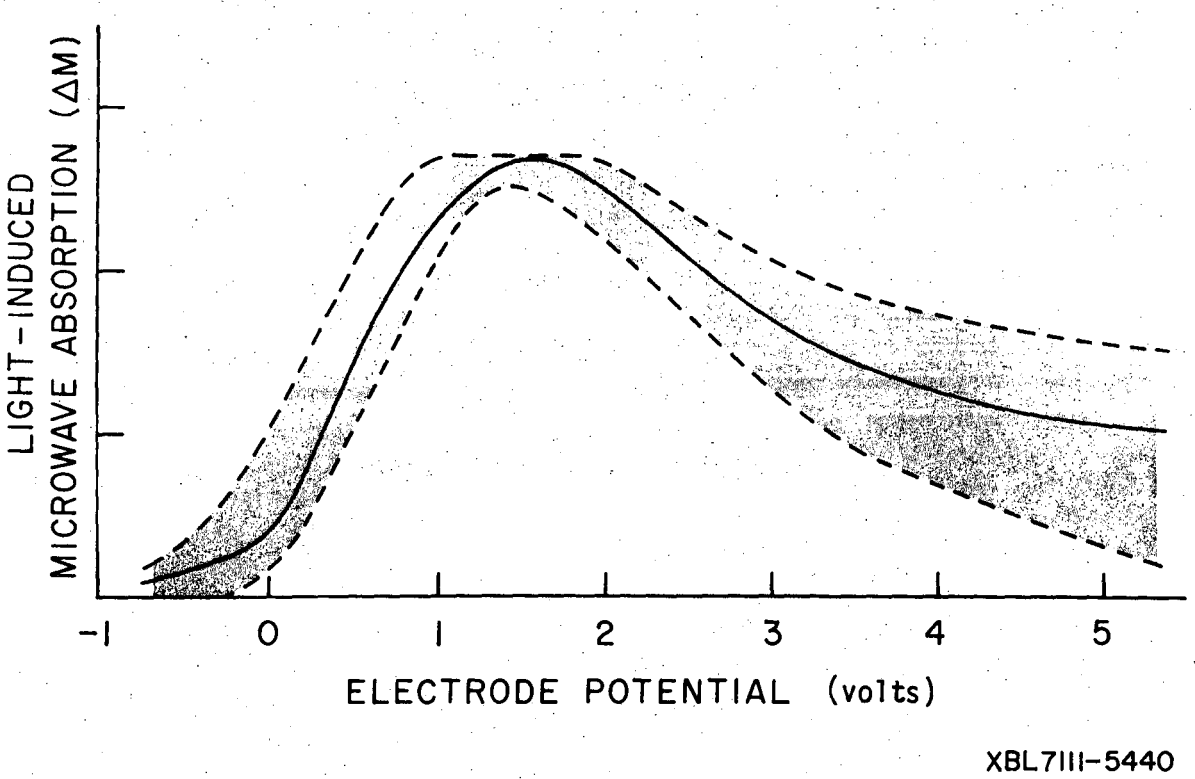

Figure 14. Light induced microwave absorption vs. electrode potential. ZnO crystal. pH 2, KCl 1 M electrolyte. Light induced microwave absorption changes. Vertical axis in arbitrary units. The shadowed area indicates the variability over several samples.

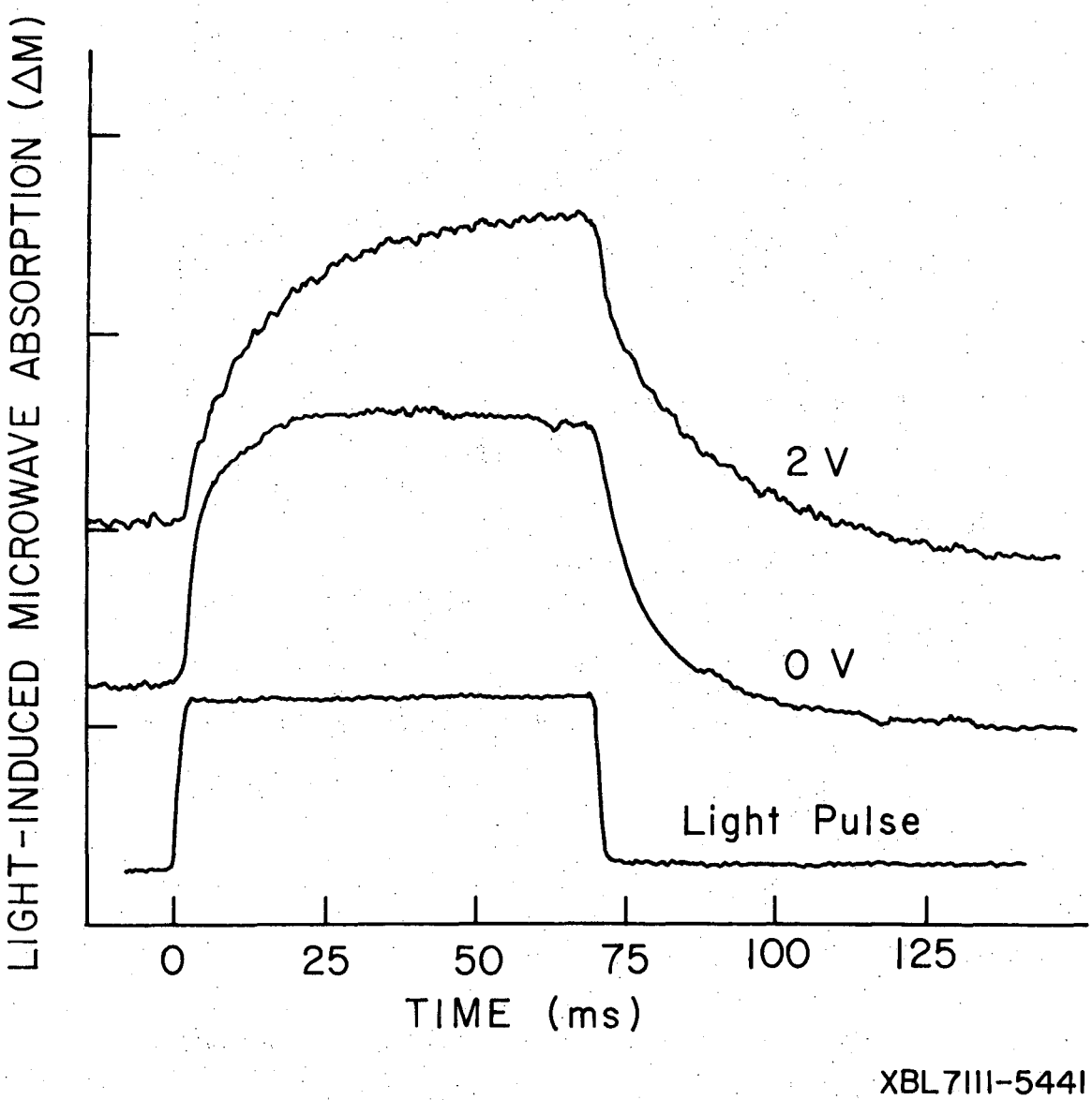

Figure 15. ZnO-KCl electrolyte system. Effect of the electrode potential on the kinetics of the light induced effect. The signal at 2 volts was several times larger than at 0 volts. The heights were equalized for better comparison of the kinetics.

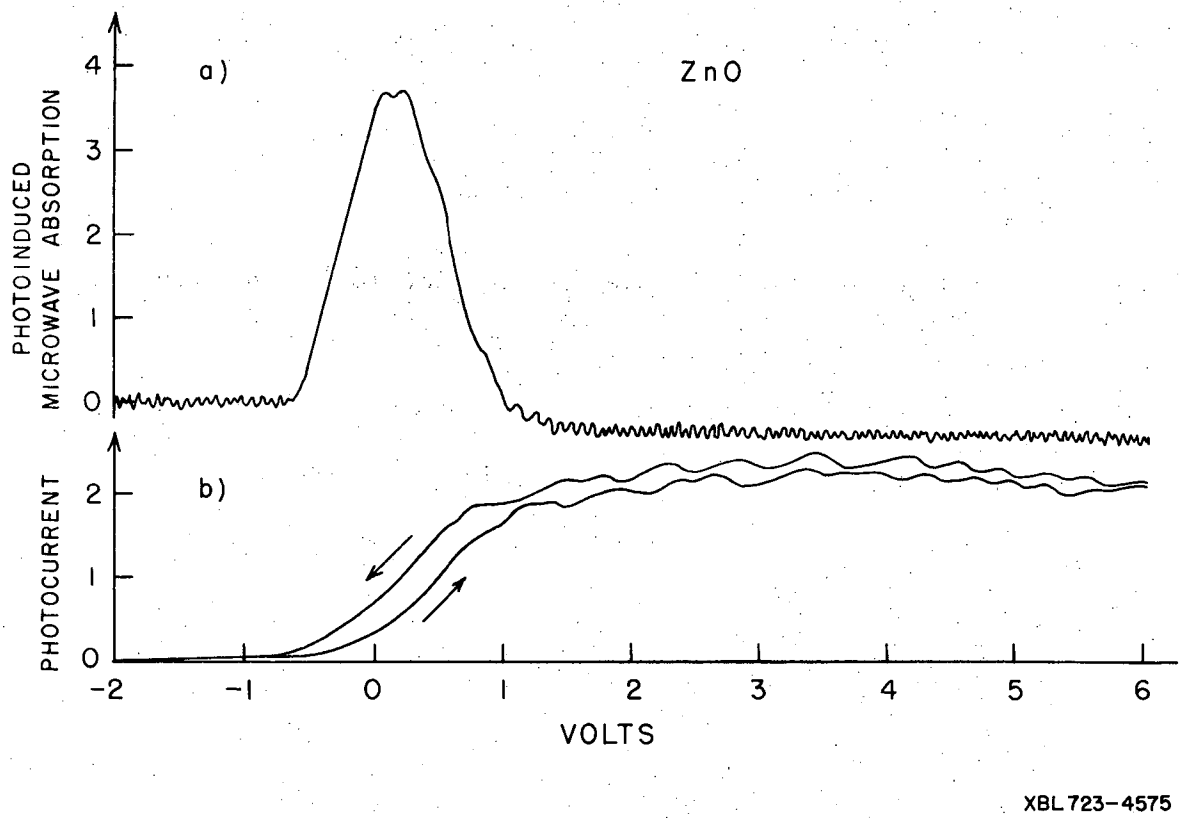

Figure 16. ZnO-KCl electrolyte system. a) Light induced microwave absorption in arbitrary units, as measured at the output of a lock-in amplifier; modulation frequency 10 Hz. b) Simultaneous recording of the D.C. photocurrents as obtained from the output of a second lock-in amplifier. Exciting wavelength: 360 nm.

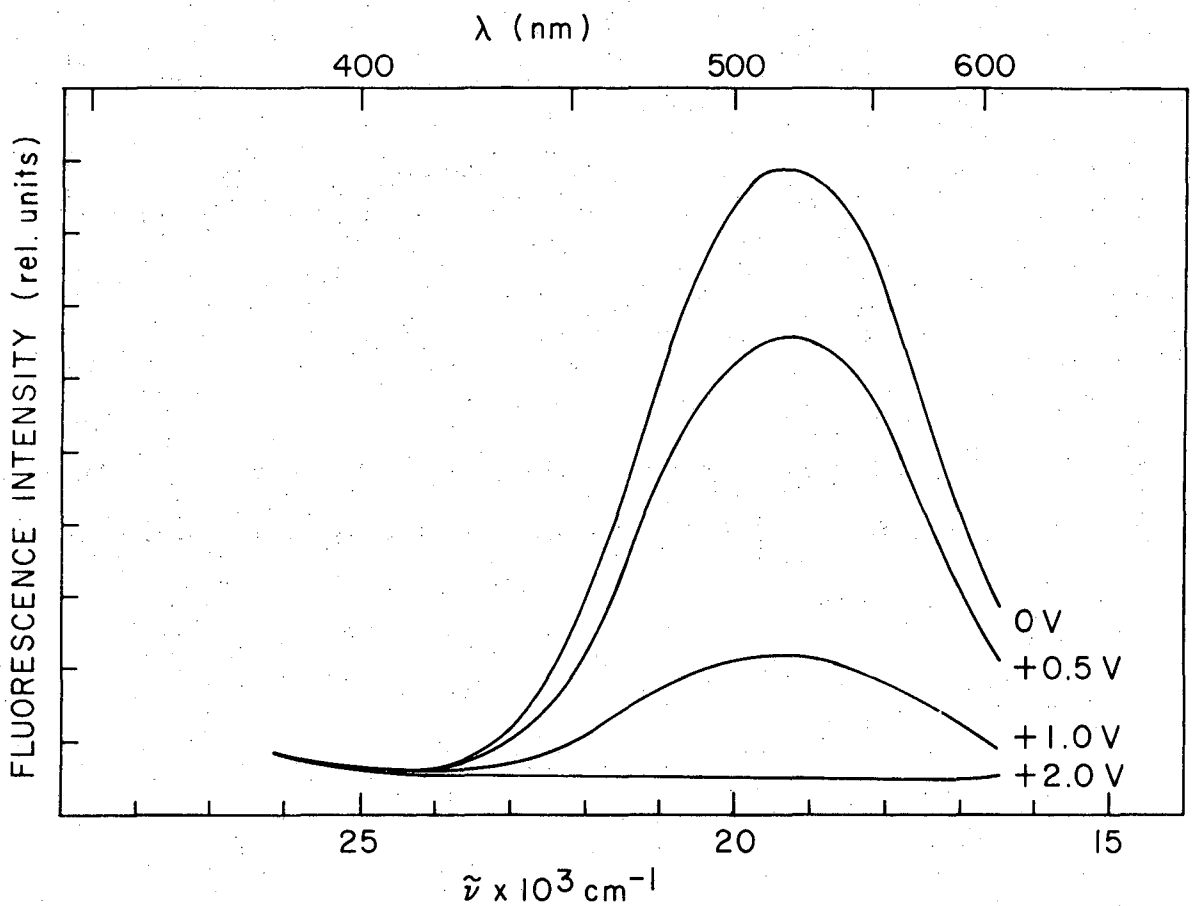

Figure 17. ZnO-KCl 1 M electrolyte system. Effect of the electrode potential on the green luminescence. Excitation wavelength 350 nm.

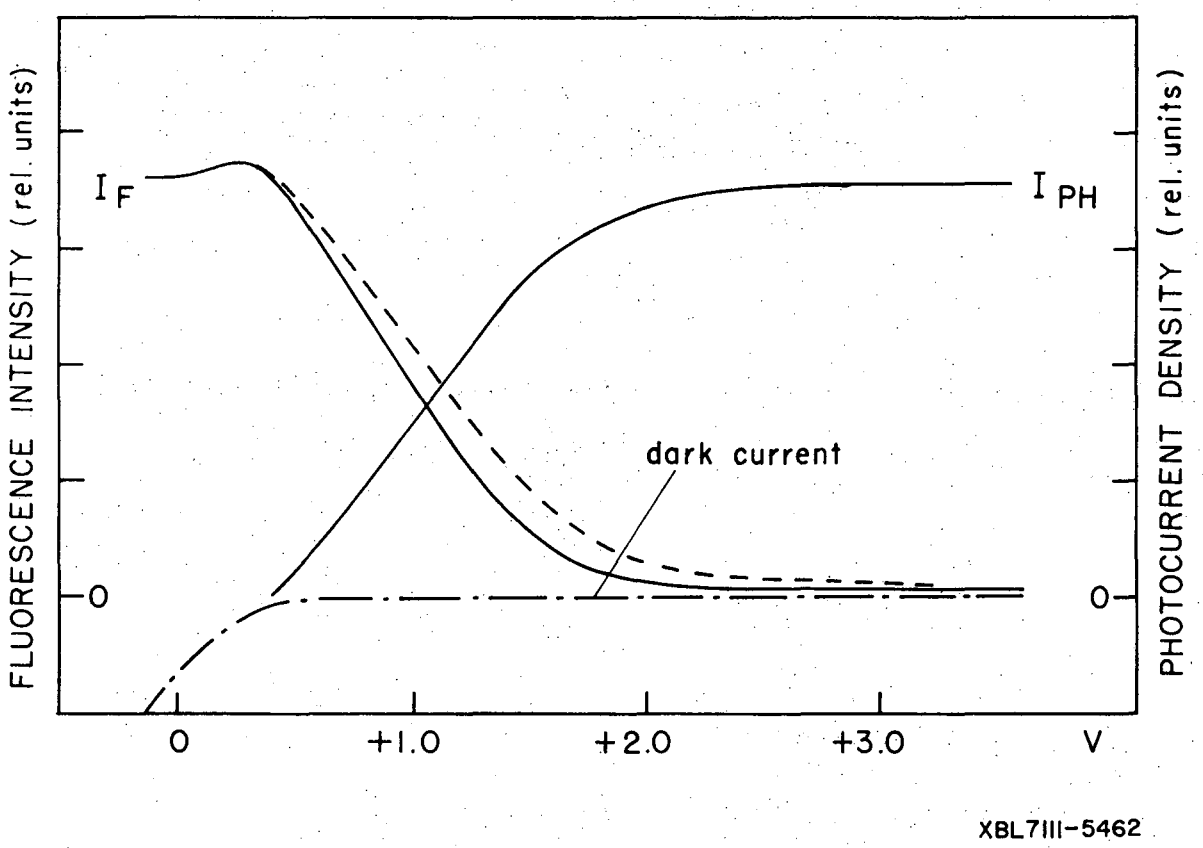

Figure 18. Zno-KCl 1 M electrolyte system. Comparison between photocurrent, I_{PH}, and luminescence intensity, I_F. —— · —— · —— Dark current.

emission and the rise in photocurrents is observed. The dark limiting current is shown as a dotted line.

D. The Exciting Wavelength Dependence

The wavelength of the exciting light was swept continuously, and the output of the lock-in amplifier sent to the recorder. The microwave photoeffect measured in such a fashion is presented in Figure 19. Since the light intensities available to us were rather small, the bandwidth of the Bausch and Lomb grating monochromator had to be opened almost to the maximum value of 10 nm allowed by the slit. Nevertheless, it is seen clearly that a voltage-dependent part at shorter wavelengths coincides with the photocurrent action spectrum shown by the dotted line. A voltage insensitive microwave component excited at around 410 $\pm$ 10 nm was observed in all cases.

When a similar experiment was performed for the fluorescence action spectrum (excitation spectrum), a closely similar effect was found for the light emission. Figure 20 shows the results. The voltage-independent component occurs at 400 nm in this case. The spectral resolution in this experiment is $\pm$10 nm. The discrepancy with the microwave peak is within the experimental uncertainty. The fluorescence action spectrum is normalized per photon absorbed, while the microwave effect is not normalized.

E. Discussion

The observed effects may be understood in terms of charge carrier generation and radiative recombination from some kind of color center.

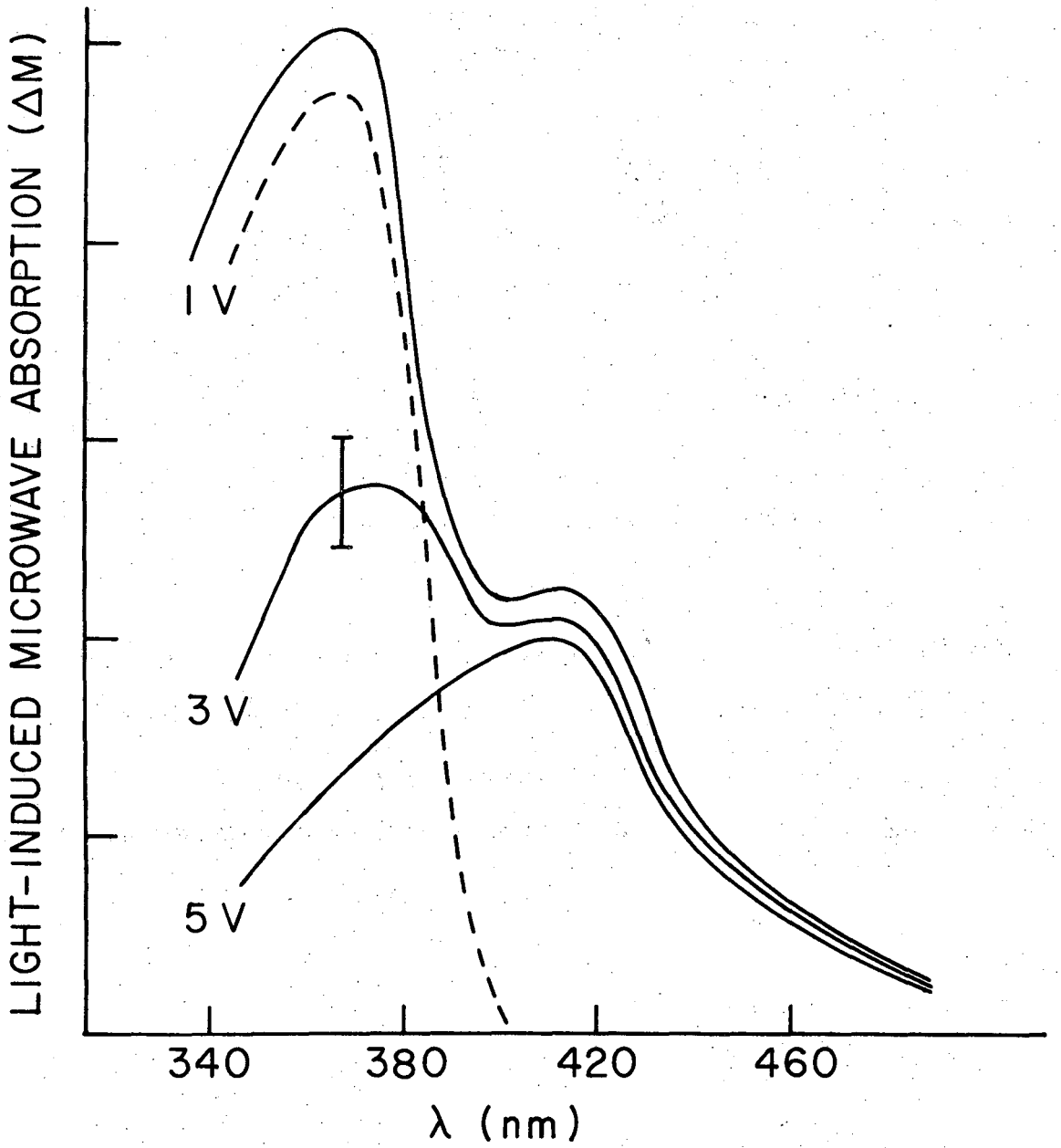

XBL7111-5439

Figure 19. Microwave photoeffect, action spectrum. ZnO-KCl 1 M pH 2 electrolyte system. ——— Microwave photoeffect at three different voltages. The vertical lines indicate the variation over a period of several hours for the same sample. ----- D.C. photocurrent. The action spectrum is not normalized.

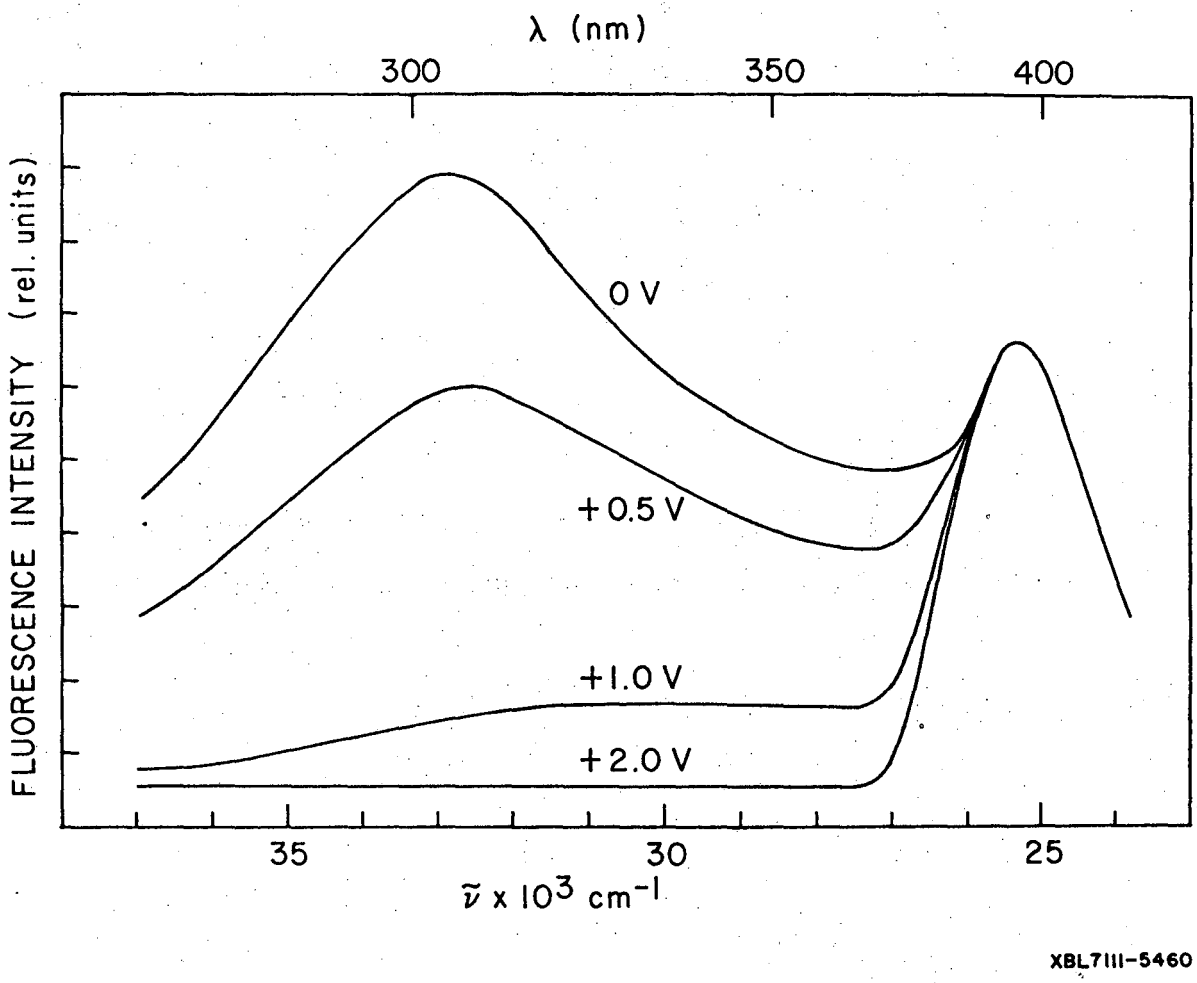

Figure 20. ZnO-KCl 1 M electrolyte system. Action spectrum of green luminescence (normalized to constant incident radiation).

A depletion layer is generated at the semiconductor solution interface. Holes are generated by light and are able to produce the measured photocurrents when the crystal is made positive with respect to the solution (anodic case). The photoinduced microwave absorption could be contributed by the generated charge carriers as well as by the relaxation of some kind of dipolar species generated by the light. This latter possibility, although rather unlikely, might arise from the Helmholtz layer in the immediate solution when perturbed by a change in the concentration of surface states. There are several points that should be introduced in this discussion. There is an exciton band in the electronic structure of ZnO at about 390 to 400 nm. The 510 nm luminescence intensity is affected by temperature.

The extinction coefficient for the longer wavelengths is much smaller than for the main absorption band at 380 nm, resulting in different penetration depths for the light.

The lifetime of the states involved has a very strong influence on the observable microwave losses. Thus, a state lasting 10^{-3} to 10^{-4} sec would contribute several orders of magnitude more than a state with a lifetime of 10^{-7} sec.

The applied electric field extracts holes from the surface, and consequently depletes the crystal of the recombination centers which give rise to the observed luminescence. The same argument applies to the photoinduced microwave effect. The exciton transition would not contribute appreciably to the photocurrents. However, luminescence could arise from such absorption by decay into the metastable

level which produces the 510 transition. An electric field would have little or no effect on such a process, as is observed. The alternative explanation, that the field independent component in the action spectrum is caused by electronic transitions to impurity levels in the crystal which do not contribute to conduction, has to be considered. Such levels acting as traps could account for the long lifetimes and the slowness of the microwave effects as compared with the photocurrents. The onset time for the photocurrents is instrument-limited and has been measured down to 10^{-5} sec. The decay times are also in the tens of microseconds. The microwave effects are in the millisecond range, indicating the possibility of trapping processes. Figure 21 shows the suggested scheme. Competition between photocurrents and luminescence and microwave photoeffects may be explained in such terms. The penetration depth argument also contributes to the explanation of the insensitivity of the long wavelength component to the field. Bulk, rather than surface, effects are produced by those wavelengths, and the field drops completely in a region much shorter than the penetration depth.

While much work remains to be done in the line of research initiated here, the present picture in terms of surface charge carriers suffices as a working model for the explanation of the observables.

Experiments with pigment molecules as charge injectors are of interest and are worthy of further study.

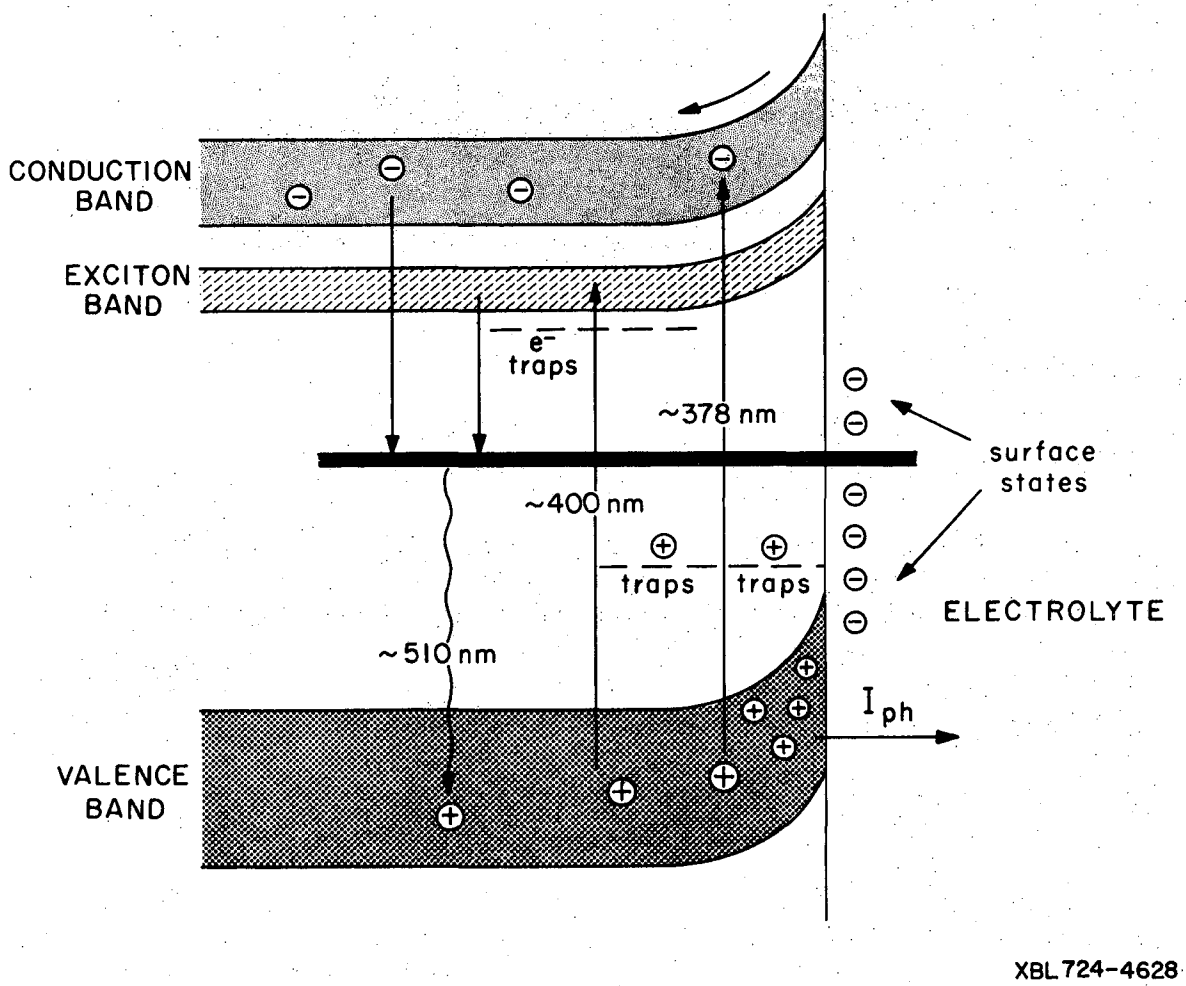

Figure 21. Working scheme for the ZnO-electrolyte system. I_{ph} - photocurrents. The black horizontal line represents the metastable level from which the 510 nm luminescence originates. See text for description.

V. MEASUREMENTS ON BIOLOGICAL MATERIAL

This chapter presents the results of measurements in higher plant material and bacterial chromatophores. The object of the experiment is to detect the possible presence of photogenerated charge carriers in the photosynthetic samples, and (if any) to establish their biological significance.

Evidence for the presence of charge carriers is obtained from measurements of: dielectric loss (or conductivity), the Hall effect, and changes in dielectric constant at 10^{10} Hz under the action of actinic illumination.

The green plant materials were films of the broken chloroplasts preparation as described in Chapter II unless otherwise stated. The samples of bacterial material were films of the isolated chromatophore fraction. Four mutants of R. spheroides were used in the experiments. The rationale for their use is as follows:

Bacteria have a photosynthetic system that is less complicated than that of higher plants. With hopes that bacteria would show some simplification in the effects, I chose R. spheroides, for which a great deal was known when I started my experiments. Evidence for the activity and composition of the photosynthetic reaction centers was, to a large extent, obtained from this species.

The existence of mutants of R. spheroides lacking carotenoids provides a simplification in the pigment contribution to the effects, and

most important of all, the existence of a non-photosynthetic mutant that lacks a functional reaction center makes this bacterium an interesting blank. This latter mutant does not exhibit the typical light induced absorbance changes at the reaction center bacteriochlorophyll absorption bands that the normal strains show, nor does it show any light induced EPR signal. This strain is designated PM-8 (Sistrom et al., 1964). The strain G.A. is the parent strain of PM-8, and should be used as a control for PM-8. It lacks most carotenoids, although retaining the neurosporene and hydroxyneurosporene. For most measurements the strain R-26, which completely lacks carotenoids, was used. The wild type R. spheroides, which contains all the pigments, was used in most of the early measurements. The measurements of action spectra and relative quantum yield were performed with the wild type strain.

The following summary of the main observations which will be presented and discussed in this chapter applies to both green and bacterial material unless otherwise stated.

1 - The photoconductivity transient response to short flashes showed rise half-times shorter than 5×10^{-6} sec at room temperature and several decay components in the 10^{-4}, 10^{-2} and 1 second ranges. The photoconductivity signals in response to high light intensity flashes ranged between 10^{-3} to 10^{-2} of the dark conductivity.

2 - The activation energy for the photoconductivity was $E_a = 0.3$ eV from 40° to -40°C; a temperature dependence of the form $\Delta\sigma = Ke^{-E_a/KT}$ was followed by the samples within this range. $\Delta\sigma$ is

the peak height of the transient photoconductivity response to short flashes and K is an amplitude coefficient.

3 - The photoconductivity action spectrum closely followed the absorption spectrum of the samples. A tendency to higher quantum yields was found at wavelengths close to the reaction center pigment absorption band. Dehydration of the sample strongly reduced the photoconductivity response to short light flashes at wavelengths around 700 nm in chloroplasts.

4 - A photoinduced microwave Hall effect corresponding to charge carriers of both signs with mobilities between 0.1 and 1 cm^2/volt sec was observed in all photosynthetic samples which also produce the light induced EPR signals characteristic of the normal functional state of the reaction center structures. A mutant of bacteria lacking such structures (or possibly having damaged reaction centers) did not show the large photoconductivity signals or the photo-production of charge carriers of both signs. Only a low quantity of negative charge carriers with low quantum yield, QY = 10^{-4}, was observed in this mutant.

5 - The negative charge carriers decayed in about 10 milliseconds after a short light flash. The concentration of positive charge carriers reached a maximum value at times ranging between 20 to 100 milliseconds, and decaying in a few hundred milliseconds. The onset time for the observed Hall effect signals was as short as the flash rise time, about 5 x 10^{-4} sec.

6 - Light induced changes in the dielectric constant of the samples having kinetic characteristics similar to those of the photo-induced losses were observed in all functional photosynthetic

materials. Values as high as $\frac{\Delta\varepsilon'}{\varepsilon_T} = 10^{-5}$ were observed in response to high intensity flashes. No changes in the dielectric constant upon illumination were observed in the bacterial mutant that lacked reaction centers. Low temperatures strongly inhibited the several second decay component of the dielectric constant transient response to short light flashes. A similar observation at low temperatures applies to the 3 to 5 second decay component of the EPR signals in both systems.

7 - The fast decaying component of the photoconductivity was affected considerably by the action of ferricyanide in both systems. Reduction of the total size of the signal and a lengthening of the 10 - 20 msec decay component was observed upon addition of ferricyanide solution.

8 - Background illumination of chloroplast film samples produced changes in the photoconductivity signal kinetics, resembling effects due to saturation of trapping levels in simple photoconductors for which there is ample theoretical foundation.

The above experimental evidence supports the following conclusions:

a - Carriers of positive and negative signs with low mobilities are generated by light in the photosynthetic samples.

b - The charge carrier generation is sensitized by the pigments that are relevant to the photosynthetic process.

c - The quantum yield of the process of carrier generation ranges from 0.1 to 1%.

d - The photochemical reaction centers are required for the generation of the charge carriers.

e - The data are consistent with a model in which charge migration and trapping processes take place in a biological matrix in which the reaction center complexes are in close association with charge donor and acceptor molecules.

f - The migration of the charge carriers may be accounted for by a tunnelling or hopping process, possibly in the way formulated by Nelson in his localized charge transport model (1963, 1965, 1969).

Some technical details needed for the interpretation of the results will be discussed along with their presentation. Control measurements in the dark for the material used in these experiments are presented in part A, the photoinduced effects are presented in part B, and part C contains some tentative speculation concerning the significance and possible location of the observed charge carriers.

A. Dark Measurements

My intention, when performing the measurements in the dark, is to gain some insight into the behavior of my samples to dehydration and temperature before introducing light as a perturbation. Possible pitfalls in the measurement of light induced effects, such as a thermal modulation of the conductivity by the light energy converted into heat, required the knowledge of the temperature dependence of the conductivity.

Absolute measurements of the dark conductivity of the samples are also needed in order to calculate the absolute photoconductivity, because the light induced effects are obtained in the form of fractional

changes, e.g., $\frac{\Delta\sigma}{\sigma}$ for the conductivity.

1. Green Plant Material

Typical values for the conductivity of a leaf segment as well as for films of osmotically broken chloroplasts are given in Table II. Films of chloroplast membrane fragments (quantasome aggregates) showed no significant differences either in conductivity or in mobility values, as compared with the chloroplast samples.

Table II. Green-Plant Material: Dark Measurements

Sample	Estimated H_2O content	Dielectric constant	Conductivity	Mobility*
	%	relative units	Ω^{-1} cm^{-1}	cm^2/volt·sec
Dry leaf	>20	3.5	7×10^{-3}	+0.6
Chloroplast	>20	3.7	2×10^{-2}	+<0.5>
	15-20	3.4	7×10^{-3}	+<0.8>
	12-15	3.3	4×10^{-3}	+<0.5>
	9-12	3.1	7×10^{-4}	+<1.1>
	5-10	2.8	2×10^{-4}	+<1.2>
	5-10	2.7	3×10^{-4}	+<1.1>
Lyophilized Chloroplast	<5	2.7	$<10^{-4}$	+1.5 - 2.0

*Average between values obtained with the magnetic field pointing in opposite directions. Differences as large as 50% were observed.

The measurements reported for chloroplasts in Table II were performed during the process of dehydration of the sample in the cavity. Dry nitrogen gas flow and microwave power absorption contributed to

the dehydration process. The nitrogen gas temperature was controlled by a servomechanism at about 25°C. The dehydration process may be followed by observing the changes in dielectric constant of the material. The values ranged from 3.8 in partially hydrated samples to 2.7 to 2.8 after several hours in the cavity. The changes in dielectric constant are measured as shifts in the resonance frequency of the cavity. These shifts made measurements of mobilities in partially hydrated samples almost impossible due to the large changes in the base lines which my system of automatic frequency control was unable to compensate.

Lower computed values for the mobilities are expected in the hydrated samples due to the fact that an overestimation of the dark conductivity results in lower computed values for the mobilities of the charge carriers (Formula 17, pg. 36, this work). Although such an effect was observed and always in the right direction, the correspondence was not linear. A decrease of the dark loss by an order of magnitude altered the mobilities by only a factor of 2 or 3. This suggests the possibility of a more complicated mechanism for the dark loss involving proton migration in dehydrated samples while other ion migration might contribute to the loss in hydrated samples.

The values for the mobilities are reported in every case as an average with the magnetic field in opposite directions. Under the reversal of the field, the signal obtained was always asymmetric, giving a different value for the mobility. Effects such as magnetoconductivity would account for such behavior, but from the fact that the sample shape and sample mounting was far from perfectly symmetric, one might expect the sample to perturb the modes unequally and, thus,

change the geometry under field reversal. The observed difference was rather constant, making this observation worthy of further study, since it is unlikely that the sample location always followed the same asymmetrical geometry. Magnetoconductivity from the resistive plugs has to be considered as an alternative explanation. They were in the cavity in order to obtain balance.

Figure 22 shows the observed change in power unbalance for two values of magnetic field. The height of the signal is roughly proportional to the magnetic field for small values of ΔP_2 as expected.

Figure 23 shows the effect of field reversal, its asymmetry and the sample behavior in a typical measurement. Figure 23(a) shows the effect of a 10 Kgauss field in both directions and the calibrating simulated effect introduced by the bucking arm calibrated attenuator. The effect in this case was twice as large in the -10 Kgauss direction as in the +10 Kgauss. In (b) the field is allowed to invert as the recorder runs. The baseline is not perfectly horizontal because this sample was still in the process of dehydration.

2. Bacterial Chromatophores

Table III contains typical data for the dark microwave parameters of the various strains. The order of magnitude of the observables is very similar to those of chloroplast and lamellar fragment samples. No difference was found in the dark measurements on the PM-8 mutant with respect to the normal strains except for the lower value of the conductivity. The dark mobility for PM-8 was consistently smaller by about a factor of 2 or 3 as compared with its parent strain G.A. The smaller mobility does not account for an order of magnitude smaller

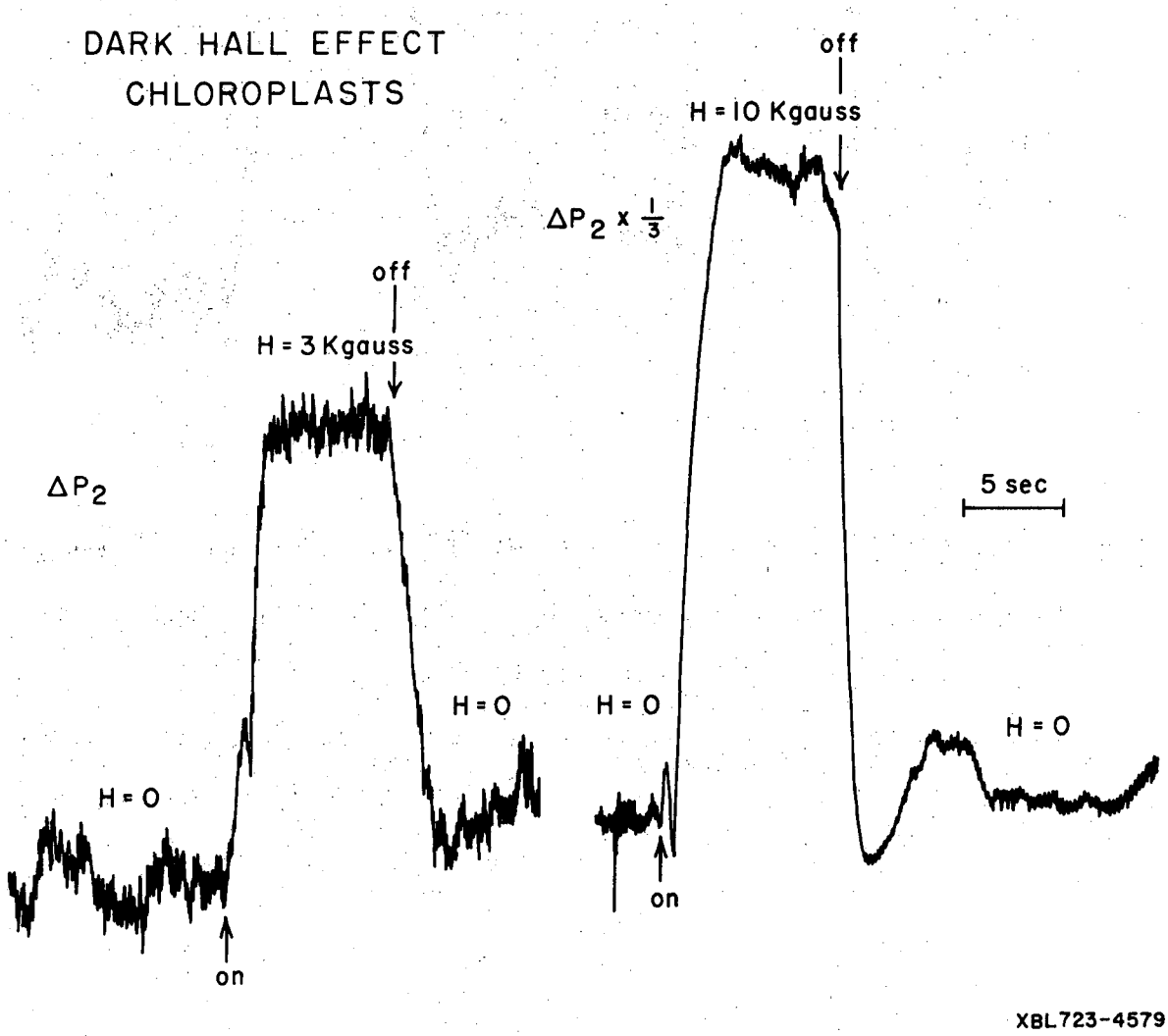

Figure 22. Dark Hall effect: chloroplasts. Left trace: Unbalance signal for a 3 Kgauss field. Right trace: Unbalance signal for a 10 Kgauss magnetic field. The receiver gain is 1/3 of the left trace. The upwards deflection of the power unbalance corresponds to positive carriers with mobility 1.2 cm^2/volt sec.

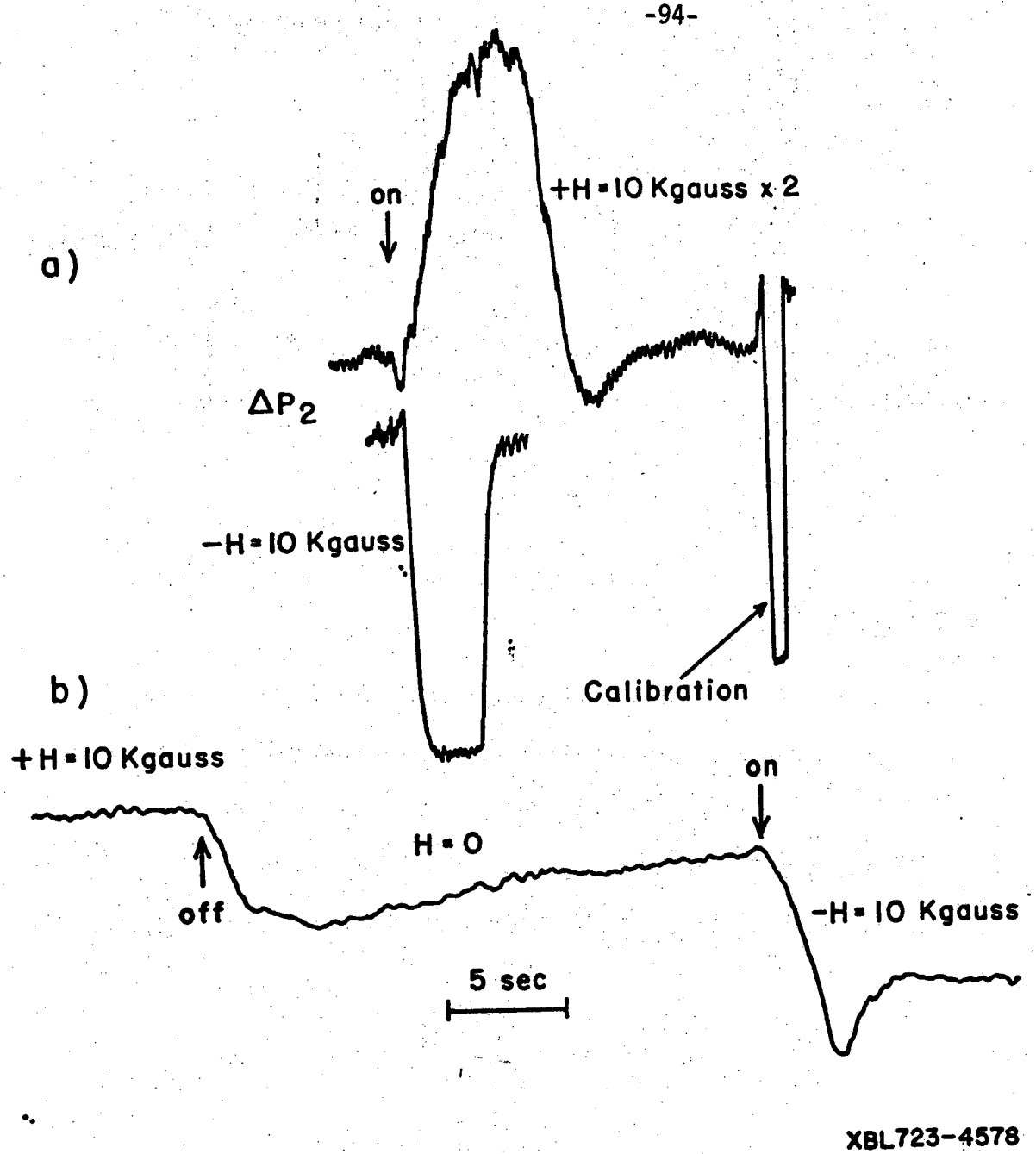

Figure 23. Dark Hall effect. Chloroplast film. (a) Power unbalance signal with the 10 Kgauss magnetic field in opposite directions. The gain for the upper trace is twice that for the lower. The inverted signal to the right in the upper trace is a calibration power unbalance signal. (b) The same experiment is performed as the recorder runs.

Table III. Dark Measurements - Bacteria

Sample	ε'	σ	$\langle\mu\rangle$
R. spheroides - strain		Ω^{-1} cm^{-1}	cm^2/volt·sec
R-26	3.1	6×10^{-3}	+1.1
G.A.	3.0	3×10^{-3}	+0.9
PM-8	3.1	4×10^{-4}	+0.5

conductivity; therefore it has to be assumed that the PM-8 mutant has a smaller concentration of dark carriers or dipoles that contribute to the conductivity than the G.A. strain.

Figure 24 shows the result of a measurement of the dark Hall effect in R-26 chromatophores.

An attempt was made to follow the temperature dependence of the dark mobilities in a chloroplast sample. At temperatures above -5°C the mobility increased with increasing temperature. Since the mobility values followed an exponential behavior as a function of the inverse of absolute temperature, I computed a value of 0.15 eV for the activation energy from the slope. I assumed a dependence of the form:

$$\mu = \mu_o e^{-E/KT}$$

The mobility reached a minimum value around -5°C and then increased at lower temperatures, from 0.4 ± 0.1 cm^2/volt·sec at -5°C to 0.8 ± 0.2 cm^2/volt·sec at -70°C. The dependence below -5°C showed the mobility to be roughly proportional to the inverse of temperature.

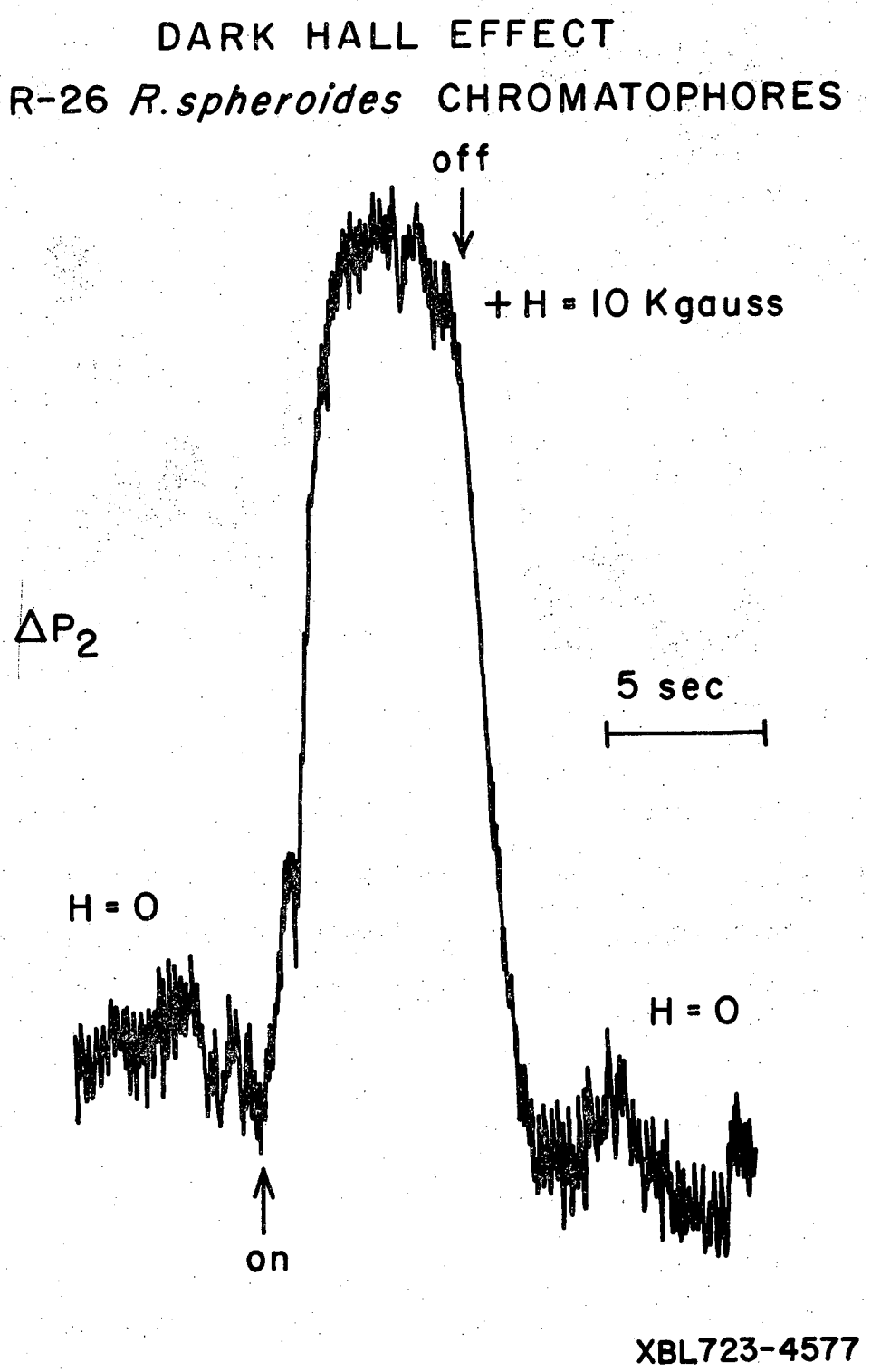

Figure 24. The trace shows the Hall effect signal. The magnetic field is turned on and off at the arrows. The deflection corresponds to carriers of positive sign, with a mobility of about +1.0 cm^2/volt·sec.

B. Light Induced Effects

1. Photoconductivity (Photoinduced Dielectric Loss)

a. Some Preliminary Observations

(1) The photoconductivity signals from all biological samples were about two orders of magnitude larger than the photosignals observed from chlorophyll microcrystals under comparable light excitation.

(2) Denaturation of the samples by heating for 5 minutes at 100°C caused the disappearance of the fast (millisecond) component; a photosignal about one order of magnitude smaller than that of the native sample, decaying in several hundred milliseconds to seconds, remained. As it will be seen later, that signal may be accounted for by a thermal effect of the light. Heating at 60°C for 10 minutes did not affect the signal. The light induced EPR signal, which was used as an indicator of biological activity, disappeared completely upon heating to 100°C, but remained unaffected by the treatment at 60°C.

(3) The photoconductivity signals in samples dried under nitrogen gas flow could be elicited indefinitely. Freeze dried samples showed a much reduced fast component that disappeared after several flashes. Rehydration, followed by the milder nitrogen gas flow dehydration, recovered the fast component, which was present after several hundred flashes.

(4) Sonication of the material did not affect the signals.

The above observations apply to all the green plant samples. At this point it was clear that the photosignals required the integrity of some sample components able to withstand temperatures not higher than 60°C, while neither the thylakoid membranes integrity nor redox

reactions involving soluble components was involved in the observed effect.

Following these qualitative observations a quantitative analysis of the kinetics, the temperature behavior, the light intensity behavior, and the light wavelength dependence (action spectrum) of the photoconductivity signals are presented.

b. Kinetics

1) Chloroplasts

Figure 25 shows the typical photoconductivity signal from a chloroplast film sample. The kinetic analysis is presented in Figure 26. The decay clearly resolves into two first order components: a fast 5.5 millisecond, and a slow component decay with a half-time of 300 milliseconds. Any slower component present in this sample would not be detected since the pulsing rate was about 1 Hz. A decay component of several seconds, which may account for as much as 20% of the signal, has been observed in all samples when dark adaptation periods of several minutes were allowed between light pulses. The fast component never varied by more than a few milliseconds among several samples, while the other two were very dependent on sample conditions such as state of hydration, previous dark time, and the age of the samples.

To determine the kinetics of the onset of the signals, I used first the 20 microsecond Xenon flash unit. A chloroplast sample, dried under nitrogen gas flow, gave a photoconductivity transient signal which rose as fast as the response time of the detector amplifier which in this experiment was about 10^{-5} sec. Figure 27 shows the oscilloscope trace.

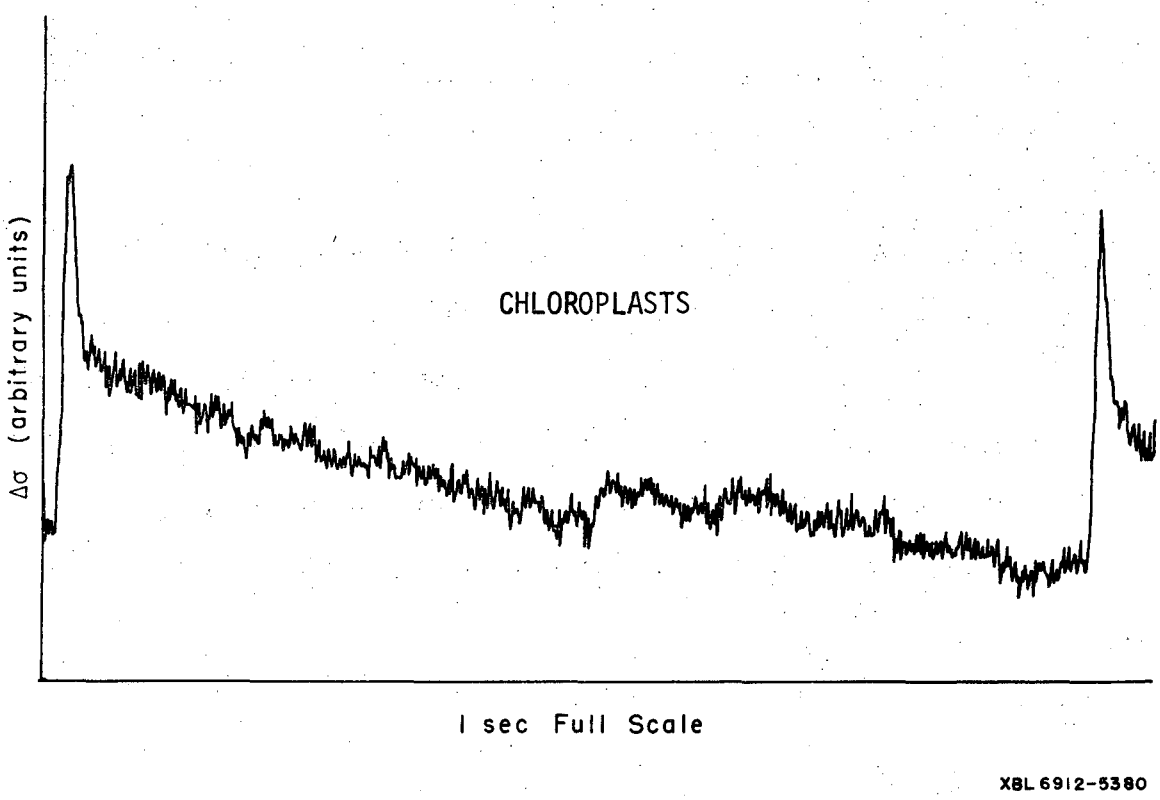

Figure 25. Photoconductivity signal. Chloroplast sample dried under nitrogen gas flow. Illumination: 10 msec pulses of white light. Source: Tungsten iodine lamp. Light intensity 10^6 erg/sec per cm^2. Pulsing rate 1 Hz. The typical biphasic decay is observed. The signal was recorded from the computer averager after 20 passes. The discontinuity at the center of the figure is due to microphonic noise.

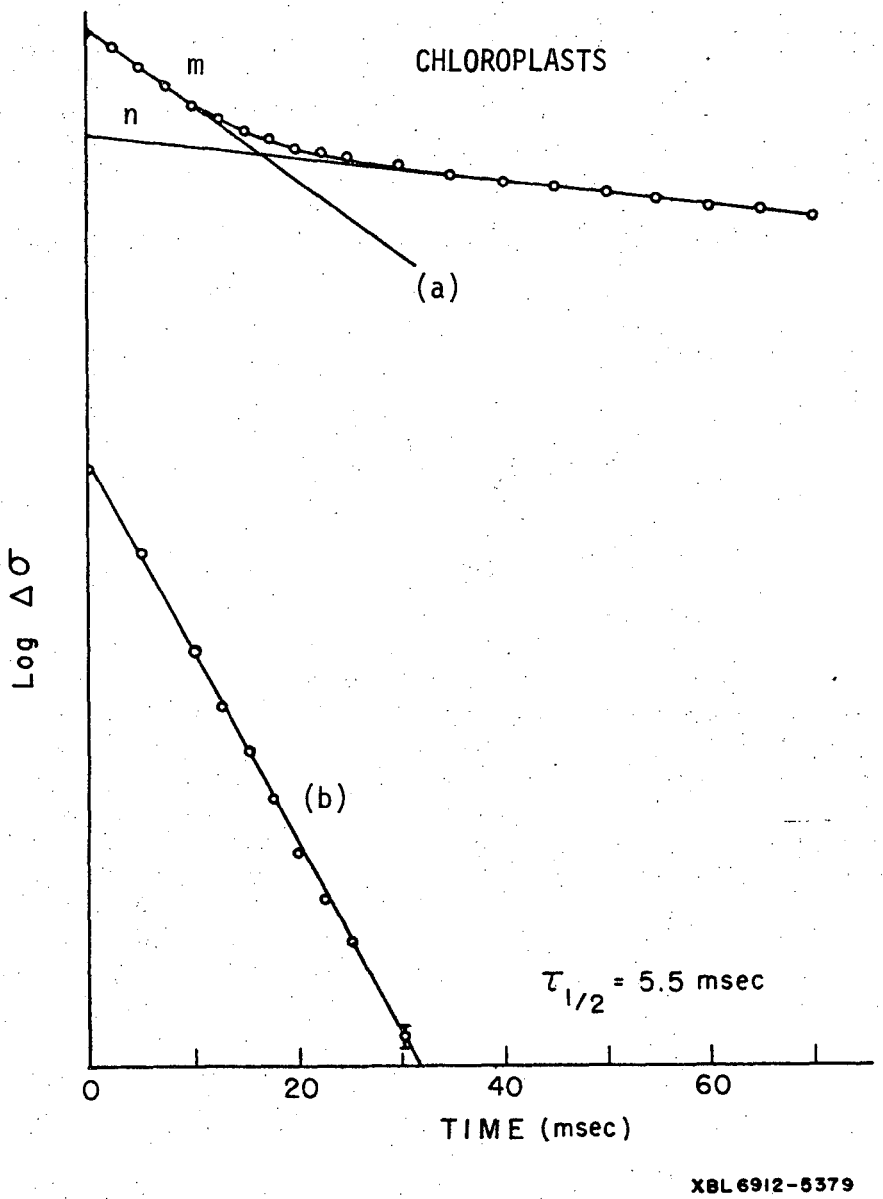

Figure 26. Kinetic analysis of the signals shown in Figure 25. (a) Log vs. time plot of the data obtained from the trace in Figure 25. It may be decomposed into two exponential decays. (b) Fast decay extracted by subtraction of trace (n) from (m). The decay half-time of the signal is 5.5 msec.

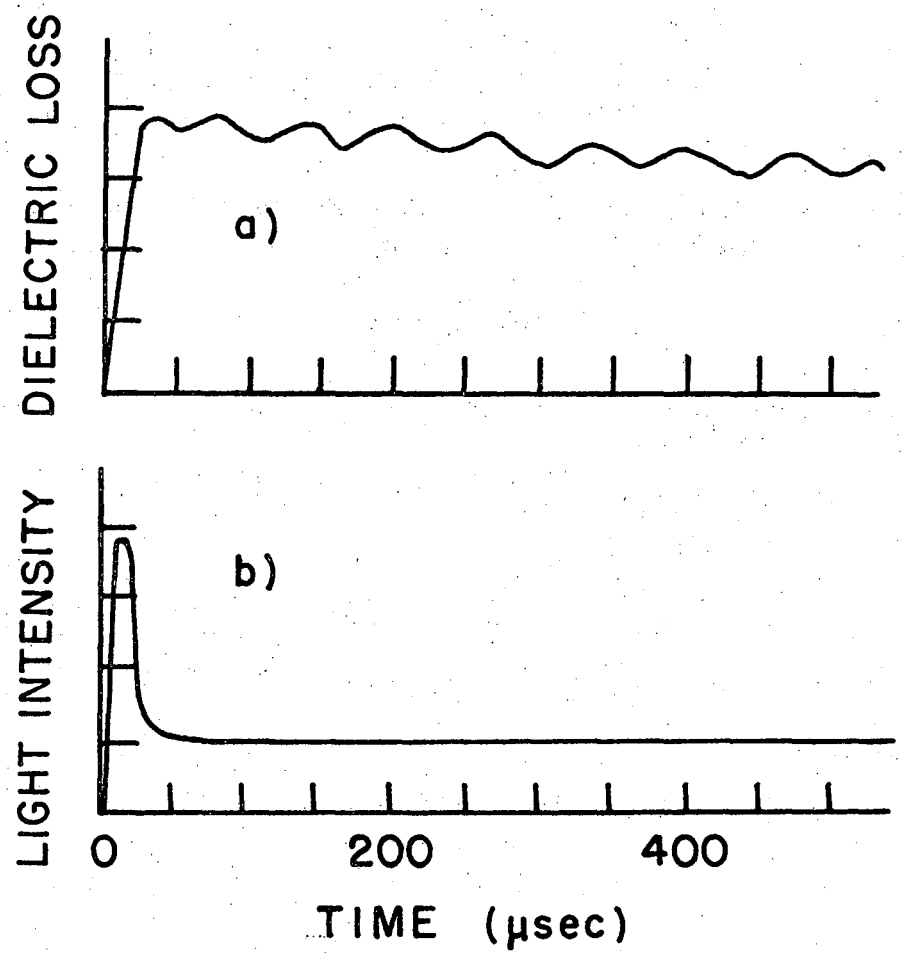

XBL723-4574

Figure 27. Photoconductivity rise kinetics, as traced from the oscilloscope photograph. (a) Photoconductivity signal from a chloroplast sample. The time response of the recording system was 10^{-5} sec. The signal to noise ratio was about 4. The signal rises with the time constant of the detector. (b) Trace showing the form of the light flash as obtained from a PIN photodiode, time response 10^{-8} sec. The light energy corresponds to about 10 millijoules at the sample location.

To investigate the rise time further, I used a passively Q-switched ruby laser, which provided about 50 times more light energy at the sample site than did the xenon flash. The increased signal to noise ratio clearly established that the rise half-time of the photoconductivity signal was as short as the response time of the detection system, which in this experiment was improved to 4×10^{-6} sec. The theoretical time response limit for the microwave measurements in cavities with unloaded quality factors of the order of 10^4 is about 10^{-6} sec. The few microsecond time response of my system was determined by the electronics. Measurements in cavities of lower Q-values would permit reaching a lower limit of 10^{-7} sec.

The laser experiments revealed a component, not observed with the xenon flash, with a decay half-time of around 200 microseconds. No decay components were observed between 200 microseconds and the 4 microsecond response time of the amplifier. Any component decaying in times shorter than a few microseconds would be recorded at the instrument-limited time of 4 microseconds.

2) Bacterial chromatophores

The photosignals from chromatophores showed a biphasic decay with a fast component in the millisecond range and a much slower component in the range of several seconds. The fast decay component was exponential in all cases. Figure 28 shows the fast decay of the photoconductivity signal of a R-26 chromatophore sample in response to 20 microsecond flashes. Figure 29 depicts its kinetic analysis. Figure 30(a) is the photoconductivity signal from a R-26 sample in response to 20 microsecond flashes at three values of light flux. The time response of the detection channel was 10 microseconds in that experiment.

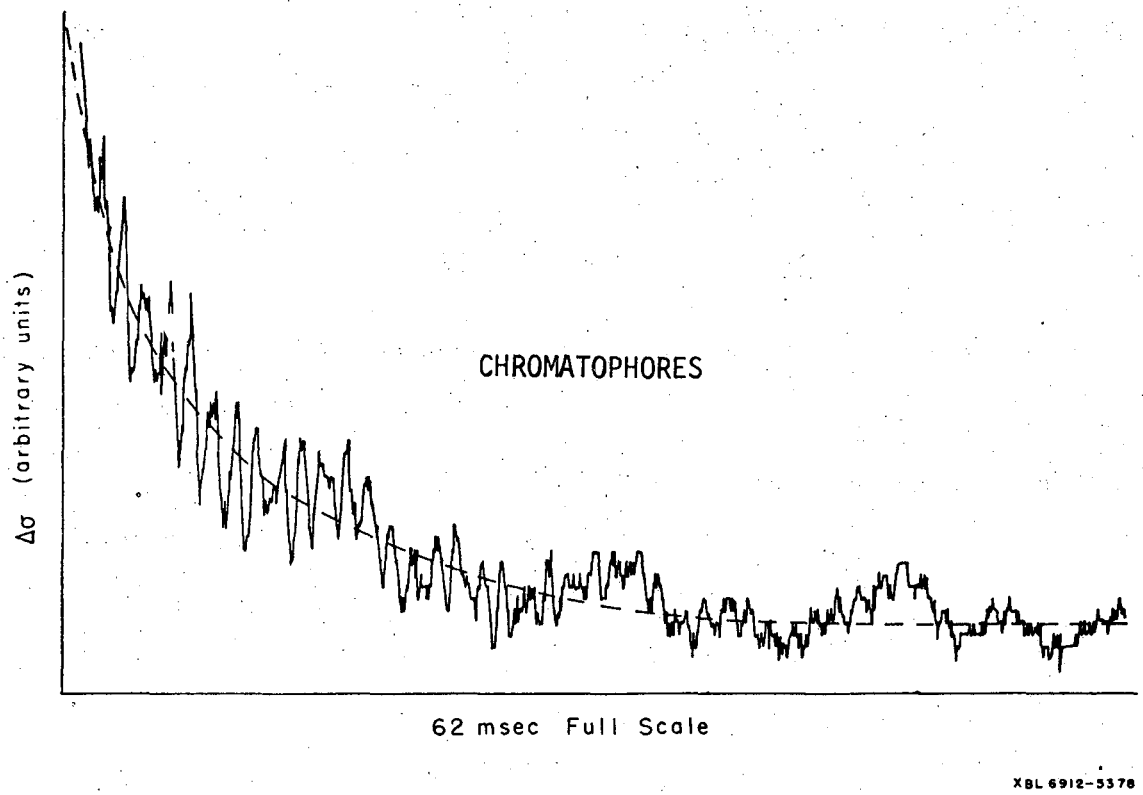

Figure 28. Fast decay component of R-26 chromatophores. Photoconductivity signal in response to a 20 microsecond flash. Light wavelength 600-900 nm. Light energy: 5 millijoule/pulse. The trace was recorded in a computer averager.

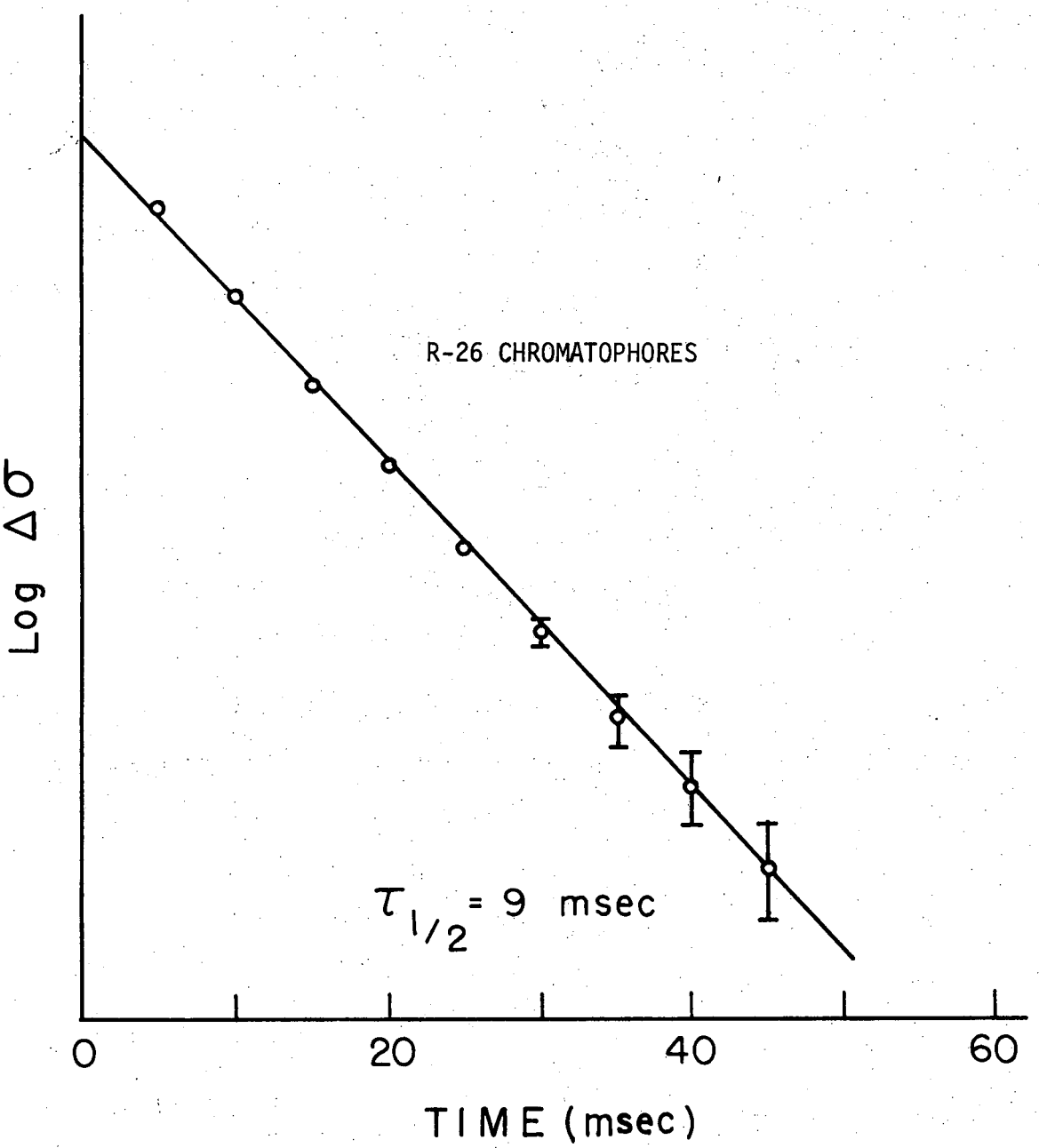

XBL 6912-5383

Figure 29. Kinetic analysis corresponding to Figure 28. The plot log $\Delta\sigma$ vs. time indicated a first order decay with a half-time of 9 milliseconds.

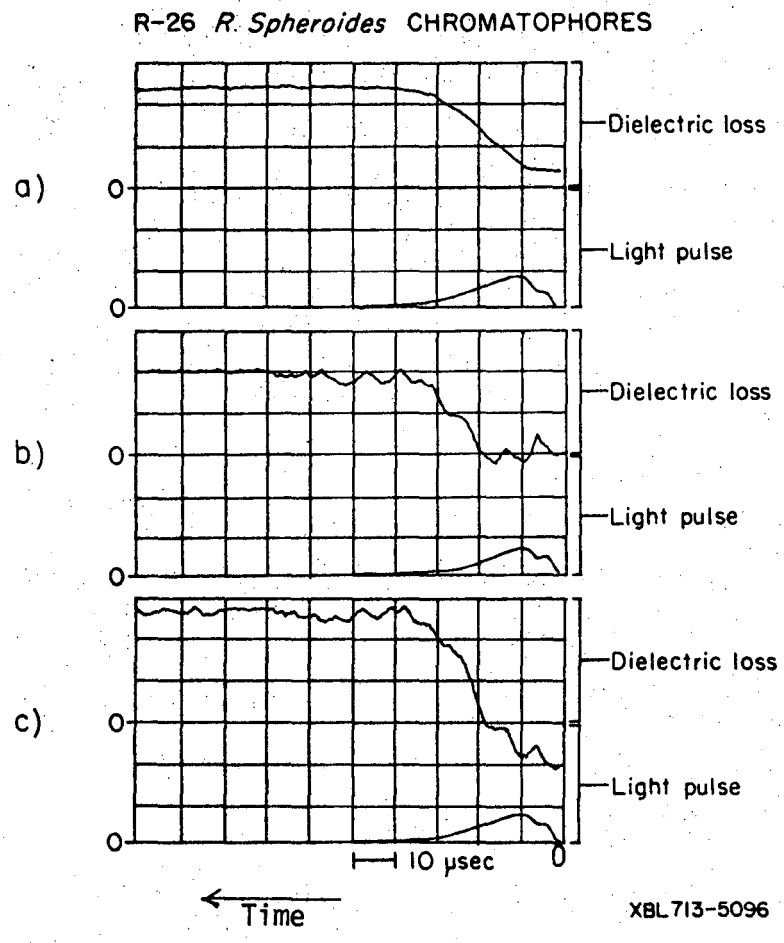

Figure 30. Photoconductivity signal in response to 20 microsecond light flashes (traced from the oscilloscope photograph). Trace (a): The light pulse is shown in the lower part of the oscilloscope scale; it was recorded with a PIN photodiode (time response 10^{-7} sec). The light energy was about 10 millijoules of white light per flash at the sample location. The upper part shows the photoconductivity signal; the rise time is instrument limited to about 10 microseconds. Trace (b): The light intensith is 60% of that in trace (a). The gain of the microwave detector is twice than in (a). Trace (c): The light intensity is 10%, and the gain is 10 times larger than in trace (a).

It may be seen that the onset of the signal is instrument limited. The lower trace is the light pulse as recorded by a PIN photodiode. The time response of the light measuring set-up was less than a microsecond.

Experiments with the ruby laser showed that the photoconductivity signal of a sample of R-26 chromatophores rose with time time constant of the detection system which was about 5 microseconds in those experiments.

An additional component with a decay half-time of 200 microseconds was observed.

c. Light Intensity Dependence

1) Chloroplasts

A plot of the fractional change in conductivity, $\frac{\Delta\sigma}{\sigma}$ vs. light energy per flash (20 microsecond flashes) shows that broken chloroplast samples followed a dependence of the form:

$$\frac{\Delta\sigma}{\sigma} = K I^n \quad , \quad \text{where}$$

$n = 1 \pm 0.15$ and I is the average number of photons per flash, varying from 10^{14} to 5×10^{16}.

Saturation of the photoconductivity signals was achieved only by using the laser as a light source. Saturation was obtained at about 5×10^{17} photons per pulse.

Long light pulses (20-100 milliseconds) were more effective for saturation of the photoconductivity signals. Light pulses (20 msec long) having the same total energy as the 20 microsecond flashes (10^6 ergs) completely saturated the photoconductivity. It should be noted that the peak power of the radiation is much smaller in the light pulse

than in the flash. A more detailed study of the phenomenon showed that long pulses produced a biphasic rise, with a fast component that practically followed the rise of the light pulse, and a slower one that reached a steady state value when the pulse length was increased to about 100 msec. Since it was not possible to standardize the samples' behavior to obtain reasonably reproducible results for experiments in which long light pulses were used, I proceeded with the use of pulses lasting less than 10 milliseconds for the rest of the work.

2) Bacterial chromatophores

As with the green plant material, the light intensity dependence of the photoconductivity signals in bacterial chromatophores was linear over a large range of intensities. Saturation was observed only in experiments with the laser at light intensities close to 10^{17} photons per pulse.

The photosignals for R-26 chromatophores at three intensities of the 20 microsecond flashes are shown in Figure 30. The rise time of the signals is instrument limited to about a rise time of 10 microseconds.

Figure 31 is a plot of photoconductivity vs. light intensity for two different illumination conditions, the 20 microsecond flash and long pulses of 20 millisecond provided by the tungsten-iodine stepping motor source. As was observed for green material, long pulses containing the same energy per pulse as the short pulses were more effective in showing saturation effects of the photoconductivity. The photoconductivity response to the long pulses shows signs of nonlinearity at 10^{15} photons per pulse. Figure 32 shows the photoconductivity signal in response to four consecutive 20 microsecond flashes

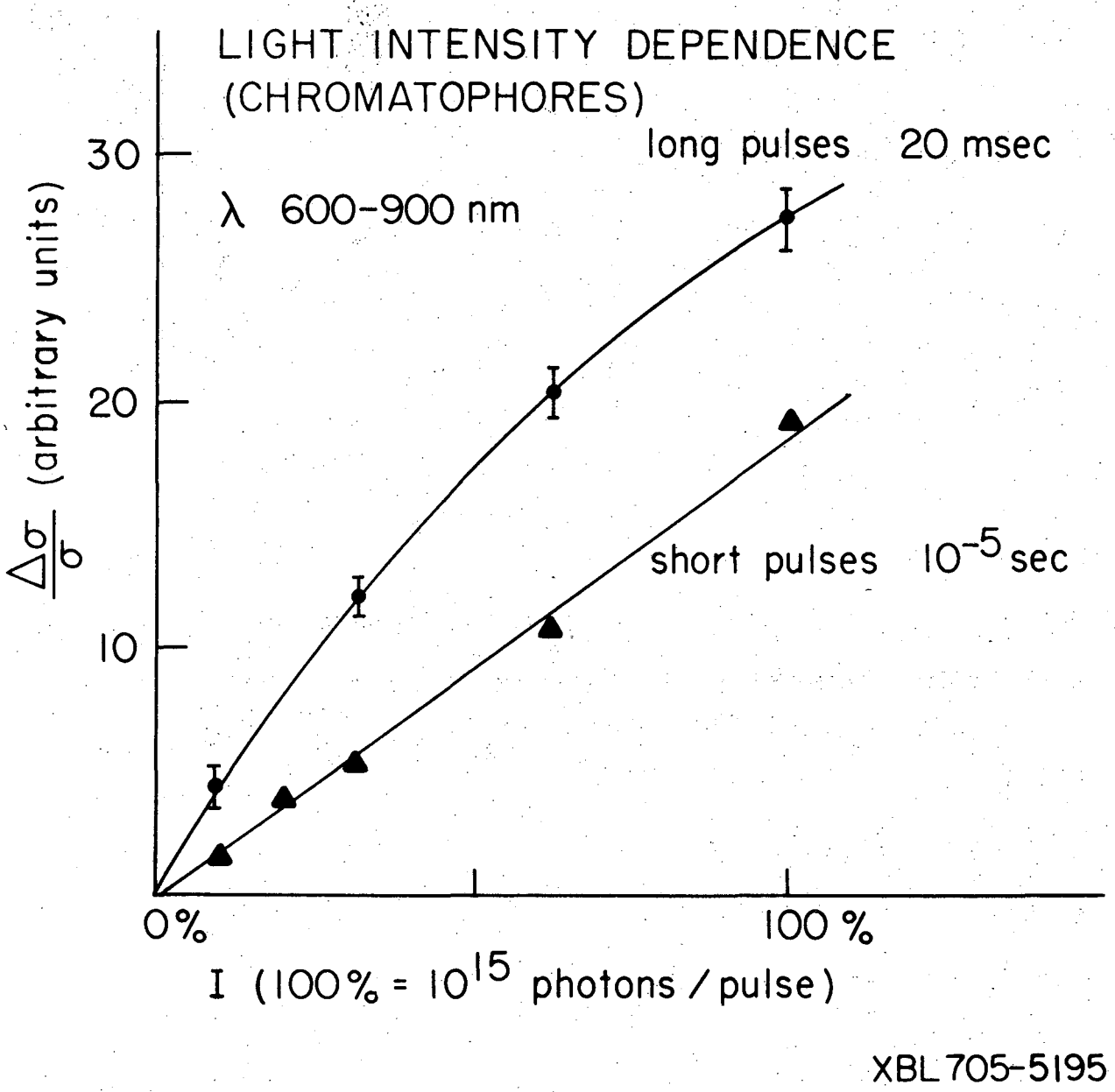

Figure 31. The photoconductivity responded linearly to light intensity for short flashes up to 10^{15} photons/flash. Evidence of saturation may be observed for the longer pulses.

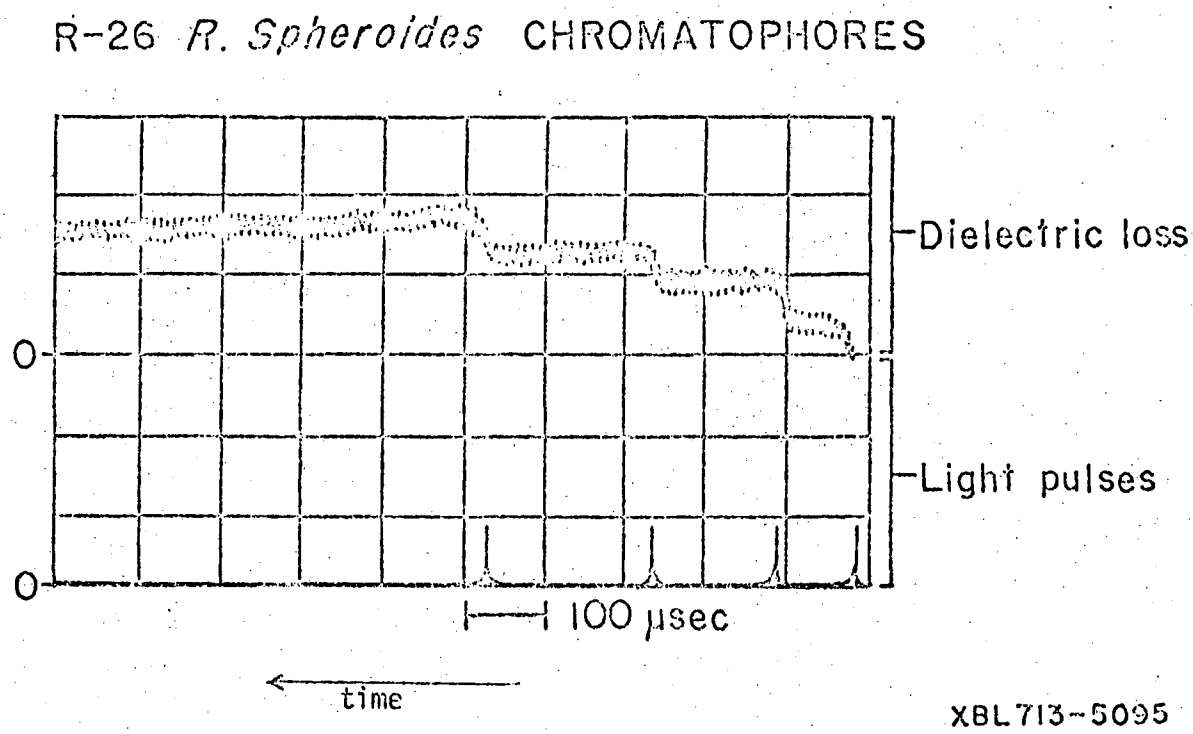

Figure 32. Response of the system used in Figure 30 to four consecutive flashes. The light intensity corresponds to that of trace (a) of Figure 30.

of equal intensity of about 5 millijoules/flash. The sample shows no sign of saturation.

d. Temperature Dependence

1) Chloroplasts

Experiments on chloroplast films showed that the peak photoconductivity, $\Delta\sigma$, followed a dependence on temperature of the form:

$$\Delta\sigma = K e^{-E_a/KT}$$

between 40° and -40°C. At the lower temperature a phase transition was observed, resulting in a sudden change in the cavity quality factor. Such a transition was not observed in the samples dried to constant weight in a P_2O_5 desiccator. I attribute the effect to the freezing of bound water (Kuntz, 1969). Figure 33 shows the temperature dependence of the photoconductivity of a chloroplast sample dried under nitrogen gas flow. The activation energy was about 0.3 eV above the transition temperature for both chloroplast and quantasome aggregate samples.

As the temperature was lowered, the slow component of the decay (seconds range) was either inhibited or frozen-in at -5°C. The fast component (10-20 millisecond) slowed continuously until at -80°C the decay half-time was several hundred milliseconds. The remaining signal at -80°C was about 0.5% of that at room temperature. At -150°C the decay rate and the signal intensity increased to about 100 milliseconds and 5% of the room temperature value, respectively.

2) Bacterial chromatophores

A plot of the logarithm of the peak photoconductivity as a function of the inverse of the absolute temperature gives a linear behavior

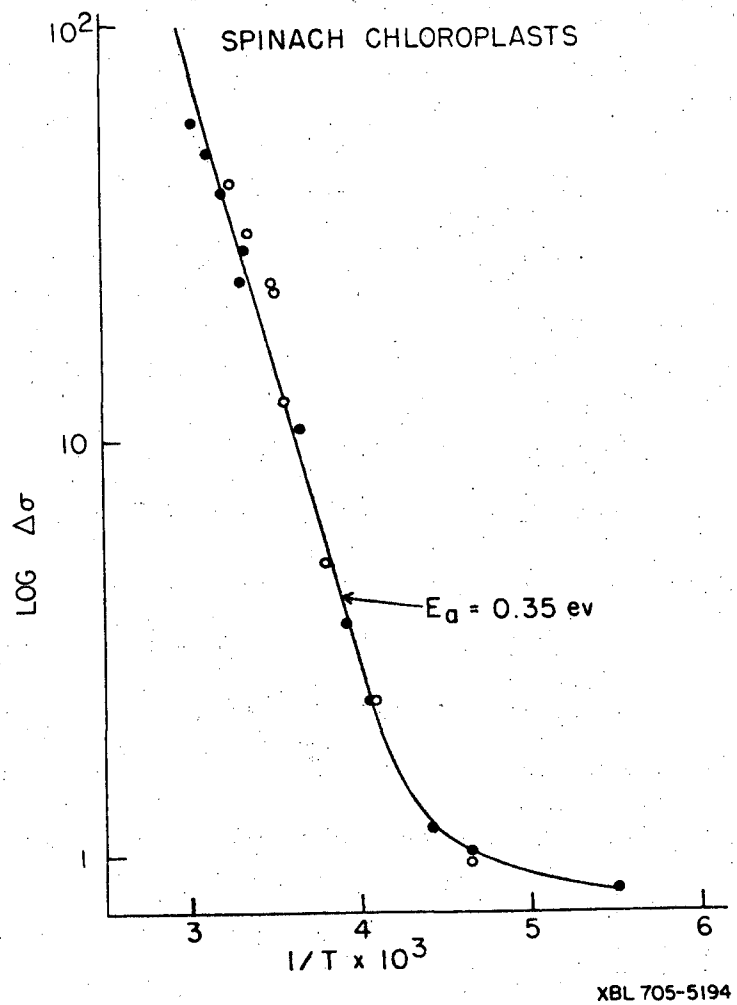

Figure 33. Temperature dependence of the photoconductivity of chloroplasts. Ten msec pulses of white light as described in Figure 25 were sent to a chloroplast sample. The temperature was modified by nitrogen gas flow as described in Chapter II. The signal peak height is labeled $\Delta\sigma$. A plot log $\Delta\sigma$ vs. 1/T where T is the absolute temperature, shows a dependence of the form: $\Delta\sigma = Ke^{-E_a/KT}$ over an extended range. The full dots indicate data when the temperature was lowered and the open dots the peak conductivity values as the temperature rose back. The activation energy, E_a, from 1/T x 10^{-3} to 4 x 10^{-3} was in this sample E_a = 0.35 eV.

between 40 and -40°C with an activation energy of about 0.3 eV for practically all samples.

The decay time of the millisecond component was temperature dependent in all samples including the PM-8 chromatophores. Figure 34 shows the effect of lowering the temperature for the PM-8 sample. An activation energy calculated for the decay half-time of the fast component of that sample gives a value close to 0.2 eV. That value was typical of most bacterial chromatophore samples. The bacterial chromatophores also showed a phase transition at about -35 to -40°C. A similar transition was observed by de Vault and Chance in frozen Chromatium cell preparations when measuring the cytochrome oxidation absorbance changes. As for the green plant material, I attribute the effect to the freezing of bound water (Kuntz, 1969).

The several-second component of the decay was completely frozen at -35°, but in distinction with the behavior of the chloroplast samples, the fast component of the decay was much less affected by temperature. It steadily increased to about 50 msec at -40°C, remaining rather constant down to -150°C. The magnitude of the remaining signal was also comparatively larger than in chloroplasts. About 10% of the photoconductivity at room temperature remained at -150°C.

Table IV summarizes the photoconductivity results in R. spheroides chromatophores discussed this far.

e. Action Spectrum and Relative Quantum Yield

1) Chloroplasts

The relative quantum yield was obtained as the ratio between the photoconductivity and the absorbance at the same wavelength. This ratio would be proportional to the number of charge carriers per photon

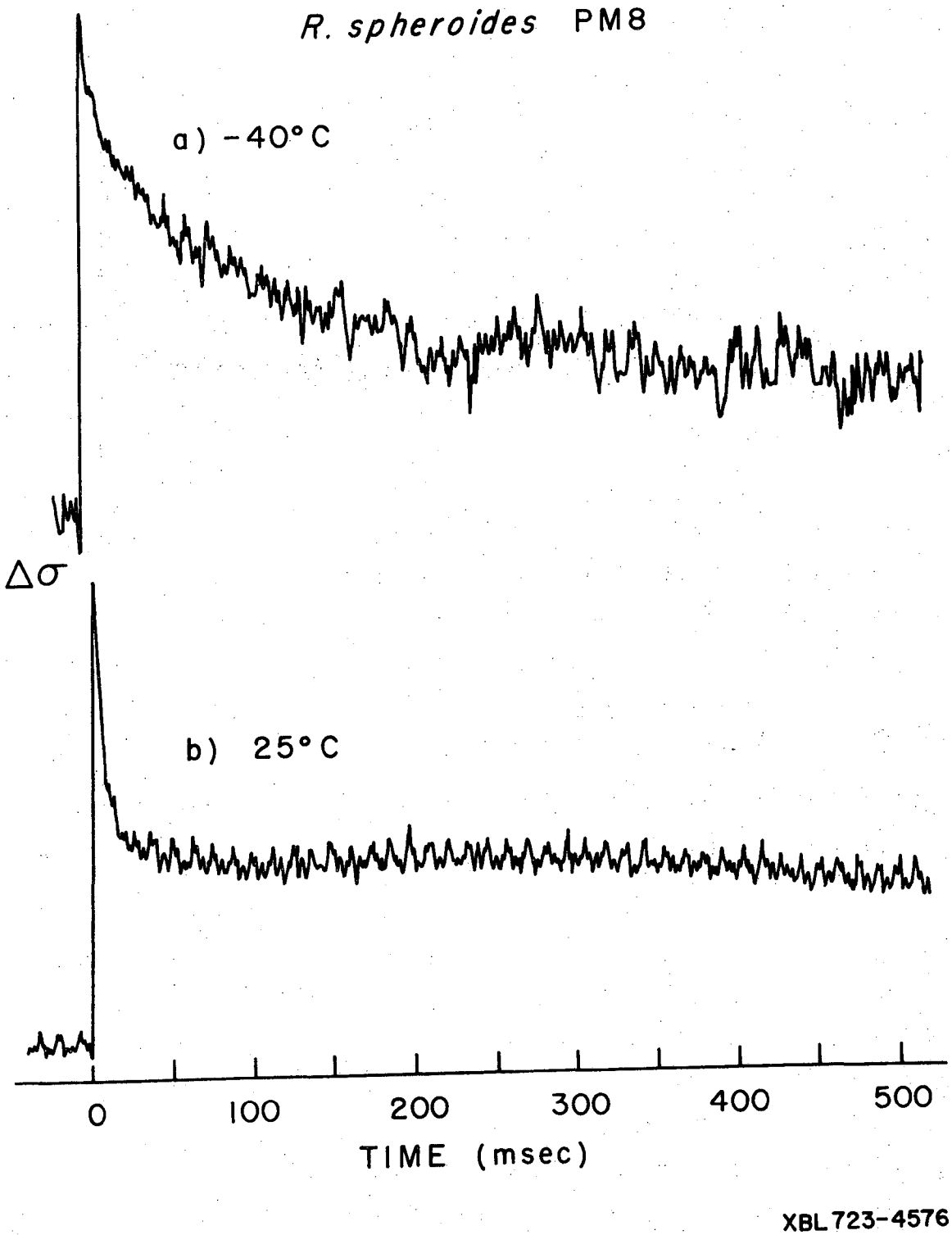

Figure 34. Temperature dependence of the decay kinetics. Photoconductivity of a film of R. spheroides, strain PM-8, in response to one millisecond flashes.

Table IV. Bacterial Chromatophores

R. spheroides Photoconductivity Measurements

Sample	Light intensity dependence**	Saturation intensity	$E_{activation}$	Kinetics Decay rise		
	n	I_{sat}	eV	fast* (msec)	slow (sec)	sec
R-26***	1 ± 0.2	$\sim 5 \times 10^{16}$ photons/flash	0.3 ± 0.1	10-20	4-5	$< 5 \times 10^{-6}$
G.A.	1 ± 0.2	---	0.3 ± 0.1	8-50	1-5	$< 10^{-3}$
PM-8	1 ± 0.1	---	0.2 calculated from the decay half-times vs. temperature	5-10	5-10	$< 10^{-3}$

* First order decays.

** It is assumed that a dependence of the form $\Delta\sigma = KI^n$ is followed by the samples. I is the light intensity (not larger than 10^{15} photons/pulse).

*** A rise kinetic component with a half-time of 200 microseconds was observed for this mutant under laser excitation.

provided the mobility of the carriers is not affected by light.

The chloroplast films were not optically clear. Measurements of the absorption spectrum were not very reproducible between different samples, probably due to self-absorption effects and scattering. For that reason a much smaller amount of material was used in order to obtain chloroplast films with a reasonably good absorption spectrum.

This latter restriction produced a poorer signal to noise ratio than in most other photoconductivity measurements.

Figure 35 shows the action spectrum, absorption spectrum and their ratio, which is labeled relative quantum yield, of a chloroplast sample. The action spectrum shows a shoulder at around 700 nm which is not visible in the absorption.

Measurements performed by Blyumenfeld et al. (1970), with better spectral resolution, show two regions of spectral sensitivity, one around 650-680 nm and another at about 700 nm. An interesting observation, that I was able to reproduce, was that very careful desiccation (lyophilization and immediate sealing of the samples) results in the disappearance of the photoconductivity signal at 700 nm. The 650-680 region is not affected. It is known that the EPR signal is completely "frozen-in" under such conditions. It might be of interest to determine the light induced absorbance change simultaneously with the photoinduced EPR signal and the photoconductivity. It is known that the light induced absorbance changes originating at the reaction centers are also affected by the hydration state of the samples. Recent reports show that a chlorophyll-water interaction might play an important role in the process of charge separation (Katz, 1971).

In section A it was shown that the dark losses were temperature dependent. Therefore it was necessary to determine the relevance of a possible artifactual signal arising from thermal modulation of the dark losses. Two experiments were performed on chloroplasts in an attempt to investigate the thermal effect of the light.

In a first experiment I found that the thermal activation energy for the dark conductivity of a chloroplast sample was about 0.4 eV.

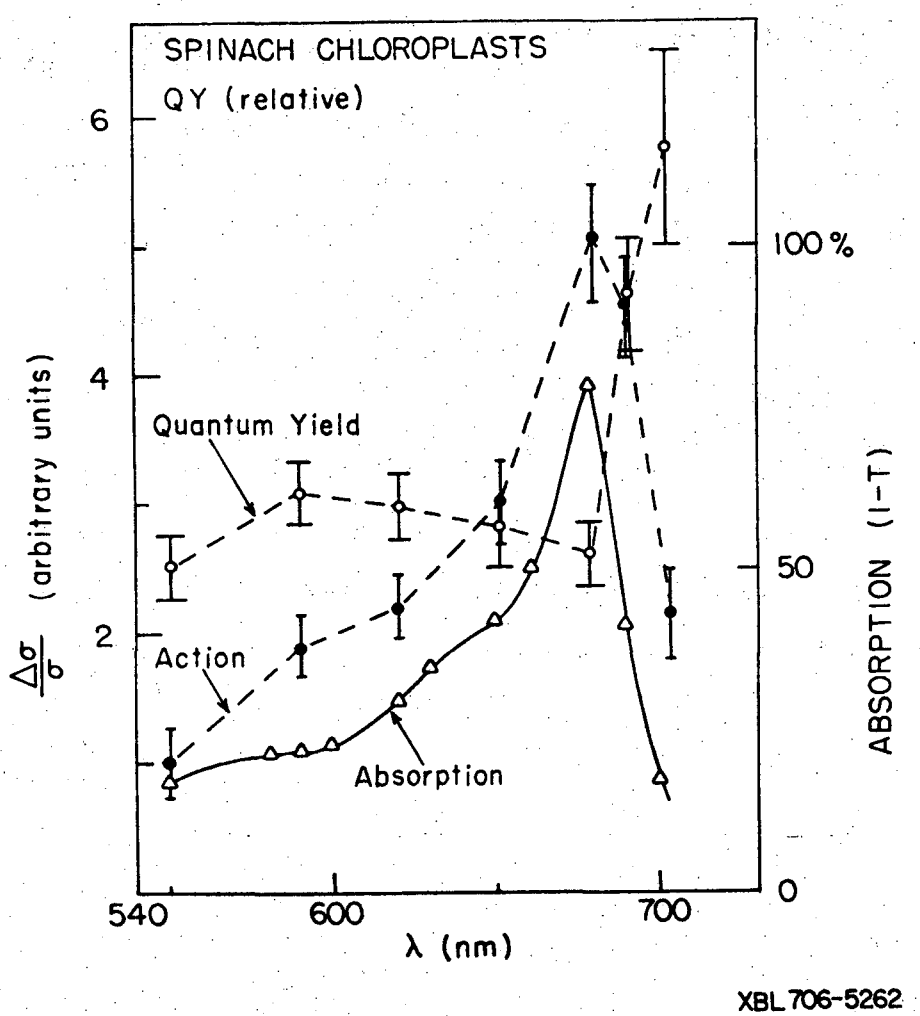

Figure 35. Photoconductivity action spectrum and relative quantum yield. o: Action spectrum of the fractional photoconductivity. The points are normalized to constant incident light intensity. The 550 nm reading was arbitrarily given a value of 1. ●: Ratio $\frac{\Delta\sigma}{\sigma}$/% absorbance (labeled relative quantum yield). Δ: Absorption spectrum of the chloroplast film.

(The four conductivity values taken between 5 and 40°C followed very closely an exponential behavior when plotted versus the inverse of absolute temperature.) Assuming a heat capacity of 1 cal/degree gram, the temperature rise of a 20 mg sample would be about 10 millidegrees when a light pulse of 1 millijoule is completely degraded into heat. The predicted value for the fractional change in conductivity due to heating under such conditions is $(\frac{\Delta\sigma}{\sigma})_{heat} = 3 \times 10^{-4}$. The actual experiment performed under the above conditions using the one millisecond strobe flash attenuated to about one millijoule per pulse gave a photosignal $\frac{\Delta\sigma}{\sigma} = 6 \times 10^{-3}$, which is about 20 times larger than the predicted thermal modulation.

In a second experiment infrared light between 2 and 4 microns, where the sample is known to absorb, produced a change in conductivity of a chloroplast sample which was less than 5% of that produced by an equal incident power per unit area of visible light between 550 and 700 nm.

Both experiments lead to the conclusion that the possible thermal modulation of the dark losses, due to the conversion of the absorbed visible radiation into heat, does not account for the photoconductivity signals. The conversion of light into heat might account for the small photosignals observed in samples heated at 100°C for several minutes, which showed slow rise and decay times in the many hundreds of milliseconds, and were about 10% of the signal obtained from the native samples.

2) Bacterial chromatophores

Since the chromatophores produced clear films, it was possible clearly to rule out the direct heating effect of the light. An infrared

absorption spectrum, Figure 36, shows that the sample of R-26 absorbs strongly between 3 and 4 microns. Infrared radiation was obtained from a 1200 Watt tungsten projection lamp and by a combination of filters constrained to a band between 1.5 and 6 microns. The upper limit determined by the absorption of the pyrex glass optics and a glass light pipe. The incident infrared light power per unit area was about 3 times larger than that of visible illumination provided by a combination of the same light source with a 4 cm water filter and an interference filter with a band pass between 600-900 nm. The photoconductivity signals from the R-26 chromatophore sample in response to the infrared illumination were smaller than the noise level of my detection system. Illumination with the 600-900 nm source resulted in photoconductivity signals that were about 10 to 15 times larger than the noise level. Therefore I conclude that to this limit, the direct heating effect of light was not responsible for the observed photoconductivity effects at microwave frequencies.

Figure 37 shows the results of a measurement of the action spectrum for a wild type R. spheroides chromatophore sample. The absorption spectrum was obtained from the same sample in a Cary 14 spectrophotometer. The quantities were already defined in Figure 35. This sample also shows, as did the chloroplasts, a tendency to a larger relative quantum yield at long wavelengths.

2. Photo-Hall Measurements

a. Chloroplasts

As was described in Chapter II, a power unbalance signal is obtained from the balanced bimodal cavity when a magnetic field is applied. If the sample is located exactly at the antinode of the

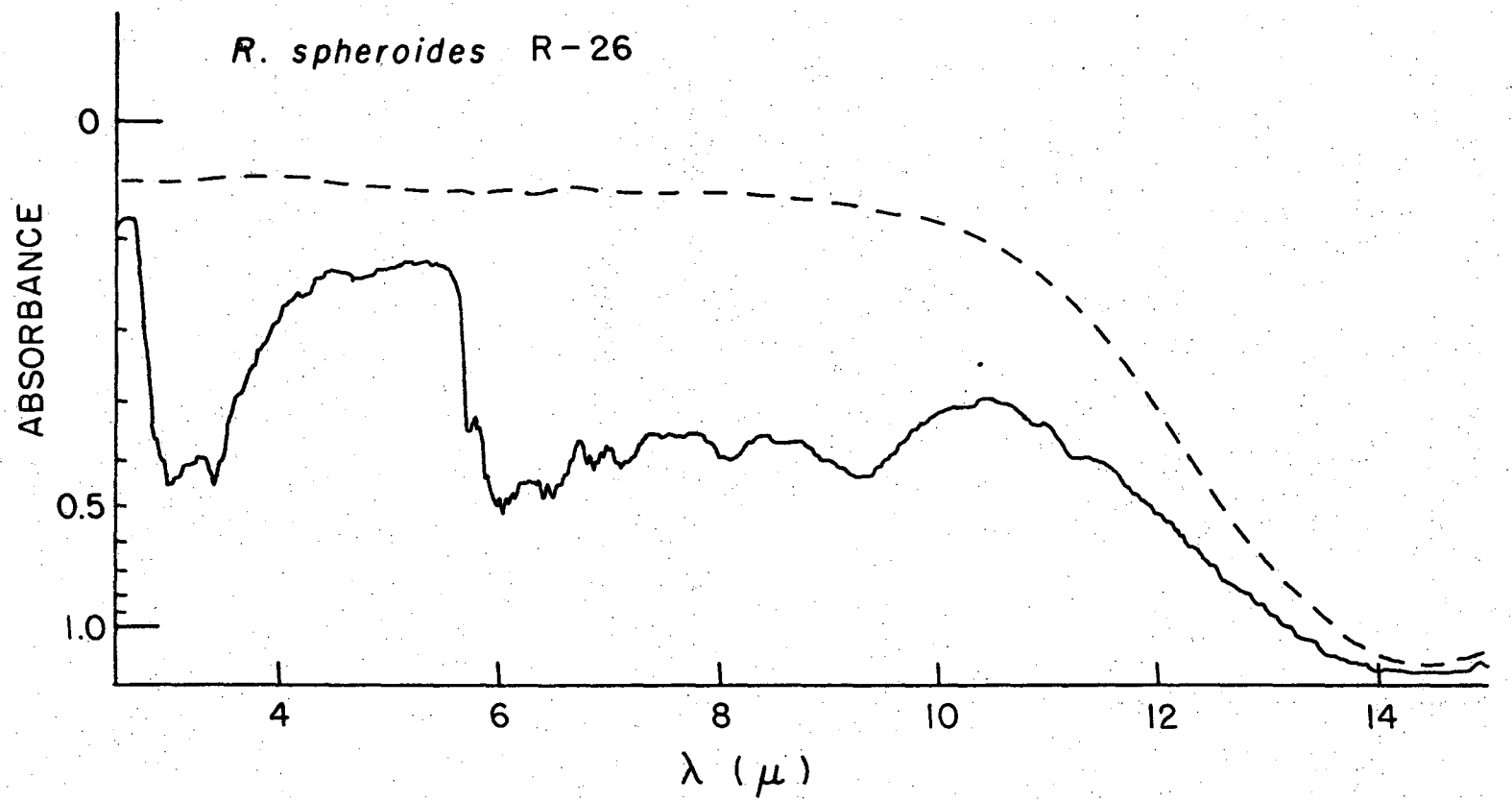

XBL706-5263

Figure 36. Infrared absorption spectrum of a film of R-26 chromatophores. -----Absorbance of the CaF_2 crystal which was used as a support for the film. ——Absorbance of the chromatophore film on the CaF_2 crystal. The instrument was a Perkin Elmer NaCl infrared spectrometer.

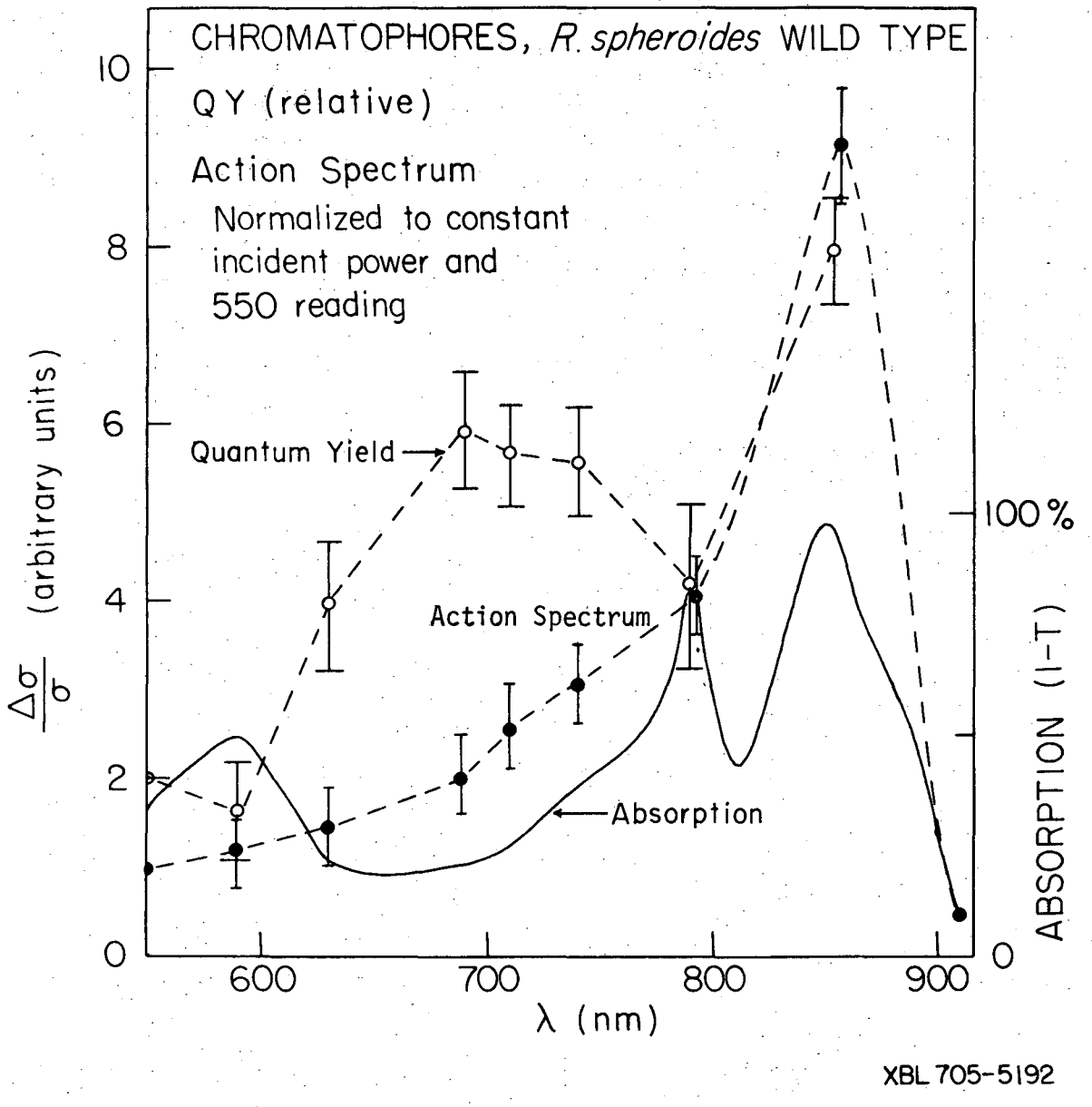

Figure 37. Photoconductivity action spectrum of a wild type R. spheroides chromatophore film. The quantities are as defined in Figure 35.

cavity electric field, the signal may be interpreted as due to the Hall effect resulting from the presence of mobile charge carriers in the sample.

When light is introduced as an additional perturbation, as discussed in Chapter II, two possible contributions to the observed signal have to be considered when interpreting the results. First, the effect of inhomogeneous illumination of the sample could result in a spurious rotation signal in the absence of a magnetic field, and second, a component of the unbalance power always results from the photoconductivity of the sample. This latter signal is not a change in coupled power due to a rotation, but simply a reduction in the intensity of the cavity fields due to the photoinduced sample losses. Therefore, before application of a magnetic field there may be an initial signal. Only the changes in coupled power due to the action of the magnetic field is to be considered as the Hall effect signal.

A method for extracting the Hall effect signal due to the photocarriers is to apply a pulse of light to a sample in the balanced cavity in the absence and in the presence of a magnetic field. The difference between the measured power unbalance signals is the rotation signal due only to the photocarriers. A control procedure to determine that the observed signal is indeed a rotation is to reverse the magnetic field direction. A Hall effect power unbalance signal adds to the zero-field signal with the magnetic field in a given direction and subtracts from it when the field is reversed.

Figure 38 shows the result of such a measurement in a chloroplast film sample. One millisecond light flashes produced the zero-field signal shown as trace (c). Traces (a) and (b) result upon application of a magnetic field of 10 Kgauss in opposite directions.

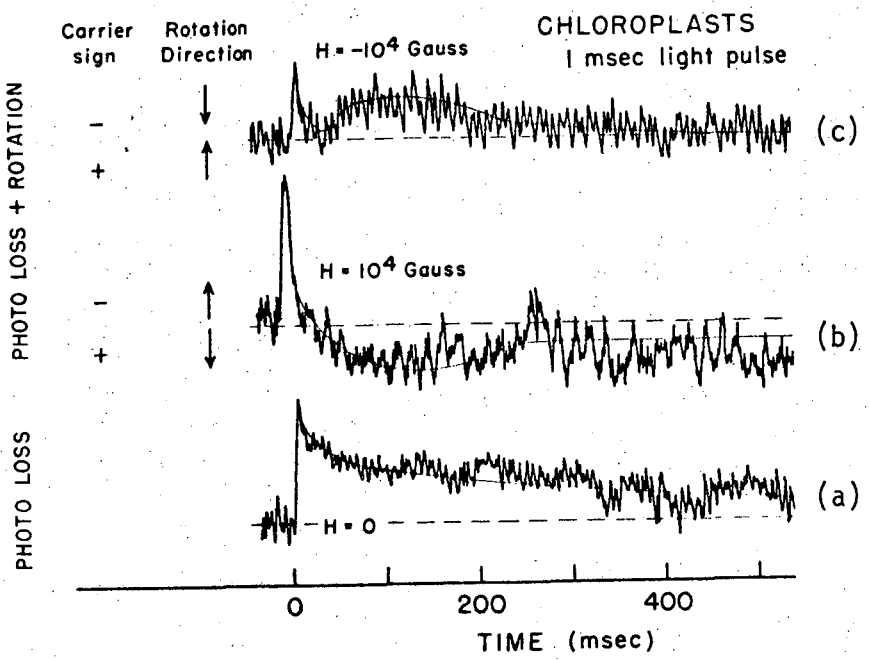

Figure 38. Hall effect. Pulsed measurement on chloroplasts. The experiment is described in the text. The direction in which the power unbalance should point for a given carrier sign is shown at the left. Trace (a): Zero field signal. Possibly contributed by the photoconductivity signal and some spurious rotation due to asymmetry in the location and illumination of the sample. Trace (b): A signal in the millisecond range corresponding to carriers of negative sign is added to the zero-field signal of trace (a). A slow rotation component is seen as a decrease in coupled power which peaks at about 100 milliseconds. Trace (c): The signal corresponding to carriers of negative sign points downwards and is subtracted from the zero-field signal. The slow component points in the reverse direction and also maximizes at about 100 msec.

The algebraic sum of trace (c) plus (b) should give back the signal of trace (a) with no field present. A fast component of a rotation signal is added in (b) and subtracted in (a) to the zero-field signal. A slow component with opposite sign shows a maximum at about 100 milliseconds. The averaging technique was employed for this measurement. Microphonic noise makes it rather difficult to follow the behavior of the slow component at times longer than 500 milliseconds. Nevertheless it is clear from this experiment that two rotation signals having different signs and different relaxation times are produced by illumination of the sample.

Figure 39 depicts the results of a similar experiment for 50 msec light pulses provided by the tungsten-iodine laser stepping motor system. A more complicated decay pattern, which may be decomposed into three or four rotation components, appears. This result is in agreement with previous observations (pg. 27, Chapter IV, this work) that longer illumination times result in a more complicated behavior of the photoconductivity kinetics and light intensity dependence.

The mobility of the photocarriers is computed from the peak value of the rotation signal. The values for the experiment in Figure 38 are:

$$\mu_- = 0.6 \text{ cm}^2/\text{volt}\cdot\text{sec}$$

$$\mu_+ = 0.4 \text{ cm}^2/\text{volt}\cdot\text{sec}$$

The procedure for the calculation of the Hall mobilities is given in Chapter II. However, it has to be noted at this point that only the photoinduced changes in the diagonal and off-diagonal elements of the conductivity tensor should enter the computation of the photo-mobilities. The former is simply the photoconductivity of the sample.

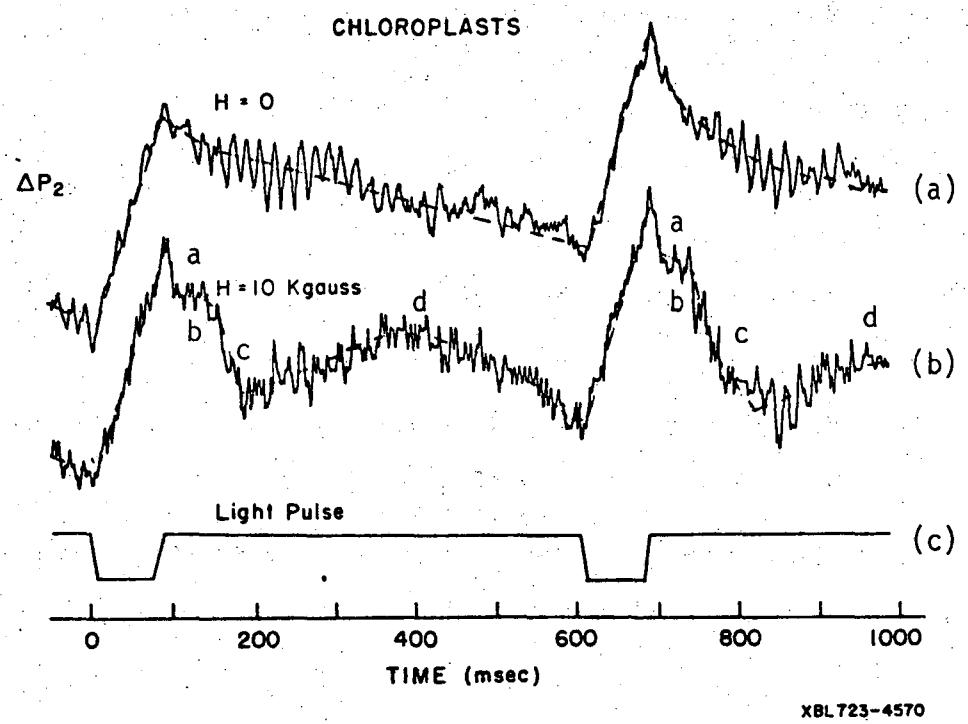

Figure 39. Photo Hall effect, pulsed measurements. The experiment is similar to the one described in Figure 38, the only difference being in the length of the light pulses and the pulsing frequency, which in this case is 1.8 Hz. Trace (a): The zero field signal as recorded from the computer averager after 50 passes. Trace (b): The photosignal with a 10 Kgauss magnetic field applied to the sample. For the direction of the applied magnetic field an increase in power unbalance corresponds to positive carriers (upwards deflection). The main feature of Trace (b) is the appearance of a sequence of components, two possibly pointing downwards (negative carriers, a and c) and one or two in the reverse direction (b and d). Trace (c): The light pulses recorded simultaneously by a silicon S1020 photocell.

The latter is given by the rotation photosignal. The Hall angle is given by their ratio. The photoconductivity was measured in the bi-modal cavity by unbalancing the cavity with the capacitive plugs. The photo-rotation measurements were performed by unbalancing the cavity with the resistance plugs. The two measurements were performed sequentially with the same sample under identical conditions of illumination.

Table V summarizes the results of the pulsed measurements on three chloroplast samples. Sample a corresponds to the data presented in Figure 38.

Table V. Light Measurements in Chloroplast Films

Sample	$\Delta\sigma/\sigma$	σ_{dark}	Light* intensity	Carrier sign	Photo-Hall mobility, μ_L	Life-times	Δn
	$\times 10^{-3}$	$\Omega^{-1}cm^{-1}$	$\frac{joule}{flash}$		$cm^2/volt \cdot sec$	msec	# Photo-carriers
a	2	1×10^{-3}	10^{-3}	-	0.6 ± 0.3	15	5×10^{12}
				+	0.4 ± 0.2	100	
b	5	2×10^{-3}	10^{-3}	-	0.9 ± 0.4	10	10^{13}
				+	0.6 ± 0.3	150-200	
c	1	1×10^{-3}	10^{-3}	-	0.3 ± 0.2	10	10^{13}
					0.4 ± 0.2	100	

* 1 msec xenon flash, white light

The photocarrier concentration was calculated by assuming that the photoconductivity signal results from a change in the concentration of carriers alone. Rigorously, $\Delta\sigma/\sigma = \Delta n/n + \Delta\mu/\mu$, but it is assumed in the calculation that the second term is smaller than the first. The calculation is as follows:

If $\sigma_{dark} = nq\mu$, where σ is the conductivity, q is the carrier charge and μ the mobility, then it is assumed that $\Delta\sigma = \Delta nq\mu$.

Since $\Delta\sigma/\sigma_{dark}$ and σ_{dark} are measured, the value of $\Delta\sigma$ is computed. Then:

$$\Delta n = \frac{\Delta\sigma}{q<\mu>} \quad \# \text{ carriers/cm}^3$$

I used for the calculation an average value of μ, between positive and negative values, e.g. $<\mu> = 0.5$ cm^2 volt·sec for sample (a). Δn is obtained as a carrier concentration. To compute the absolute number of generated photocarriers, that value was multiplied by the sample volume.

b. Bacterial Chromatophores

The chromatophore samples behaved in a fashion similar to the green material. A sign reversal of the rotation signal was observed in all the normal mutants. Figure 40 shows the rotation signal in an R-26 chromatophore sample. Trace (a) is the light pulse as measured by the silicon photocell. The frequency components below 10 Hz are excluded by use of the amplifier roll-on filter. This procedure was used to enhance the observation of the sign reversal which in previous measurements was perturbed by the low frequency microphonic noise components. Trace (b) shows the rotation signal for chromatophores. A downwards deflection corresponds to negative charge carriers. A field of 10 Kgauss is applied in the experiment. The positive carrier rotation component maximizes in the chromatophore sample about 10 msec after the flash, by contrast with the chloroplast samples that gave a positive carrier component in the 100 msec range. Trace (c) is the photoconductivity response of the same sample. Fortunately, it was

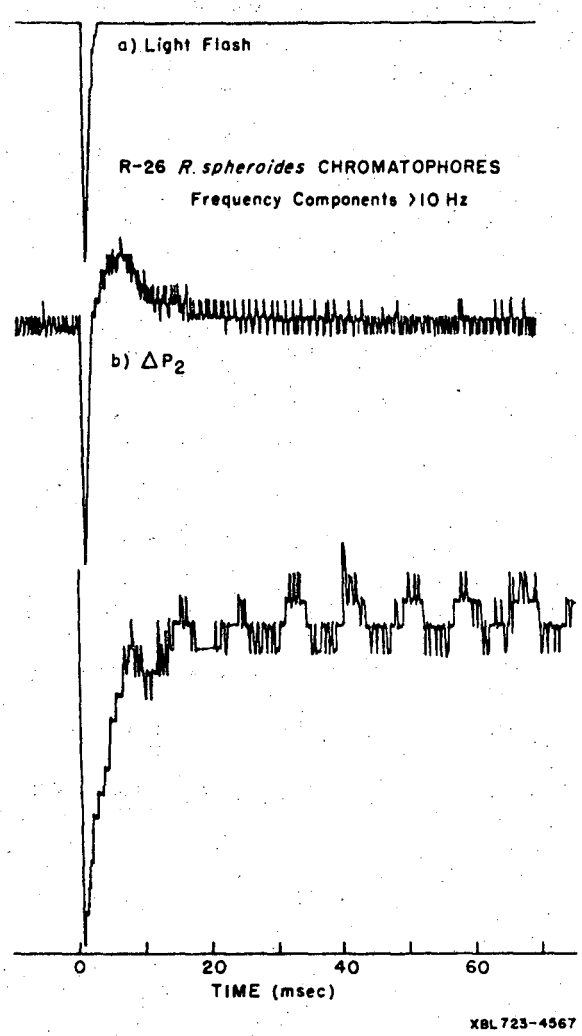

Figure 40. Photo Hall mobility measurement of R-26 chromotophores. (a) The light flash is recorded by the silicon photocell. (b) Power unbalance signal due to a Hall effect rotation. A downward deflection indicates carriers of negative sign. (c) Photoconductivity signal from the same sample (shown pointing downwards for convenience).

possible with this sample to minimize the baseline spurious rotation and photoconductivity signal to a level below the noise. Therefore, trace (b) is seen as a pure rotation signal. Trace (c) was obtained with reactive unbalance of the cavity where rotations do not contribute to the photosignals.

Table VI summarizes the measurements of photomobilities for the R. spheroides mutants.

The typical sign reversal was not observed on the PM-8 mutant samples.

Table VI. Photo-Hall Mobility Measurements

Bacterial Chromatophore Films

Sample	$\Delta\sigma/\sigma$	σ_{dark}	Light* intensity	Carrier sign	Photo-Hall mobility, μL	Life-times	Δn
		$\Omega^{-1}cm^{-1}$	$\frac{joule}{flash}$		$cm^2/volt \cdot sec$	msec	# Photo-carriers
R-26 (Ave. 3 samples)	3×10^{-3}	2×10^{-3}	10^{-3}	-	0.8 ± 0.3	5-8	10^{12}
				+	0.3 ± 0.1	20-50	
G.A. (Ave. 3 samples)	2×10^{-3}	1×10^{-3}	10^{-3}	-	0.4 ± 0.2	5-10	10^{12}
				+	0.2 ± 0.1	30-100	
RM-8	1×10^{-4}	10^{-4}	10^{-3}	-	0.1 ± 50	5	10^{10}

* 1 msec xenon flash, white light

Since there are other mechanisms which could give rise to a Faraday rotation, such as the interaction of paramagnetic center with the microwave magnetic field, the sample position was varied along the Z axis of the cavity and the dark and photoinduced rotations were measured. It was clear that the maximum value for the effect was

obtained with the sample located at the center of the cavity where the electric field is a maximum. Other effects, such as gross orientation of sample components in a magnetic field due to anisotropy in the magnetic susceptibility, although not impossible, have to be considered very unlikely to occur in our dehydrated specimens. Such orientation effects have been detected for whole thylakoid structures in solution (Geacintov et al., 1971).

3. Quantum Yield and Pigment Units

The values of the pnotomobilities now available permit an order of magnitude estimation of the quantum yield for the process of carrier generation by light.

Several experiments for the determination of the necessary parameters for the evaluation of the quantum yield were performed on chloroplast and R-26 bacterial chromatophore film samples. The dispersion in the values for samples of the same batch never exceeded a factor of two.

Measurements were performed of the absolute conductivity, the photoconductivity, the light energy per pulse, the sample optical density at the actinic light wavelength, the total chlorophyll (or bacteriochlorophyll) content, and the sample volume.

An outline of the calculation follows: The conductivity, σ, is given by $\sigma = nq\mu$, where n is the carrier concentration, q the charge, and μ the charge mobility. It is assumed that a light pulse produces an excess carrier concentration Δn, and the mobility is constant. Hence,

$$\Delta n = \frac{\Delta\sigma}{q\mu}$$

The total number of carriers generated over the volume of the sample is n_s: $n_s = \Delta n \cdot v_s$, where v_s is the volume of the sample.

The Quantum Yield, QY, is given by:

$$QY = \frac{n_s}{(h\nu)_\lambda}$$

where $(h\nu)_\lambda$ is the total number of photons absorbed by the sample.

The maximum value for the quantum yield is obtained in the linear range of photoconductivity response to light intensity. This is the case for the biological samples tested at low light intensities.

The size of the pigment unit that generates a single carrier is estimated from the value of the photoconductivity at saturating light intensities. The number of pigment molecules per charge carrier is denominated Pigment to Carrier Ratio, PCR:

$$PCR = \frac{\text{Total number of chlorophyll molecules/sample}}{\text{Maximum number of carriers/sample}}$$

where the maximum number of carriers = $\Delta\sigma$ (saturation) / $e\mu$.

The results for two selected samples are given in Table VII. In every case, QY is evaluated at low light intensities and PCR at saturation. Two values are reported for QY and PCR. They correspond to the upper and lower limit set by the dispersion in the experimentally observed mobilities. The values used for the photomobilities were 1 cm^2/volt·sec and 0.1 cm^2/volt·sec as the upper and lower limit, respectively.

Both calculations were performed with values of photoconductivity obtained from the peak height of the signals. Therefore, if there are kinetic components rising and decaying in times much shorter than the few microsecond time response of the microwave instrument, the magnitude of the observed signals might be considerably smaller than the

Table VII. Light Intensity Saturation and Quantum Yield Data for Two Selected Samples

Sample	I	$\Delta\sigma/\sigma$	Total Chl	σ_{dark}	Sample volume	*QY = Quantum yield (1)	**PCR = Pigment to carrier ratio (1)
	photons / flash		mg / sample	Ω^{-1} cm^{-1}	cm^2	carriers / photon	pigment molecules / carrier
Chloroplasts	10^{14}	5×10^{-5}					
N_2 dried	10^{15}	7×10^{-4}					
Sample OD_{694} = 1.8	10^{16}	6×10^{-3}					
Light source:	5×10^{16}	1.5×10^{-2}	34×10^{-3}	4×10^{-3}	4×10^{-2}	10^{-3} - 10^{-2}	10^3 - 10^2
ruby laser	10^{17}	2.0×10^{-2}					
λ = 694 nm	10^{18}	2.2×10^{-2}					
R-26							
Chromatophores	10^{14}	4×10^{-4}					
Sample OD_{850} = 1.4	10^{15}	3.6×10^{-3}	15×10^{-3}	2×10^{-3}	1×10^{-2}	10^{-3} - 10^{-2}	5×10^2 - 5×10
Light source:	10^{16}	1.2×10^{-2}					
20 μs xenon flash	10^{17}	1.3×10^{-2}					
Filter bandwidth							
750-900 nm							

*Computed for the linear response region (10^{14} photons/flash) of the photoconductivity.

**Computed for the saturating light intensity photoconductivity value.

(1) The two values reported correspond to the upper and lower limits, determined by the dispersion in the values of the photomobilities used in the calculation. The details of the calculation are given in the text.

true peak values, thus resulting in an underestimation of QY. Moreover, any refinement in the above calculations, such as the effects of trapping, would result in an increased value for the "true" quantum yield.

4. Effects of Some Chemical Agents on the Photoconductivity

Assuming that the observed effects are indeed due to photogenerated charge carriers, it is not clear how they are related to the functioning of the photosynthetic apparatus.

My approach was to apply to the samples some chemical agents known to perturb the photosynthetic apparatus, and as an indicator of the activity I tested the same samples for the presence of light-induced EPR signals.

I proceeded to investigate the action of substances such as DCMU, (3-(3',4'-dichlorophenyl)-1,1-dimethylurea), PMS, (phenazine methofulfate), O-phenanthroline, ascorbate, and some redox agents such as ferricyanide and ferrocyanide ions and dithionite, by incubating the samples with the agents before the mounting and dehydration procedure.

Observations under those conditions are very irreproducible. Once the sample is dehydrated the chemicals crystallize in the sample and it is difficult to distinguish between any true effect and gross denaturation. Therefore, I proceeded to mount the samples following the geometry used for the ZnO crystals. The suspension of photosynthetic material is spun down in a cylindrical (4 mm diameter) tube and mounted in the cavity as described in Chapter IV. Photoconductivity measurements without any addition are taken; and then the sample is resuspended, incubated with the desired chemical agent, centrifuged again and repositioned in the cavity.

The alternative method of adding a small crystal of the desired chemical to the supernatant solution, followed by observation of the changes as it dissolved and diffuses into the chloroplast sample, proved to be very useful because it introduced a rather small perturbation to the microwave system tuning. The presence of a sample with different composition and different dielectric constant, implying a different resonance frequency for the cavity, does not permit any quantitative conclusion from this kind of experiment. Nevertheless, qualitative observations regarding changes in kinetic properties are valid.

The only consistently reproducible observation was the action of K ferricyanide solution. A drop of a 10% solution of ferricyanide in the supernatant resulted in the gradual disappearance of the fast decay component. Since I cannot compare signal intensities (the system required retuning), it is impossible to distinguish between inhibition or stabilization of the decay component. Figure 41 shows the effect on chloroplasts. The upper trace (a) shows the signal before any addition. The fast component accounts for as much as 50% of the total photoconductivity signal. The middle trace (b), taken about 2 minutes later, shows the gradual lengthening of the fast decay (or alternatively its partial inhibition). The last trace (c), taken 5 minutes after trace (a), shows the virtual disappearance of any decay component shorter than hundreds of milliseconds.

Ferricyanide produces stabilization of the EPR signal at g = 2 in chloroplasts as well as in bacterial chromatophores, possibly by maintaining the reaction center chlorophyll species, which is assumed to produce the signal, in its oxidized radical cation state.

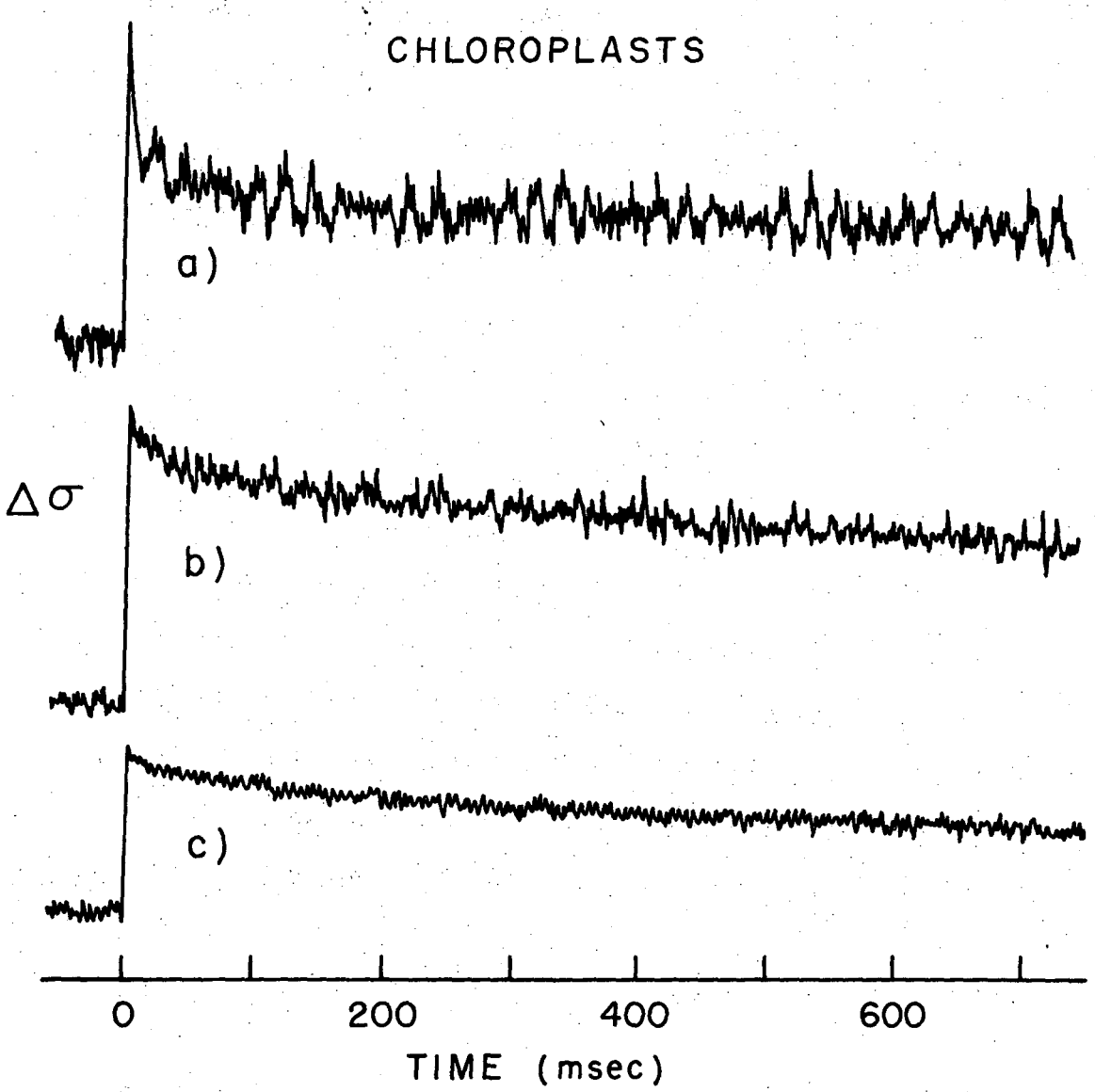

Figure 41. Effect of Ferricyanide. XBL723-4568

(a) Photoconductivity signal to the 1 msec flash from a "wet" chloroplast sample (see description in text). (b) A drop of a 10% solution of K ferricyanide was added to the supernatant in the sample holder. The trace was recorded 2 min after the addition. (c) Trace recorded 5 min after the addition of ferricyanide solution. The fast component is absent.

Mixtures of ferri-ferrocyanide had measurable effects only when the molar ratio was larger than 5, which corresponds to redox potentials larger than +0.48 volts. The EPR signals are half-inhibited by redox potentials around +0.45 volts.

The observations in bacterial chromatophores are qualitatively similar to those in chloroplasts. Ferricyanide-ferrocyanide mixtures inhibited the fast decaying component at ratios larger than 5-6.

No difference in kinetic behavior was found in the PM-8 samples after addition of a solution of ferricyanide. However, I can make no statement regarding effects on the signal intensity.

Addition of a drop of detergent solution to the supernatant had no effect on the signals. Triton X at 2% (w/v) concentration and Na dodecylsulfate at 2% (w/v) were tested. No effects from the detergents were found on the EPR signal in either chloroplasts or chromatophores.

5. Photoinduced Change in Dielectric Constant

a. Chloroplasts

For most of the measurements discussed thus far a servo-control of the microwave oscillator frequency to that of the cavity was the usual procedure. Much of the microphonic noise, which arises from variations in the resonant frequency of the cavity, is avoided by utilizing such an AFC system. Microphonics are contributed by changes in cavity volume, possible motion of the sample holder, and sample vibrations. In such a configuration, only a change in ε'' contributes to the signal. Therefore, one can obtain a pure absorption signal even in the presence of dispersion, e.g., change in ε'. The contrary is not true. To obtain values for changes in ε', the AFC system is disconnected and a double

phase-sensitive detector is utilized to distinguish the in-phase (absorption) from the out-of-phase (dispersion) signals. For very small changes, the 90 degree out-of-phase signal is predominantly proportional to the change in dielectric constant, but for large changes some mixture of the two components is obtained. During dehydration, the samples undergo large changes in ε': in such cases absolute values for ε' are obtained by measuring the resonant frequency of the cavity. Illumination of highly hydrated samples produces changes in temperature, and consequently in ε'. This process can be followed as a slow (many seconds) change in the AFC error signal upon illumination. These effects are reduced to a minimum when the sample has lost most of its water content. A rather fast component can be detected in the 90 degree channel following light pulses. The rise and decay kinetics resemble those of the absorption signals. The order of magnitude of the fractional changes in ε' was about 10^{-5} to 10^{-6} for the 1 msec light pulses by the xenon strobe. The light energy was a few millijoules/pulse, of white light.

It was frequently observed that the changes in ε' followed more closely the behavior of the slow (a few hundred millisecond) component of the photoconductivity signal decay than that of the fast component. For instance, the changes in the dispersion channel seemed to disappear, or to become very slow at temperatures close to -50°C, while the signal in the absorption or photoconductivity receiver were still present and decaying in tens of milliseconds.

b. Bacterial Chromatophores

The normal strains showed light induced changes in the values of dielectric constant. The G.A. mutant produced values of fractional changes in ε' as high as 10^{-5} for 5×10^{-3} joule (1 msec) flashes. Strain R-26 always gave values 4 to 5 times larger than G.A. for samples of comparable size. Typically, for R-26, $\Delta\varepsilon'/\varepsilon' = 5 \times 10^{-5}$.

An interesting observation in the reaction centerless mutant PM-8 chromatophores is that the films obtained from this strain under nitrogen gas desiccation conditions did not show, at my sensitivity level which was about $\Delta\varepsilon'/\varepsilon' \cong 10^{-7}$, any changes in the dispersion channel produced by light pulses. A test of the same sample,for light induced absorbance changes at 870 nm and for EPR signals, was negative, as expected from known literature data.

6. Background Illumination Effects

It is very often found in the field of photoconductivity that the kinetics of the photosignals in the presence of traps do not reflect the true recombination lifetime of the photocarriers, but rather the rate at which the traps are emptied. A common method for studying such situations is to illuminate the sample with a steady light superimposed on the pulsed light. The steady light generates a high concentration of carriers which keeps the traps practically full. Trapping effects are thus reduced and a change in kinetics--usually the appearance of faster rise and decay components--is observed. Such components might be related to the direct generation and recombination process or to some other faster intermediate trapping step.

The long decay times that I observed in the photosynthetic material, as well as the presence of a biphasic rise when I used long pulses of high light intensity, were suggestive of trapping effects. Direct recombination processes would result in much faster kinetics.

In a search for such phenomena, background illumination was added to the modulated illumination.

Light from 400 to 600 nm of 10^{-3} watts/cm^2 intensity was superimposed on 100 msec light pulses of 550 to 700 nm light of intensity 5×10^{-3} watts/cm^2. The repetition rate was 1 pulse per second. Figure 42(a) shows the photoconductivity response of a chloroplast sample under the conditions described above. Apparently the signal shows only the slow component of the decay, a situation typical of very low light intensity pulses, such as those applied here. When background light was added to the pulses, the rise and decay kinetics showed the appearance of a faster component. This is shown in Figure 42(b). The action spectrum for this effect indicated that light of any wavelength absorbed by the sample is equally efficient. Another observation in Figure 42(b) is that the photoconductivity signal did not change in magnitude; only the kinetics were modified.

The transient photoconductivity signal in Figure 42(b) has been labeled at several points with the letters A, B, C, D, and E, to facilitate its analysis. Hornbeck and Haynes (1955) found strikingly similar effects in Silicon samples. The signal is interpreted by them as follows: the conductivity rise from A to B originates from the charge pairs generated by light, until a steady state concentration of carriers is reached at point B. The increase in conductivity from B to C is

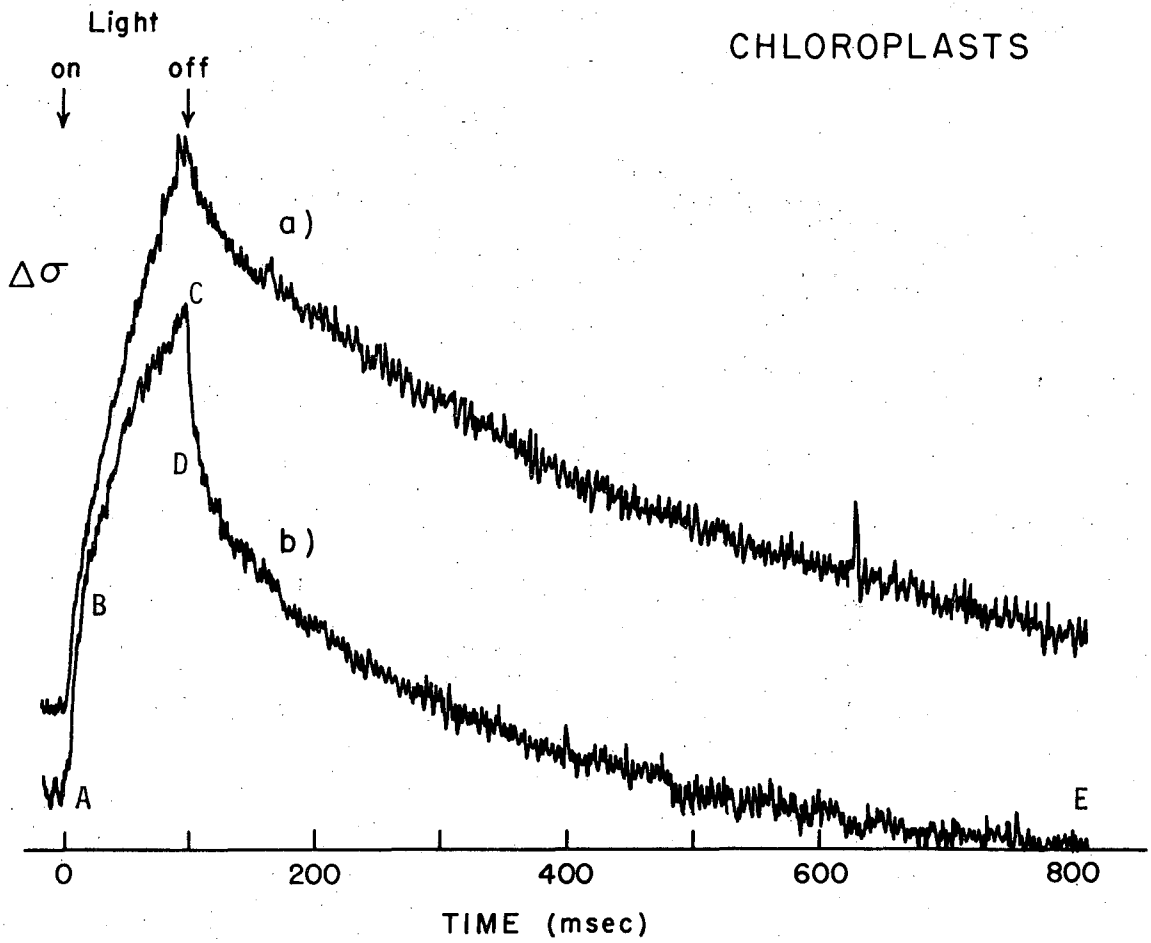

Figure 42. Effect of Background Illumination.

(a) Photoconductivity signal in response to low light intensity pulses of 100 msec. Total energy per pulse is 10^{-4} joules. No background illumination is applied. (b) Photoconductivity signal when background illumination was applied simultaneously with the same light pulses. The photoconductivity at point C (peak value) is $\Delta\sigma = 4 \times 10^{-7}$.

evidence of the trapping of one of the charge species. The complementary (free) charge contributes to the conductivity. At point C a final steady state is obtained. The light is shut off at C; a sudden drop from C to D is interpreted as caused by the direct recombination of charge pairs until the bands are practically depleted. At point D the conductivity is still larger than that at point A by $\Delta\sigma_{DE}$. This latter value is caused by the detrapped carriers complementary to the species in the traps. The transient change from D to E is due to the thermal emptying of the traps. If the detrapping rate constant is smaller than the recombination constant, the decay rate from D to E is practically the rate at which the traps are emptied. A very simple kinetic scheme is used in order to interpret the results and a brief description of it follows.

The system consists of a valence band, a conduction state (which in chloroplasts does not necessarily involve a typical conduction band), and a density of trapping states at a discrete energy level below the conduction state, E_T. Thus there is an energy of activation $E_T-E_c=E_a$ for the trapped carriers to reach the conduction state. The following diagram shows the energy levels.

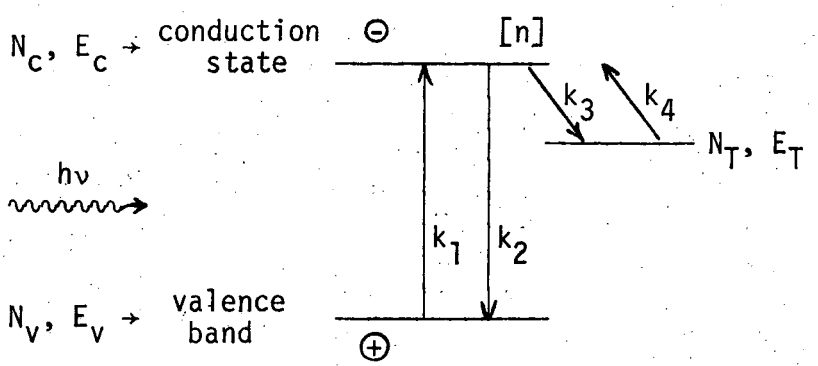

Let n equal the excess density of electrons in the conduction states, with respect to the thermal equilibrium values, n_T equals the excess density of electrons in the traps, ϵ is the absorption coefficient, L is the photon flux, S is the cross section for electron capture by the traps, v is the thermal velocity of the electrons, and N_T is the density of normally empty traps.

The rate constants for the system are as follows: k_1 is the kinetic constant for the production of charge pairs, k_2 is the recombination constant, k_3 is the rate of trapping and k_4 is the rate of detrapping of electrons from the traps.

The value of k_3 is a function of the trapping cross section, the velocity of the carriers, and the density of empty traps at a given time. Thus $k_{3_{max}} = N_T \cdot S \cdot v$ when the trapping sites are empty .

The observed change in conductivity after illumination is given by:

$$\Delta\sigma = ne(\mu_+ + \mu_-) + n_T e \mu_+$$

where it is assumed that for every trapped electron there is a free hole left in the valence state. At low light intensities the second term represents the major contribution to the conductivity. The first term becomes dominant at high light intensities or at very short times after the light is turned off (a time of the order of the recombination time). The differential equations for this case are as follows:

$$\frac{dn}{dt} = \epsilon I (N_v - n) + k_4 n_T - Svn (N_T - n_T) - k_2 n \qquad (1)$$

$$\frac{dn_T}{dt} = n (N_T - n_T) Sv - k_4 n_T \qquad (2)$$

A solution of the simultaneous equations for the steady state gives:

$$n = \frac{(N_v - n)}{k_2}\,\varepsilon I \quad \text{and} \quad n_T = N_T\left[\,1 + \frac{k_4}{nSv}\,\right]^{-1}$$

A similar system in which the trapped species is a hole instead of an electron yields the same differential equations and consequently equivalent solutions. Solutions for the transient changes in carrier concentration after the light is shut off and under the action of steady background illumination are given by H and H. Approximations concerning the various kinetic constants, which may not apply to the chloroplast sample, are used in the treatment. Nevertheless, the calculations of some parameters are possible without the use of the exact solutions.

The trap density may be estimated from $\Delta\sigma_{DE}$, which is mainly due to the complementary (free) species. Although there is no "a priori" reason to consider the hole as the trapped species, the negative sign of the first temporal component of the photo-Hall effect suggests that such is the case. Therefore, $N_T = \Delta\sigma_{DE}/q\mu_-$.

The initial trapping rate is closely given by the initial slope of BC, $\left.\frac{dn_T}{dt}\right]_B^o$, using eq. (1):

$$\left.\frac{dn_T}{dt}\right]_B^o = (N_T S v)\, n_B$$

where n_B is the excess concentration of carriers in the bands at point B and is given by $\Delta\sigma_{AB}$, as: $n_B = \frac{\Delta\sigma_{AB}}{q\mu}$. Therefore, a calculation of S, the cross section for trapping, is possible by assuming v to be the thermal velocity of a free electron. At room temperature $v = 10^7$ cm/sec.

Figure 42(b) gives the following parameters:

$$\left.\frac{dn_T}{dt}\right]_B^o \cong 10^{-5}\ \Omega^{-1}\ cm^{-1}\ sec^{-1} / e\mu_-$$

$$n_B \cong 1.6 \times 10^{-7}\ \Omega^{-1}\ cm^{-1} / e\mu_-$$

$$N_T \cong 10^{12}\ cm^{-3}$$

$$S \cong 10^{-16} - 10^{-17}$$

Total chlorophyll in the sample $\cong 10^{15}$ molecules

Pigment to trap ratio = $10^2 - 10^3$

The value of S is of the order of the area of a small organic molecule. The upper and lower limit values are determined by the value of the photomobilities which range from 1 to 0.1 cm^2/volt·sec.

It is interesting to note that a calculation of the pigment to carrier ratio, from the saturation experiment, gives for a similar sample PCR = $10^2 - 10^3$. Therefore, the number of mobile carriers is comparable to the number of traps. The fact is indeed suggestive that the observed charge carriers at low light intensities are the complementary species to a trapped charge, which might be the chlorophyll cation radical.

The behavior of the signals in the absence of background illumination may be understood in the following terms: The probability for an electron (hole) to be trapped when all trapping sites are empty is much larger than the probability for recombination; the charges generated by the light will tend to fill up the traps before building up a steady state concentration of charges in the bands. When background illumination is present, a fraction of the traps is filled leading to a decrease in the probability for trapping. When the recombination rate becomes larger than the trapping rate, a steady state charge concentration, n_B, is

built up in a time of the order of $1/k_2$ before appreciable trapping occurs, resulting in the fast rise component observed in Figure 42(b).

C. Discussion

The similarities between the photoconductivity and the EPR signals suggest a close functional relation between the species that originate the effects. Tables VIII and IX summarize the available observations. The observed similarity in behavior between the photoconductivity and the EPR signal does not necessarily imply that they originate from the same species; the EPR signal could originate from a trapped hole (bacteriochlorophyll cation radical, for instance) and the photoconductivity arise from the complementary charge, if free. The appearance, but not necessarily the decay, of one species would then very closely follow the other.

Previous work by several investigators has shown that the probable assignment for the paramagnetic species that gives the photoinduced EPR signal is the chlorophyll (or bacteriochlorophyll) cation radical. It has been a very striking fact, however, that the EPR signal from the complementary (reduced) species has not been observed. A single photon produces only one spin. A migrating charge does contribute to the paramagnetism of the material, but its paramagnetic resonance signal might not be observed under conventional conditions. Efforts by Feher have indeed shown a broad light induced EPR signal at very low temperatures in R. spheroides reaction center preparations. The signal was tentatively assigned to an iron ion, which was assumed to belong to the primary acceptor molecule. Recent work has shown that total removal of the iron does not affect the appearance of the photoinduced EPR

Table VIII. Comparison between Photoconductivity and EPR Signals - Chloroplasts

Parameter	Photoconductivity	EPR Signals	Reference
Decay half-times	0.2 & 10-20 msec; 3-5 sec	3-5 sec	Bolton (1968); Androes (1962).
Rise kinetics	$<4 \times 10^{-6}$ sec	$<10^{-3}$ sec	
Effect of temperature			
-15°C	Blocks decay of 3-5 sec component	Blocks over-all decay	"
-150°C	Very small signal remains Rise: 100 msec Decay: 100 msec	Photosignal is frozen-in	"
40°C to 0°C	Signal decreases with an activation energy $E_a = 0.3$	1. Signal slightly decreases from 40°C to 25°C. 2. Signal slightly increases from 25°C to 0°C	Androes (1962); Heise (1962)
100°C	Destroys signal	Signal disappears	Treharne et al. (1963)
60°C	No effect	No effect	"
Addition of Ferricyanide	Inhibits or stabilizes the 20 msec component	Stabilizes the signal decay	This work
Light intensity saturation	Two to three orders of magnitude larger than the intensity to saturate CO_2 fixation	Two orders of magnitude larger intensities than that which saturates CO_2 fixation	Androes et al. (1962)

Table IX. Comparison between Photoconductivity and EPR Signals - Bacterial Chromatophores

Parameter	Photoconductivity	EPR Signal	Reference
Decay half-times (25°C)	0.2 & 10-20 msec; 5 sec	20-30 msec; 5 sec	Bolton (1968); Androes (1962).
Rise kinetics (25°C)	$<5 \times 10^{-6}$ sec	$<10^{-3}$ sec	
Effects of temperature			
-15°C	Blocks the 5 sec decay	Blocks the 5 sec decay	"
-150°C	A signal remains having a rise time $\tau_{1/2} < 10^{-3}$ sec and a half-decay $\sim$50 msec	The fast component of the signal remains. Rise time and decay half-time $\sim$30 msec	"
40°C to 0°C	Photosignal decreases with an activation energy E_a = 0.3 eV	Signal decreases slightly from 25°C to -15°C	Androes (1963); Heise (1962).
100°C	Destroys signal	Destroys signal	This work
60°C	No effect	No effect	"
Saturating light intensity	Orders of magnitude larger than that which saturates CO_2 fixation	Orders of magnitude larger than that which saturates CO_2 fixation	Treharne (1963)
Effect of adding ferricyanide	Inhibits or stabilizes the 20 msec decay component	Stabilizes the over-all signal	Loach et al. (1963)
Biological perturbation Non-photosynthetic PM-8 *R. spheroides* mutant	Shows a very small photoconductivity signal corresponding to a very small quantum yield for carrier generation.	Shows no EPR signal induced by light	Clayton (1964)

signal attributed to bacteriochlorophyll and also of a second light induced signal with a g value of 2.0047 at 9 GHz. This second signal was previously observed by Loach (1971) and has not been assigned to any molecular component yet.

I suggest the possibility that the photoconductivity signals may correspond to the mobile negative charge species complementary to the trapped positive hole. The first temporal component of the photoconductivity signal exhibits a Hall effect corresponding to negative carriers, a fact consistent with the above interpretation.

Experiments with the reaction centerless mutant of R. spheroides showed a very small photoconductivity signal (which under my experimental conditions may well be accounted for by the thermal effect of the light), and produced no measurable photo-EPR signal. This evidence suggests that the reaction center structures must be present for the photogeneration of the mobile carrier species to occur.

The charge separation process produces an extra dipole moment which would cause changes in both the polarizability and in the dielectric constant of the sample. The polarizability changes have been observed previously in R. spheroides chromatophore films, by Arnold and Clayton in 1960. The fact that the reaction centerless mutant showed no photoinduced changes in dielectric constant as were observed in the G.A. mutant leads to the conclusion that the observed effects of illumination on the dielectric constant are indeed produced by the charge separation process at the reaction center structures.

The available evidence does not permit an identification of the slow positive component of the Hall effect photosignal. The time at which the signal maximizes is close to the decay half-time of the slow

decay component of the EPR signals, and is also in the kinetic range of several light induced absorbance changes.

It has been suggested in the past (De Vault, 1966) that some sort of semiconductivity mechanism could account for the temperature dependence of the cytochrome oxidation in Chromatium. Although highly speculative, the possibility that the electron transfer reactions between the reaction center complexes and the primary and secondary electron donors and acceptors contribute to the photoconductivity should be further investigated. Measurements on mutant organisms defficient in some of the components of the redox chain might provide the necessary evidence to confirm or to rule out such a possibility.

The mechanism for the observed charge migration cannot be understood in terms of a band model. The small values for the photomobilities and the temperature dependence of the photoconductivity are similar to some organic semiconductors: for those materials other mechanisms for the transport have been suggested. These are the hopping and tunneling models, applied to conduction in organic dyes (Nelson, 1965) and proteins (Eley, 1961).

Some of the arguments introduced by Nelson in his localized model for the charge splitting and migration process in photosynthesis predict effects similar to those observed in this work.

In essence Nelson suggests that the charge generation and transport in dye systems do not require the cooperative effects which appear in the band models, and supposes the molecules to maintain their individual character when aggregated (or even in crystals). Such an assumption is supported by the fact that experiments in dyes adsorbed on a

variety of substrates had almost no effect in the ionization potentials; the molecules see the environment as a classical dielectric medium. The charge carrier separation takes place between two adjacent molecules. The carriers are able to diffuse, possibly by tunneling, and are always essentially localized on a molecule at any instant. The charge migration in such a model would resemble a process of transport under multiple trapping. Calculation of the migration transfer rates for such a model gives values as high as 10^{13} sec^{-1}. The calculated mobilities are of the order of 1 cm^2/volt·sec, which are very close to those observed experimentally in this work for most samples. Such transfer is rather "chemical" in nature, as Nelson himself recognizes (1967). He also states that such charge transfer may take place easily between unlike molecules thus allowing the possibility of a similar kind of charge transfer between the primary donors and acceptors. Since the time that Nelson first offered these suggestions (1963) it has been proposed that the most likely explanation for the charge migration between some components of the redox chain is indeed a tunneling process (Chance, 1967). In Nelson's view the charge pairs located on adjacent molecules are equivalent to oxidized and reduced states which would behave as a cation or anion radical, respectively.

Nelson also offers an alternative mechanism to account for the observed photomobilities by considering, instead of tunnelling, a hopping type process of charge migration. The question of how fast such hopping may take place requires some consideration. Starting from Einstein's diffusion formula, $\mu = De/kT$, where the diffusion constant is $D \cong a^2/\tau$, a is the distance between hopping sites, and τ is the average time between hoppings; gives for our $\mu = 0.1$ cm^2/volt·sec

and 10 Å spacing at room temperature

$$\tau = \frac{ea^2}{kT\mu} = \frac{1.6 \times 10^{-19} \text{ Coulomb } [10^{-7}]^2 \text{ cm}^2}{1.38 \times 10^{-23} \frac{\text{joule}}{\text{degree}} \times 300 \text{ degree} \times \frac{10^{-1} \text{ cm}^2}{\text{volt} \cdot \text{sec}}}$$

$$\tau_h = 4 \times 10^{-13} \text{ sec},$$

a very short time indeed. If the vibration time is shorter than τ_h, namely $\tau_h > \tau_{vib}$, it is reasonable to apply a localized model for the charge migration, while in the case $\tau_h << \tau_{vib}$ we are in the domain of a typical band model. Since both transport processes, tunnelling and hopping, may result in a temperature dependent mobility, no distinction is possible from the available experimental data.

Previous unsuccessful efforts to detect photocarriers in green plant material by McCree (1965) can be understood by considering his experimental conditions. McCree employed light modulation and lock-in detection at frequencies of 80 Hz and higher. The photoconductivity signals that I observed in green plant material showed decay half-times longer than the inverse frequency of McCree's modulation, which would result in a large attenuation of the signal. The values that I computed for the quantum yield for charge carrier generation are orders of magnitude larger than those of McCree but are smaller than the values of one spin per photon, found by Bolton et al. (1969) for the EPR signals from bacterial reaction center preparations.

The rather low value of one charge per 100 to 1000 photons that I found in both systems may be understood by considering that only that fraction of carriers which are detrapped at a given time contribute to the conductivity. Evidence that such trapping processes take place in the materials is provided by the effects of background illumination.

The possible meaning of the observed trapping in terms of chemical species in the biological structures requires some comment.

Primary electron donors and acceptors, as well as any of the members of the electron transport chain that are bound to the membrane structures in a "solid state" matrix, may be regarded as charge traps. Such a system would give a trap distribution with the primary acceptor acting as a shallow trap. Effects such as thermoluminescence would result from the thermal depletion of these traps. The activation energy for the process of emission of luminescence is around 0.4 eV (Laime et al., 1972), very close to the values that I observed for the photoconductivity. The temperature dependence of the photoconductivity would be determined to a large extent by the trap depth, because the concentration of mobile photocarriers results from a thermal equilibrium between the trapped states and the conduction state. The energy of activation for the process should provide the value for the trap depth.

Activation energies reported by Arnold (1968) for the thermoluminescence of chloroplast samples are in the range of those observed here for the photoconductivity. Since the effects may be interpreted as arising from the depletion of the same trap, further efforts to clarify this point are worthy.

To conclude this discussion, I would like to point out an observation regarding the kinetic analysis of the sign inversion observed in both the bacteria and chloroplast samples.

If we assume that the negative charge carrier rotation transient is the parent of the positive carrier species, the following reaction scheme follows:

$$A \xrightarrow{k_1} B \xrightarrow{k_2} C$$

where A represents the negative carrier, B the positive, and C is the trapped species.

In the following equation the concentration of component B is given by B = [B],

$$[B] = e^{-k_2 t}\left[\frac{[A_o]k_1}{k_2-k_1}\left(e^{(k_2-k_1)t}-1\right)\right]$$

The time at which [B] reaches its maximum value, t_{max}, is given by:

$$t_{max} = \frac{2.303}{k_2-k_1} \cdot \log\frac{k_2}{k_1}$$

where $[A_o]$ is the initial concentration of A.

Because of their opposite signs, the B component subtracts from the A component and leads to an apparently faster decay of the first component than is actually the case. A very good fit of the position of the time at which B reaches its maximum, t_{max}, is obtained for values of $k_1 = 2\ k_2 = 200\ sec^{-1}$ in bacteria and $k_1 = 30\ k_2 = 33\ sec^{-1}$ in chloroplasts.

Nishimura (1968), applying laser pulse excitation for the measurements of cytochrome oxidation in Porphyridium cruentum cells, found an absorbance transient at 430 nm that resembles to a great extent the sign inversion kinetics in bacterial chromatophores. Nishimura interprets the observed effect as the oxidation of a type f cytochrome in about 14 microseconds followed by its slower reduction in a period of about 10 milliseconds by a b-type cytochrome. The similarity of the light induced absorbance change kinetics with that of the Hall effect suggests the possibility that such cytochrome reactions represent the trapping processes mentioned above.

In conclusion, this work provides a positive answer to the question concerning the photoproduction of mobile charge carriers of both signs in photosynthetic structures. The carrier mobilities observed at microwave frequencies are not compatible with those predicted for a model based on conduction bands in semiconductors as were employed in earlier models of the functioning of the photosynthetic apparatus. Rather, they are consistent with hopping or tunneling processes. The charge carriers are not observed in materials lacking the reaction centers. Thus, it appears probable that the charge splitting occurs either in the reaction centers or in structures closely associated with them.

Future work in which this microwave technique is applied to simultaneous measurements of possibly related parameters including EPR, delayed luminescence, and light induced absorbance changes might contribute to a better understanding of the role of the observed charge carriers in the photosynthetic process.

APPENDIX I

.CALCULATION OF THE FILLING FACTOR

The calculation of the filling factor, η, for a sample in the form of a piece of cylinder located at the antinode of the electric field in a TE_{011} cylindrical cavity follows.

The following diagram shows the geometry under consideration:

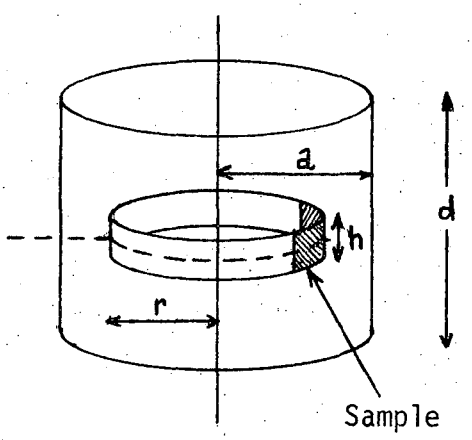

The fields in a TE_{011} cylindrical cavity are given by:

$$H_r = H_o\, J_o'(k_c r)\, \cos(\pi z/d) \left[1+(k_c a)_{01}, d/\pi a\right]^{-1/2}$$

$$H_z = H_o\, J_o(k_c r)\, \sin(\pi z/d) \left[1+(\pi a/[k_c a]_{01}, .d)\right]^{-1/2}$$

$$E_\phi = -[\mu/\varepsilon]^{1/2}\; H_o\, J_o'(k_c r)\, \sin(\pi z/d)$$

$$H_\phi = E_r = E_z = 0$$

The electric field has components only in the coordinate and the H components are only given for completeness. Form the definition of the filling factor;

$$\eta = \frac{\int_{sample} E^2\, dv}{\int_{cavity} E^2\, dV} = \frac{\langle E^2\rangle_{sample}}{\langle E^2\rangle_{cavity}} \times v/V$$

where E is the value of the microwave electric field, $\langle E^2\rangle_{sample}$, is the average value of the square of the field in the sample and $\langle E^2\rangle$ cavity is the same quantity in the cavity;

$$\langle E^2\rangle_{sample} = \frac{.1}{v} \int_{sample} H^2\, dv$$

$$\langle E^2\rangle_{cavity} = \frac{1}{V} \int_{cavity} H^2\, dV$$

$J_o(k_c r)$ is the cylindrical Bessel function of zero order and $J_o'(k_c r)$ its derivative. The root $(k_c a)_{01'} = 3.832$ and the maximum value for $J_o'(k_c r)$ is $J_o'(k_c r)_{max} = 0.5819$, and $J_o(k_c a) = 0.4028$; $J_o(0) = 1$.

Therefore:

$$E^2 \text{ cavity} = H_o/\ \pi a^2 d\ \mu/\epsilon \int_0^{2\pi} d\phi \int_o^a J_o'^2 (k_c r)\ r\ dr \int_0^d \sin^2 \pi z/d)dz$$

The Jahnke and Emde tables give:

$$\int_0^r J_n^2 (k_c r)\ r\ dr = r^2/2\ [\ J_n^2 (k_c r) - J_{n-1}(k_c r).\ J_{n+1}(k_c r)\ ]$$

and $$J_n'(k_c r) = (n/k_c r)\ J_n(k_c r) - J_{n+1}(k_c r)$$

$$2n/k_c r\ J_n(k_c r) = J_{n-1}(k_c r) + J_{n+1}(k_c r)$$

Therefore for J_o' :

$$\int_0^r J_o'^2 (k_c r)\, r dr = r^2/2 \left[J_o^2 (k_c r) - (2/k_c r) J_o(k_c r) \cdot J_1(k_c r) + J_1^2 (k_c r) \right]$$

for the boundary conditions; $E(a) = 0$, $J_o' (k_c a) = 0$ and $J_{\pm 1}(k_c a) = 0$ because $J_o'(k_c r) = -J_1(k_c r) = J_{-1}(k_c r)$.

Hence:

$$\int_0^r J_o'^2 (k_c r)\, r\, dr = r^2/2\, J_o^2 (k_c r)$$

and for r=a:

$$\int_0^a J_o'^2 (k_c r)\, r\, dr = a^2/2\, J_o^2 (k_c a) = a^2/2 \times (0.4028)^2$$

Since $\int_0^{2\pi} d = 2\pi$, and $\int_0^d (\sin^2 \pi z/d)\, dz = d/2$, then:

$$\langle E^2 \rangle_{cavity} = - \mu/\epsilon (H_o^2 / \pi a^2 d)(d/2)\, (2 \pi a^2/2)\, 0.16$$

$$\langle E^2 \rangle_{cavity} = - \mu/\epsilon \;\; 0.16/2 \times H_o^2$$

The value for $\langle E^2 \rangle_{sample}$, assuming that the sample is entirely located at r=d/2 and at $J_o'(k_c r)_{max} = 0.5819$, is

$$\langle E^2 \rangle_{sample} = -\mu/\epsilon\, H_o^2\, (0.5819)^2 \int_{sample} (\sin^2 \pi z/d)\, dz$$

$$\langle E^2 \rangle_{sample} = -\mu/\epsilon\, H_o^2\, (0.5819)^2 \left[1/2(\pi z/d) \right]_0^d - 1/4 \sin 2\pi z/d \Big|_0^d$$

For a sample size such that h= d/10, the value for $\sin^2 \pi z/d$ does not change appreciably. In such case for $z = d/2 \pm d/10$ and $\sin^2 \pi/2 = 1$ the filling factor, η , is given by:

$$\eta = \langle E^2 \rangle_{sample} / \langle E^2 \rangle_{cavity} \quad (v/V) = \frac{- \mu/\varepsilon \; H_o^2 \times 0.58}{- \mu/\varepsilon \; H_o^2 \times 0.16/2} \quad (v/V)$$

$$\eta = (0.58)^2/0.08 \quad (v/V) = 4.2 \; v/V$$

Since the sample has the shape of a thin disc, for which an exact calculation is complicated, this filling factor does not apply exactly to the experimental situation. Measurements performed in the bimodal cavity on the same sample, in order to test the value experimentally, gave for our geometry:

$$\eta = 3 \pm 0.5 \quad v/V$$

Since the bimodal cavity geometry is ideal for a flat cylindrical sample and the filling factor has been confirmed experimentally (Von Aulock and Rowen,1957), I feel that the value given above is acceptable with an uncertanty of ± 20%. It is more than sufficient accuracy for my measurements since no arguments in terms of absolute values of the conductivities have been made.

APPENDIX II

ELECTRIC FIELD EFFECTS

An electric field applied simultaneously with the microwave field might contribute to a better understanding of the mechanisms involved in the losses.

Carr (1963-1965) has studied extensively the effect of electric fields on the dielectric properties of liquid crystals at microwave frequencies. Some helpful conclusions concerning the relevance of the dipolar losses may be obtained from such measurements. An external D.C. or low frequency A.C. field, much larger than the microwave field, aligns the dipoles, thus removing them from the action of the microwaves. The fields needed for such effects are rather small, e.g., several hundred volts per cm.

It has also been shown that constant fields have an effect upon the charge carrier conductivity. A typical band model accounts reasonably for the effect observed in germanium (Nag. and Das, 1963). The effects on charge carrier loss were of the order of a few percent for fields of 2 to 4 Kvolts/cm. An accompanying change in the dielectric constant induced by the electric field was also accounted for by the band model.

The effect of an electric field on the photoinduced microwave loss and luminescence properties of a ZnO semiconducting electrode is reported in this thesis in Chapter III. It is shown there that extraction

of surface photocarriers by the action of the field efficiently competes with the microwave loss.

With these facts in mind I decided to apply simultaneously a static electric field to the biological samples in the microwave cavity, to observe its effects (if any) on the losses.

Technically it is not an easy experiment, because most cavity configurations would permit the introduction of electrodes in the cavities but not the light. A reentrant cylindrical cavity gives the desired geometry but the dimensions involved led to the necessity of sample micromanipulation techniques and contacting a sample is a rather difficult procedure. Figure 44 shows the cavity which was made from an old V-58 Klystron by Varian Associates (Palo Alto, Ca.). The sample chosen for the experiment was a 1 mm by 1/2 mm piece of spinach leaf. The leaf provides its own support for the photosynthetic apparatus and an electric field penetrates the sample to some extent, due to the high water content and the large ionic concentrations. There are many factors which could invalidate the results. Electrostriction or changes in the volume due to the electric field would give some change in instrumental parameters such as filling factor. Orientation of the water dipoles by the field might extract them from the action of the microwave field, thus decreasing the microwave losses.

It is the light induced part that could give an interesting answer, if it is affected preferentially by the static field. Indeed, such an effect was observed.

Figure 45 shows the response of the leaf sample to light pulses lasting 50 msec. A decay time of about 100 msec was observed in this

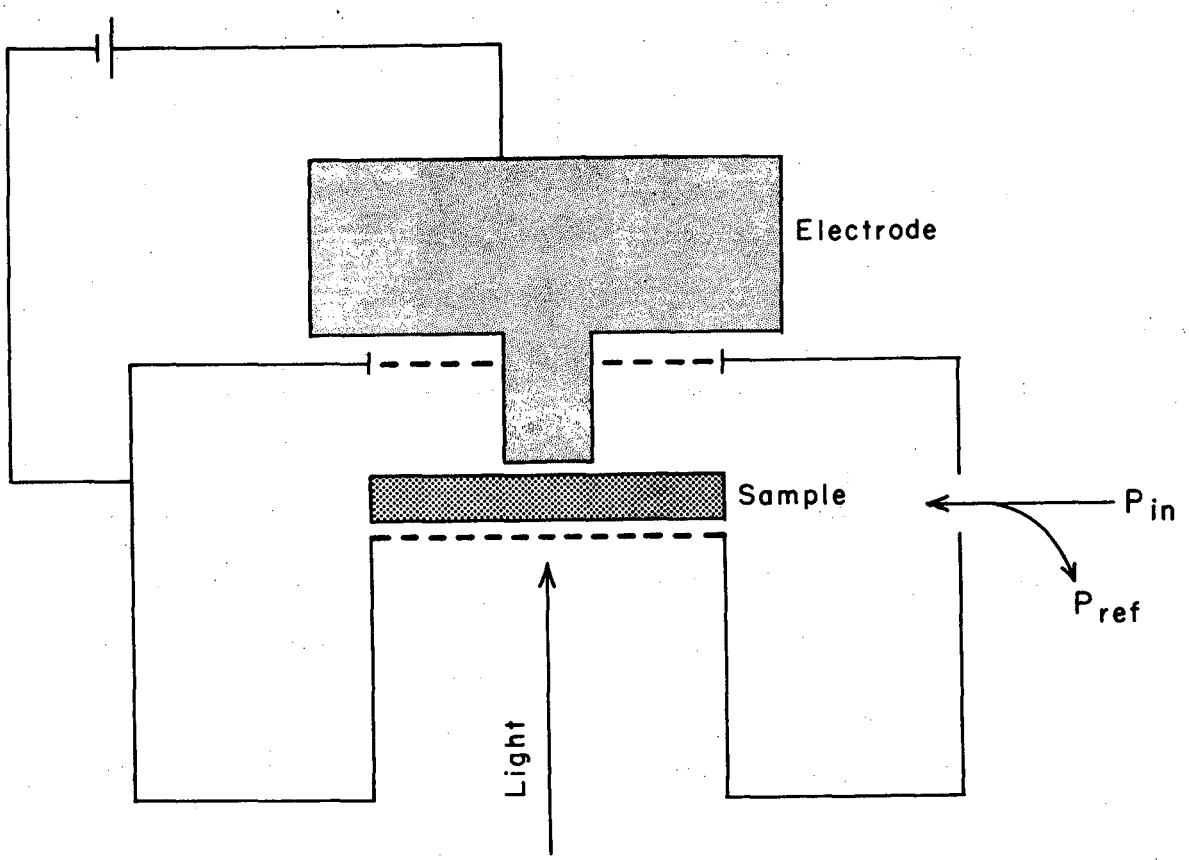

XBL723-4584

Figure 44. Electric field effect arrangement. A typical reentrant cavity resonator made from a V-58 klystron (Varian Associates); the broken lines indicate the grid that makes the cavity wall at such points. Light was sent to the sample through the lower grid, which was also used as an electrode. The upper electrode was made of copper. Coupling to and from the cavity was provided in the klystron, as well as the frequency tuning system (neither shown in the figure).

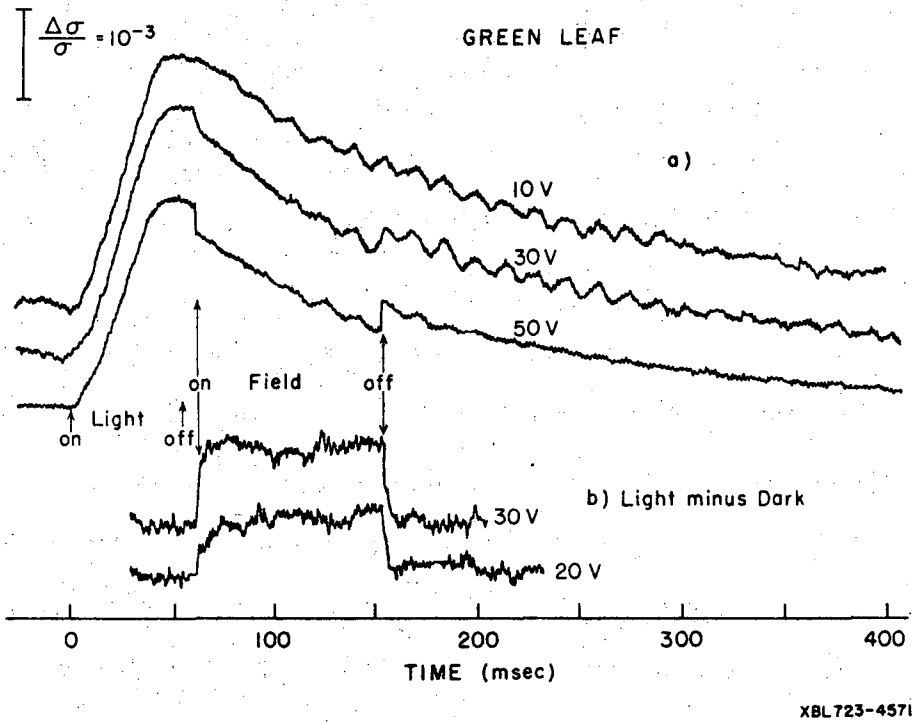

Figure 45. Effect of an electric field. (a) The photoconductivity signal from a piece of spinach leaf to 50 msec light pulses with a 100 msec electric field pulse applied at the points indicated by the arrows. The effect of the direction of the effect indicates a decrease in losses. Three different values of voltage are shown. (b) The effect of the electric field pulses under constant illumination minus the effect in the dark is shown for 20 and 30 volt pulses. The signals were recorded in the computer averager and the subtraction of an equal number of passes in the dark as in the light was performed electronically.

sample. The effect of an electric field pulse at three different voltages is shown in Figure 45(a). The distance between electrodes was 0.02 cm, giving 2.5 Kvolt/cm for the average value of the field when a potential of 50 V was applied. The effect was a decrease in the losses proportional to the field strength. The onset time was dependent on the field values. The lower part of Figure 45, (b), shows the light minus dark results. A constant illumination of about 5×10^4 erg of red light was sent to the sample using a red cut filter Corning glass #3-63. Infrared radiation was filtered with a 4 cm water filter and a 1-58 Corning glass filter. The signal resulting from averaging 50 pulses of electric field with light-off was subtracted electronically from the same number of pulses with constant light-on. Results for 20 and 30 V are also shown. The field dependence of the rise time is also evident in this experiment. The equivalent experiment, but for light-minus-light or dark-minus-dark, yields a null average as expected.

The effect with light-on is estimated to be about 5 times larger than that with light-off. Since no measurements were made in a completely dark adapted sample I cannot conclude whether the observed dark effect is some residuum of the previous action of the light or just the action of the field upon the permanent dipoles that contribute to the dark losses.

An electric field of a few Kvolt per cm has been shown to induce light emission from chloroplast and Chlorella suspensions (Arnold, 1970; Ellenson, 1971). Comparison of such effects with the results shown in Figure 45 suggests that the decrease in loss might be

associated with the radiative recombination of some mobile charge carrier species.

The experiment described here is a very modest attempt to give a yes or no answer to the question of whether the electric field would have an effect on the photoinduced losses. It is very clear to me that much work has to be done in order to understand the effect. I introduced it in this work for two reasons. First it is consistent with other evidence that the photoinduced loss is the result of a mobile charge carrier; and second, it suggests some relation with the luminescence processes, and I feel that it might incite some constructive argument.

REFERENCES

Anderson, A. F. H., and Calvin, M., Archives of Biochem. and Biophys. 107, 251 (1964).

Androes, G. M., Singleton, M. F., and Calvin, M., Proc. Natl. Acad. Sci. 48, 1022 (1962).

Appfel, J. H., and Portis, A. M., J. Phys. Chem. Solids 15, 1 (1960).

Arnold, W., J. Phys. Chem. 69, 788 (1965).

Arnold, W., and Azzi, J. R., Biology Div. Oak Ridge Natl. Lab., Oak Ridge, Tennessee (1968).

Arnold, W., and Azzi, J., J. Photochem. Photobiol. 14, 233 (1971).

Arnold, W., and Clayton, R. K., Proc. Natl. Acad. Sci. Wash. 46, 769 (1960).

Arnold, W., and Kohn, H., J. Gen. Physiol. 18, 109 (1934).

Arnold, W., and Sherwood, H., Proc. Natl. Acad. Sci. Wash. 43, 105 (1957).

Arnon, D. I., Allen, M. B., and Whatley, F. R., Nature 174, 394 (1954).

Baranov, E. V., and Akimov, I. A., Doklady Akad. Nauk SSSR 154, 1, 184-187 (1964).

Bassham, J. A., and Calvin, M., The Path of Carbon in Photosynthesis, Prentice Hall, New Jersey, 1957.

Bay, Z., and Pearlstein, R., Proc. Natl. Acad. Sci. U.S. 50, 1071 (1963).

Bierman, A., Physical Review 130, 2266 (1963).

Biggins, J., and Park, R. B., Plant Physiol. 40, 6, 1109 (1965).

Birnbaum, G., and Franeau, J., J. Appl. Phys. 20, 817 (1949).

Blyumenfeld, L. A., et al., Dokl. Akad. Nauk SSSR 193, 3 (1970).

Bolton, J. R., Clayton, R. K., and Reed, D. W., Photochem. Photobiol. 9, 209 (1969).

Bogomolni, R. A., and Klein, M. P., International Converence on the Photosynthetic Unit, Gatlinburg, Tennessee, 1970, Abstracts G-2.

Bolton, J. R., Cost, K., and Frenkel, A. O., Arch. Biochem. Biophys. 126, 383 (1960).

Brody, S. S., and Rabinowitch, E., Science 125, 555 (1957).

Calvin, M., 11th Brookhaven Symp. in Biology 160 (1958).

Calvin, M., and Bassham, J. A., U.S. Atomic Energy Commission Report UCRL-2853 (1955).

Carr, E. F., J. Chem. Phys. 43, 11, 3905 (1965).

Clayton, R. K., Photochem. Photobiol. 5, 679 (1969).

Clayton, R. K., Brookhaven Symp. in Biology No. 19, 62 (1967).

Clayton, R., Fleming, H., and Szuts, E. Z., Biophysical J. 12, 46 (1972).

Cohen-Bazire, G., Sistrom, W. R., and Stanier, R. Y., J. Cell. comp. Physiol. 49, 25 (1957).

Commoner, B., Heise, J. J., and Townsend, J., Proc. Natl. Acad. Sci. U.S. 42, 710 (1956).

Commoner, B., Townsend, J., and Pake, G., Nature 174, 4432, 689 (1954).

Cost, K., Bolton, J. R., and Frenkel, A. W., Photochem. Photobiol. 10, 251 (1969).

Chance, B., Nature 169, 215 (1952).

Chance, B., Science 120, 707 (1959).

Chance, B., et al., "Early Chemical Events in Photosynthetic Kinetics of Oxidation of Cytochromes of Types c or f in Cells, Chloroplasts and Chromatophores," Brookhaven Symp. in Biology No. 19, 115-131 (1966).

deVault, D., and Chance, B., Biophys. J. 6, 825 (1966).

Douglas, F., and Albrecht, A. C., Photoelectric Response from Chlorophyll a Microcrystals in Suspension, Department of Chemistry, Cornell University, Ithaca, New York.

Dratz, E. A., Schultz, A. J., and Sauer, K., Brookhaven Symp. in Biology No. 19, 303 (1966).

Duysens, L. N. M., Ph.D. Thesis, Utrecht, The Netherlands, 1952

Duysens, L. N. M., "Primary Photosynthetic Reactions in Relation to Transfer of Excitation Energy," Brookhaven Symp. In Biology. No. 19, 71 (1966).

Eley, D. D., and Pethig, R., Bioenergetics 2, 39 (1971).

Eley, D. D., and Pethig, R., Bioenergetics 1, 109 (1970).

Eley, D. D., and Smart, S., Biochim. Biophys. Acta 102, 379 (1965).

Emerson, R., J. Gen. Physiol. 12, 609 (1929).

Emerson, R., Science 125, 746 (1957).

Emerson, R., and Arnold, W., J. Physiol. 15, 391 (1932).

Emerson, R., and Arnold, W., J. Gen. Physiol. 16, 191 (1932).

Emerson, R., Chalmers, R., and Cederstrand, C., Proc. Natl. Acad. Sci. U.S. 43, 133 (1957).

Emerson, R., and Lewis, C. M., Am. J. Bot. 26, 808 (1941).

Emerson, R., and Lewis, C. M., Am . J. Bot. 30, 165 (1943).

Engleman, T. W., Arch. Ges. Physiol. (Pfluger's) 30, 95 (1883).

Engleman, W. T., Bot. Ztg. 39, 441 (1881).

Feher, G., Internat. Conf. on the Photosynthetic Unit, Gatlinburg, 1970.

Feher, G., The Bell System Tech. J. 36, 449 (1957).

Feher, G., Photochem. Photobiol. 14, 373 (1971).

Fleischman, D. E., Photochem. Photobiol. 14, 277 (1971).

Fleischman, D. E., and Clayton, R. K., Photochem. Photobiol. 8, 287 (1968).

Förster, T., Z. Naturforsch. 4a, 321 (1949).

Förster, T., Znn. Physiol. 2, 55 (1948).

Förster, T., Naturwissenschaften 33, 166 (1946).

Frank, J., and Teller, E., J. Chem. Phys. 6, 861 (1938).

Frank, J., and Livingston, R., Revs. Mod. Phys. 21, 505 (1949).

Frank, J., Rosenberg, J. L., and Weiss, C., Jr., Luminescence of Organic and Inorganic Materials, Eds. H. P. Kallman and G. H. Spruch, John Wiley & Sons, New York, 11-29, 1962.

French, C. S., J. Gen. Physiol. 21, 71 (1937).

French, C. S., Myers, J., and McCloud, ., Comparative Biochemistry of Photoreactive Systems, Ed. M. B. Allen, Academic Press, New York, p. 361, 1960.

Gaffron, H., and Wohl, K., Naturwissenschaften 24, 81, 103 (1936).

Geacintov, N. E., Pope, M., and Fox, S., J. Phys. Chem. Solids 31, 1375 (1970).

Geacintov, N. E., Van Nostrand, F., Pope, M., and Tinkel, J. B., Biochim. Biophys. Acta 226, 486 (1971).

Ginzton, E. L., Microwave Measurements, McGraw Hill, New York, 1957.

Goedheer, J., Nature 176, 928 (1955).

Goedheer, J., Biochim. Biophys. Acta 35, 1 (1959).

Haxo, F. T., and Blinks, L. R., J. Gen. Physiol. 33, 389 (1950).

Hill, R., Proc. Roy. Soc. (London) 127, 192 (1939).

Hill, R., and Bendall, F. F., Nature 186, 137 (1960).

Ilten, D. F., and Calvin, M., J. Chem. Phys. 42, 11, 3760 (1965).

Ilten, D. F., Kronenberg, M. E., and Calvin, M., Photochem. Photobiol. 7, 331 (1968).

Jensen, R. G., and Bassham, J. A., Proc. Natl. Acad. Sci. U.S. 56, 4, 1095 (1966).

Katz, J. J., Conference on Primary Photochemistry of Photosynthesis, Argonne, Ill., 1971.

Katz, E., Photosynthesis in Plants, Iowa State College Press, Ames, Iowa, 1949.

Kamen, M. D., Primary Processes in Photosynthesis, Academic Press, New York, 1963.

Kittel, Introduction to Solid State Physics, John Wiley & Sons, New York, 1971.

Kittel, Quantum Theory of Solids, John Wiley & Sons, New York, 1963.

Klein, M. P., and Barton, G. W., Jr., Rev. Sci. Instr. 34, 754 (1963).

Kok, B., Currents in Photosynthesis, Ed. J. B. Thomas and J. C. Goedheer, A. Donker, Rotterdam, p. 383, 1966.

Kok, B., et al., Brookhaven Symp. in Biology No. 19, 446 (1967).

Kok, B., Biochim. Biophys. Acta 48, 527 (1961).

Kok, B., and Businger, J. A., Nature 177, 135 (1956).

Kusnezov, N., Microwave Propagation in Aromatic Compounds, Series No. 60, Issue No. 389, June 13, 1961, AF 49 (638)-1043, Electronics Research Lab., U.C. Berkeley.

Kuntz, I. D., Jr., Brassfield, T. S., Law, G. D., and Purcell, G. V., Science 163, 1329 (1967).

Laime-Böszörmenyi, Paillotin, G., Fallot, P., and Roux, E., Photochem. Photobiol. 15, 139 (1972).

Latimer, P., Bannister, T. T., and Rabinowitch, E., Science 125, 585 (1956).

Lewis, G. N., and Kasha, M., J. Am. Chem. Soc. 67, 994 (1945).

Loach, P. A., Androes, G., Maksim, A. F., and Calvin, M., Photochem. Photobiol. 2, 443 (1963).

McCree, K. J., Biochim. Biophys. Acta 102, 96 (1965).

McElroy, J., Feher, G., and Mauzerall, D., Biochim. Biophys. Acta 172, 180 (1969).

McElroy, J., Feher, G., and Mauzerall, D., Biophys. J. 10, 204a (1970).

Memming, R., and Tributsch, H., J. Phys. Chem. 75, 4, 562 (1971).

Moss, T. S., Optical Properties of Semiconductors, Academic Press, Inc., New York, 1959.

Nag, B. R., and Das, P., Phys. Rev. 132, 2514 (1963).

Nelson, R. C., J. Chem. Phys. 27, 864 (1957).

Nelson, R. C., J. Chem. Phys. 47, 11, 4451 (1967).

Nelson, R. C., J. Phys. Chem. 69, 3, 714 (1965).

Nelson, R. C., Photochem. Photobiol. 8, 441 (1968).

Nishimura, M., Comparative Biochemistry and Biophysics of Photosynthesis, University of Tokyo Press, Tokyo, p. 198, 1968.

Olson, J. M., and Chance, B., Arch. Biochem. Biophys. 88, 26, 40 (1960).

Park, R., J. Cell Biol. 27, 1, 151 (1965).

Park, R. B., and Biggins, J., Science 144, 1009 (1964).

Park, R. B., and Branton, D., "Freeze-Etching of Chloroplasts from Glutaraldehyde Fixed Leaves," Brookhaven Symp. in Biology No. 19, 341 (1966).

Park, R. B., and Pon, N. G., J. Mol. Biol. 6, 105 (1963).

Park, R. B., and Sane, P. V., Ann. Rev. Plant Physiol. 22, 395 (1971).

Parson, W. W., Biochim. Biophys. Acta 153, 248 (1968).

Parson, W. W., Biochim. Biophys. Acta 189, 384 (1969).

Parson, W. W., Biochim. Biophys. Acta 189, 397 (1969).

Parson, W. W., Biochim. Biophys. Acta 253, 187 (1971).

Parson, W. W., and Case, G. D., Biochim. Biophys. Acta 205, 232 (1970).

Pearlstein, R., "Migration and Trapping of Excitation Quanta in Photosynthetic Units," Brookhaven Symp. in Biology No. 19, 8 (1966).

Pearlstein, R., "Coherent Excitons?," International Conference on the Photosynthetic Unit, Gatlinberg, Tennessee, 1970.

Portis, A. M., J. Phys. Solids 8, 326 (1959).

Petermann, G., Tributsch, H., and Bogomolni, R. A., J. Chem. Phys. (in Press), 1972.

Portis, A. M., Klein, M. P., and Teaney, D., Rev. Sci. Instr. 32, 6, 721 (1961).

Portis, A. M., and Teaney, D. J., J. Appl. Phys. 29, 1962 (1958).

Powell, M. R., and Rosenberg, B., Bioenergetics 1, 493 (1970).

Rabinowitch, E. I., Photosynthesis, Interscience Publishers Inc., 1956.

Reed, D. W., J. Biol. Chem. 244, 4936 (1969).

Reed, D. W., and Clayton, R. K., Biochem. Biophys. Res. Commun. 30, 471 (1968).

Reed, D. V., Zankel, K. L., and Clayton, R. K., Proc. Natl. Acad. Sci. U.S. 63, 42 (1972).

Robinson, G. W., "Excitation Transfer and Trapping in Photosynthesis," Brookhaven Symp. in Biology No. 19, 16 (1966).

Rosenberg, B., J. Chem. Phys. 36, 816 (1962).

Rosenberg, B., J. Chem. Phys. 35, 982 (1961).

Rosenberg, B., Nature 193, 364 (1962).

Rosenberg, B., J. Chem. Phys. 34, 63 (1961).

Rosenberg, B., and Camiscoli, J. F., J. Chem. Phys. 35, 3, 982 (1961).

Ross, R. T., J. Chem. Phys. 46, 12, 4590 (1967).

Ross, R. T., J. Chem. Phys. 45, 1 (1966).

Ross, R. T., and Calvin, M., Biophys. J. 7, 595 (1967).

Roosbroeck van, W., "Current-Carrier Transport and Photoconductors in Semiconductors with Trapping," Bell Telephone Laboratory, Murray Hill, New Jersey, 1959.

Ruben, S., et al., J. Am. Chem. Soc. 63, 877 (1941).

Sauer, K., and Biggins, J., Biochim. Biophys. Acta 102, 55 (1965).

Sauer, K., and Calvin, M., Biochim. Biophys. Acta 64, 324 (1962).

Sauer, K., Dratz, E. A., and Coyne, L., Proc. Natl. Acad. Sci. U.S. 61, 17 (1968).

Sauer, K., and Dratz, E. A., Progress in Photosynthesis Research II, 837 (1969).

Sauer, K., and Park, R. B., Biochemistry 4, 2791 (1965).

Sauer, K., and Park, R. B., Biochim. Biophys. Acta 79, 476 (1964).

Sauer, K., Lindsay-Smith, J. R., and Schultz, A. J., J. Am. Chem. Soc. 88, 2681 (1966).

Sistrom, W. R., Photochim. Photobiol. 14, 329 (1971).

Sistrom, W. R., J. Gen. Microbiol. 22, 778 (1960).

Sistrom, W. R., and Clayton, R. K., Biochim. Biophys. Acta 88, 61 (1964).

Snowden, D. P., Ph.D. Thesis, University of California, Berkeley, 1960.

Snowden, D. P., and Portis, A. M., Phys. Rev. 120, 6, 1983 (1960).

Slooten, L., Biochim. Biophys. Acta 256, 452 (1972).

Strehler, B. L., and Arnold, W. H., J. Gen. Physiol. 34, 809 (1951).

Sun, A. S. K., "The Photochemistry and Kinetics of Electron Transport and the Pigment Systems in Chlorophyll," Ph.D. Thesis, University of California, Berkeley, 1971.

Szent-Gyorgyi, A., Science 93, 609 (1941).

Teaney, D. J., Ph.D. Thesis, "Microwave Faraday Rotation in Magnetic Materials," University of California, Berkeley, 1960.

Terenin, A. N., Acta Physicochim USSR 12, 617 (1940).

Terenin, A., and Akimov, I., J. Phys. Chem. 69, 3, 730 (1965).

Terenin, A. N., Putzeiko, Ye. K., and Akimov, I., Disc. Faraday Soc. 27, 83 (1959).

Thornber, J. P., Olson, J. M., Williams, D. M., and Clayton, M. L., Biochim. Biophys. Acta 172, 351 (1960).

Tributsch, H., J. Bioenergetics (to be published).

Treharne, R. W., Brown, T. E. and Vernon, L. P., Biochim. Biophys. Acta 75, 324 (1963).

Trukhan, E. M., Biofisika, 11, 3, 412-19 (1966).

Van Niel, C. B., Arch. Mikrobiol. 3, 1 (1931).

Vernon, L. P., Anal. Chem. 32, 1144 (1960).

Vernon, L. P., et al., Photochem. Photobiol. 14, 343 (1971).

Vishniac, W., and Ochoa, S., Nature 167, 768 (1951).

Vogelhut, P. O., "The Dielectric Properties of Water and Their Role in Enzyme-Substrate Interactions," University of California, 1962, Series No. 60, Issue 476.

Von Aulock, W., and Rowen, J. H., Bell System Tech. J. 36, 427 (1957).

Warburg, O., Krippahl, and Schroeder, W., Z. Naturforsch. 96, 667 (1954).

Warburg, O., Krippahl, and Schroeder, W., Z. Naturforsch. 96, 164 (1954).

Warburg, O., and Negelein, E. Z., Physik. Chem. 102, 235 (1922).

Weaver, E., Photochem. Photobiol. 7, 93 (1968).

Wilson, I. G., Schramm, C. W., and Kinzer, J. P., Bell System.Tech. J. 25, 408 (1946).

Willstätter, R., and Stoll, A., Untersuchungen über die Assimilation der Kohlensäure, Springer-Verlag, Berlin, 1918.

Witt, H. T., et al., Progress in Photosynthesis Research III, Ed. H. Metzner, 1361, 1969.

Witt, H. T., Naturwissenschaften 42, 72 (1955).

Witt, H. T., Rumberg, B., and Junge, W., Mosbach Symposium, Baden, 1968. Springer-Verlag, Berlin.

Youtsey, K. L., and Grossweiner, L. I., Photochem. Photobiol. 6, 721 (1967).

Ziman, Principles of the Theory of Solids, Cambridge University Press, London, 1965.

Zvalinskii, V. I., and Litvin, F. F., Dokl. Akad. Nauk SSSR 173, 230 (1970).

TECHNICAL INFORMATION DIVISION
LAWRENCE BERKELEY LABORATORY
UNIVERSITY OF CALIFORNIA
BERKELEY, CALIFORNIA 94720